ISSN 0021-9673

VOL. 470 NO. 2 MAY 26, 1989

THIS ISSUE COMPLETES VOL. 470

Int. Symp. on Current Separation Techniques for Macromolecules Uppsala, August 22–24, 1988

JOURNAL OF

CHROMATOGRAPHY

INTERNATIONAL JOURNAL ON CHROMATOGRAPHY, ELECTROPHORESIS AND RELATED METHODS

SYMPOSIUM VOLUMES

ELSEVIER

JOURNAL OF CHROMATOGRAPHY

Scope. The *Journal of Chromatography* publishes papers on all aspects of chromatography, electrophoresis and related methods. Contributions consist mainly of research papers dealing with chromatographic theory, instrumental development and their applications. The section *Biomedical Applications*, which is under separate editorship, deals with the following aspects: developments in and applications of chromatographic and electrophoretic techniques related to clinical diagnosis or alterations during medical treatment; screening and profiling of body fluids or tissues with special reference to metabolic disorders; results from basic medical research with direct consequences in clinical practice; drug level monitoring and pharmacokinetic studies; clinical toxicology; analytical studies in occupational medicine.

Submission of Papers. Papers in English, French and German may be submitted, in three copies. Manuscripts should be submitted to: The Editor of *Journal of Chromatography*, P.O. Box 681, 1000 AR Amsterdam, The Netherlands, or to: The Editor of *Journal of Chromatography, Biomedical Applications*, P.O. Box 681, 1000 AR Amsterdam, The Netherlands. Review articles are invited or proposed by letter to the Editors. An outline of the proposed review should first be forwarded to the Editors for preliminary discussion prior to preparation. Submission of an article is understood to imply that the article is original and unpublished and is not being considered for publication elsewhere. For copyright regulations, see below.

Subscription Orders. Subscription orders should be sent to: Elsevier Science Publishers B.V., P.O. Box 211, 1000 AE Amsterdam, The Netherlands, Tel. 5803 911, Telex 18582 ESPA NL. The *Journal of Chromatography* and the *Biomedical Applications* section can be subscribed to separately.

Publication. The *Journal of Chromatography* (incl. *Biomedical Applications*) has 37 volumes in 1989. The subscription prices for 1989 are:

J. Chromatogr. + *Biomed. Appl.* (Vols. 461–497):
Dfl. 6475.00 plus Dfl. 999.00 (p.p.h.) (total *ca.* US$ 3737.00)

J. Chromatogr. only (Vols. 461–486):
Dfl. 5200.00 plus Dfl. 702.00 (p.p.h.) (total *ca.* US$ 2951.00)

Biomed. Appl. only (Vols. 487–497):
Dfl. 2200.00 plus Dfl. 297.00 (p.p.h.) (total *ca.* US$ 1248.50).

Our p.p.h. (postage, package and handling) charge includes surface delivery of all issues, except to subscribers in Argentina, Australia, Brasil, Canada, China, Hong Kong, India, Israel, Malaysia, Mexico, New Zealand, Pakistan, Singapore, South Africa, South Korea, Taiwan, Thailand and the U.S.A. who receive all issues by air delivery (S.A.L. — Surface Air Lifted) at no extra cost. For Japan, air delivery requires 50% additional charge; for all other countries airmail and S.A.L. charges are available upon request. Back volumes of the *Journal of Chromatography* (Vols. 1–460)are available at Dfl. 195.00 (plus postage). Claims for missing issues will be honoured, free of charge, within three months after publication of the issue. Customers in the U.S.A. and Canada wishing information on this and other Elsevier journals, please contact Journal Information Center, Elsevier Science Publishing Co. Inc., 655 Avenue of the Americas, New York, NY 10010. Tel. (212) 633-3750.

Abstracts/Contents Lists published in Analytical Abstracts, ASCA, Biochemical Abstracts, Biological Abstracts, Chemical Abstracts, Chemical Titles, Chromatography Abstracts, Current Contents/Physical, Chemical & Earth Sciences, Current Contents/Life Sciences, Deep-Sea Research/Part B: Oceanographic Literature Review, Excerpta Medica, Index Medicus, Mass Spectrometry Bulletin, PASCAL-CNRS, Referativnyi Zhurnal and Science Citation Index.

See inside back cover for Publication Schedule, Information for Authors and information on Advertisements.

0021-9673/89/$03.50

Printed in The Netherlands

This issue is printed on acid-free paper.

For contents see p. 314.

SYMPOSIUM ISSUE

Uppsala Cathedral (after a painting from 1850 by A. Meyer)

INTERNATIONAL SYMPOSIUM ON CURRENT SEPARATION TECHNIQUES FOR MACROMOLECULES

Uppsala (Sweden), August 22–24, 1988

Guest Editor

B. D. WESTERLUND

(Uppsala)

SYMPOSIUM VOLUMES

EDITOR
E. HEFTMANN (Orinda, CA)

EDITORIAL BOARD
S. C. Churms (Rondebosch), E. H. Cooper (Leeds), R. Croteau (Pullman, WA), D. H. Dolphin (Vancouver), J. S. Fritz (Ames, IA), K. J. Irgolic (College Station, TX), C. F. Poole (Detroit, MI), R. Teranishi (Berkeley, CA), H. F. Walton (Boulder, CO), C. T. Wehr (Foster City, CA)

VOL. 470, NO. 2 JOURNAL OF CHROMATOGRAPHY MAY 26th, 1989

CONTENTS

INTERNATIONAL SYMPOSIUM ON CURRENT SEPARATION TECHNIQUES FOR MACROMOLECULES, UPPSALA (SWEDEN), AUGUST 22–24, 1988

In articles with more than one author, the name of the author to whom correspondence should be addressed is indicated in the article heading by a 6-pointed asterisk (*)

Journal of Chromatography, 470 (1989) 315
Elsevier Science Publishers B.V., Amsterdam — Printed in The Netherlands

PREFACE

The Swedish city of Uppsala has an excellent tradition in the field of macromolecular separations with peaks in the 1940s (a Nobel prize in 1948 for Arne Tiselius, who was active both in chromatography and electrophoresis) and in the 1950s (the development of the principles for size-exclusion chromatography by Jerker Porath and Per Flodin). Macromolecular separations form the basis for the largest industry in town: Pharmacia. Uppsala was thus an appropriate choice for a symposium on the separation of macromolecules. The traditions were still very much in evidence at the symposium where Jerker Porath and Stellan Hjertén, both trained by Tiselius, were highly active participants.

Macromolecules are essential components in many different kinds of materials such as biological fluids and tissues, products from biotechnical processes, many synthetic materials, etc. Different macromolecules have widely varying properties with respect to, *e.g.*, molecular weight, polarity, extent of tertiary and quaternary structures. Separation techniques are essential in the research, production and control of macromolecules. They are used for characterisation and identification purposes, for quantitative analysis as well as for preparative isolations. The very diverse characteristics of different macromolecules as well as the numerous fields of application have resulted in the development of a variety of separation techniques.

The main purpose of the symposium was to review the different separation principles that are available today, thereby helping the advanced scientist to generate new ideas for combination possibilities and for new principles, and providing the application chemist with an overview of the various techniques in order to facilitate selection of the most appropriate one for the problems at hand. The emphasis was mainly on the retention mechanisms and the main properties of the different techniques, with applications to some typical examples. The symposium covered the areas of liquid chromatography, supercritical fluid chromatography, field flow fractionation, hydrodynamic chromatography and electrophoretic techniques. The lecturers were leading scientists in their respective areas.

The symposium largely fulfilled its goal and the organizers would like to thank all invited lecturers for their high-quality contributions.

Uppsala (Sweden) DOUGLAS WESTERLUND

Journal of Chromatography, 470 (1989) 317–326
Elsevier Science Publishers B.V., Amsterdam — Printed in The Netherlands

CHROMSYMP. 1577

TEN YEARS OF CHROMATOFOCUSING: A DISCUSSION

L. A. Æ. SLUYTERMAN* and C. KOOISTRA
Department of Organic Chemistry, Eindhoven University of Technology, P.O. Box 513, 5600 MB Eindhoven (The Netherlands)

SUMMARY

The theory of chromatofocusing has been clarified, in a qualitative manner, in terms of the pH gradient, Donnan potential, non-uniformity of flow, retardation factor and the titration curve of the protein. The main equations were refined to include the effect of the moving frame. A number of representative experimental results from the literature are given to illustrate the utility and limitations of the method. Some of these data were used to substantiate the theory. It is shown that no displacement by ampholyte components can occur under the conditions of chromatofocusing.

INTRODUCTION

As the present conference was held 10 years since the first two papers on chromatofocusing (CF) appeared in this journal[1,2], it seemed appropriate to review and discuss that method. By way of introduction, a simple qualitative explanation of the principles and factors involved is in order.

THE PRINCIPLES AND THEIR VERIFICATION

The objective of CF is to elute proteins from a column in the order of their pI values, *i.e.*, to mimic isoelectric focusing (IEF). For that purpose an ion exchanger is used, usually an anion exchanger, which exhibits a certain buffering capacity, owing to the fact that it carries ionizing groups having a wide range of pK values. The column is first equilibrated to the highest pH value desired for the separation. A pH gradient is then produced inside the column by passing through it an ampholyte solution that had been adjusted to the lower limit of the desired pH range, the protein sample having been applied in the first few ml of this solution. All protein components immediately start moving down the column in the order of their pI values at the same rate as the pH gradient. The focusing effect can be understood from Fig. 1. Owing to the buffering effect of the column, the pH gradient moves at a much slower rate than does the mobile liquid. In the moving frame of the protein the liquid flows at a rate equal to its rate outside the frame minus the rate of the frame, the latter being equal to the rate of the pH gradient.

If in the middle of the protein band the pH is equal to its pI value, the protein is

0021-9673/89/$03.50

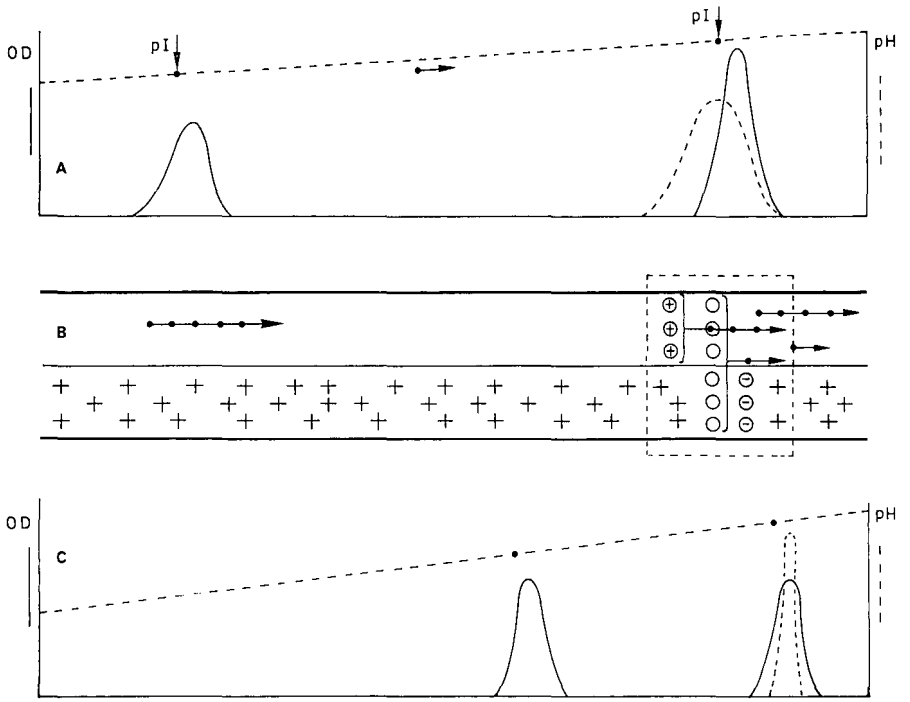

Fig. 1. Schematic representation of CF. (A) pH gradient and protein content along the length of the column shown in (B). (C) Location of protein bands in a pH gradient having twice the slope of the one in (A). Horizontal arrows indicate rates of displacement.

uncharged and therefore equally partitioned between the two phases. When the volumes of the two phases are equal, these molecules are moving at a rate half the rate of the mobile phase in the moving frame. Molecules in front of the centre are at higher pH and are negatively charged. They are therefore retained by the matrix and do not move in the frame. At the back of the centre the molecules are at a lower pH, are positively charged and are therefore expelled from the matrix. They move as rapidly as the liquid in the frame. It is evident that the band is compressed in this way. The compression is counteracted by the non-uniformity of flow, unavoidable in a column of beads. The final result is the bandwidth actually observed.

The width of a protein band depends on the steepness of its titration curve around its isoelectric point (Fig. 2). In order to carry a sufficient charge, Z, to be retained by the exchanger, protein b requires a larger pH deviation from its pI value than protein a. Therefore a larger displacement from the centre of the band is necessary for retention. Protein b will thus exhibit a wider band.

The higher the charge of the exchanger, the narrower will be the band, because less overall charge of the protein and therefore a smaller displacement from the centre of the band is needed for a molecule to be retained by the exchanger.

In Fig. 1C the pH gradient in the column is twice as steep as in Fig. 1A. The bands are, of course, twice as close as in Fig. 1A. The compression effect is also twice as large, because half the distance from the centre of the band is needed for a protein

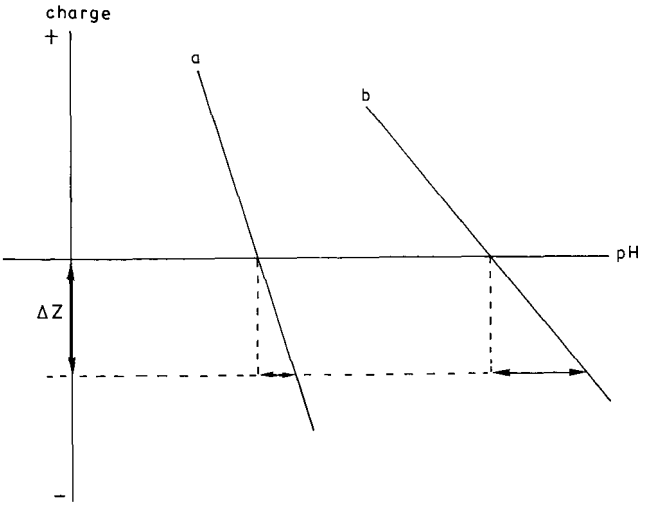

Fig. 2. Titration curves of two proteins around their pI values.

molecule to acquire the charge needed for retention. Unfortunately, a narrower band suffers more from non-uniformity of flow, and the result is a poorer separation than in Fig. 1A.

All of these factors are accounted for when the system is calculated from first principles (see Appendix I). The total width of a band, at 50% maximum, ΔpH, is described by:

$$\Delta\text{pH} = \frac{2.35}{1 - R_t}\sqrt{\frac{q}{\varphi} \cdot \frac{\text{dpH}/\text{d}V}{\text{d}Z/\text{dpH}}} \tag{1}$$

In eqn. 1 q denotes the coefficient of the non-uniformity of flow, φ the Donnan potential (multiplied by the factor F/RT) of the exchanger in the buffer concerned, dpH/dV the pH gradient, dZ/dpH the steepness of the titration curve of the protein around its pI and R_t the retardation factor, *i.e.*, the ratio of the rates of displacement of the pH gradient and the mobile phase, respectively.

When the pH gradient is not retarded, *i.e.*, when $R_t = 1$, ΔpH is infinite, signifying that no focusing occurs. The factor concerned approaches a constant when R_t decreases to realistic values like 0.1.

For optimum separation, smooth and constant pH gradients are needed. This requires proper tuning of the buffering capacity of the exchanger and of the buffer over a wide pH range. Research workers at Pharmacia managed to do so[3] and their materials are almost generally used[4].

An early application of CF is a separation of haemoglobin variants by Alexander and Neeley[5] (Fig. 3). They examined the separation on two columns of two different lengths, 26 and 54 cm. Of course, the separation is better on the longer column, as is usual in chromatography. It is interesting to compare the bandwidths; those for the protein, the exchanger and the buffer are identical; the pH gradient is the only

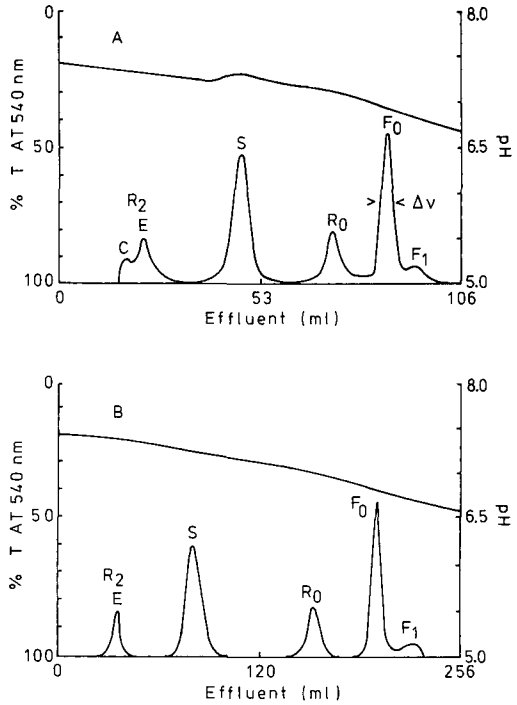

Fig. 3. Separation of haemoglobin variants. PBE 94 columns: (A) 26 cm × 0.9 cm; (B) 54 cm × 0.9 cm. Initial buffer: 0.025 *M* imidazole (pH 7.4). Limiting buffer: PB 96, 1:13 diluted, adjusted to pH 6.0. Flow-rate: 14.3 ml/h.

difference. This permits a check of eqn. 1 as far as the effect of the gradient is concerned, dpH/dV being calculated from the slope of the tangent to the pH gradient at the pH of elution, ΔpH by multiplying dpH/dV by ΔV, the bandwidth of the protein peak at half the maximum height in terms of the elution volume. The results, given in Table I, show a good correspondence between the observed and calculated ratios.

The smallest bandwidth was observed by Verbalis[6], who used a column of 100 cm and a narrow pH gradient to separate neurophysins (Fig. 4); the ΔpH was 0.015. Peaks differing in p*I* by no more than 0.02 units were reasonably separated.

Another relevant factor is the pH of an emerging protein solution, pI_{app}. It is evident from Fig. 1 that the compression causes the protein to be somewhat ahead of its isoelectric point; the protein is slightly negatively charged and partly retained by the exchanger. This permits the protein to keep pace with the slowly moving gradient.

TABLE I

EFFECT OF pH GRADIENT ON BAND WIDTH, ΔpH, OF THE HAEMOGLOBIN VARIANT F_0

	Short column	*Long column*	*Ratio*
ΔpH	0.040	0.025	obs. 1.60
Gradient	0.013	0.0043	calc. 1.75

However, there is another factor, one that causes the protein to lag behind. Owing to the positive charges, the pH is higher inside the beads than outside. Protein molecules that enter the beads will therefore undergo a shift in their overall charge in the negative direction and will thus be more retained by the beads than they would otherwise have been; they will emerge at a lower pH.

The sum of the two effects is represented by (see Appendix I):

$$\mathrm{p}I_{\mathrm{app}} - \mathrm{p}I = -\frac{\varphi}{4.6} + \frac{1}{\varphi|\,\mathrm{d}Z/\mathrm{dpH}|} \cdot \ln\frac{1 - R_t}{rR_t} \qquad (2)$$

r denoting the ratio of solvent volume inside the stationary phase and the void volumes. It is evident that this is a delicate balance that can easily turn in either direction, as borne out by the data in Table II. Low values of both φ and $\mathrm{d}Z/\mathrm{dpH}$ will cause a pronounced positive deviation (line 1), high values of both factors provide a negative deviation (line 3), whereas combinations of low φ with high $\mathrm{d}Z/\mathrm{dpH}$ (line 2) and high φ with low $\mathrm{d}Z/\mathrm{dpH}$ (line 4) tend to keep deviations low. In three of these cases $\Delta\mathrm{p}I$ can be calculated with satisfactory results.

FURTHER EXAMPLES OF SEPARATION

We now turn to a few other representative examples in the literature of what can be achieved with CF.

Aton *et al.*[8] separated rhodopsins, phosphorylated to different extents, by both IEF–PAGE (polyacrylamide gel electrophoresis) and CF. In Fig. 5 the results are plotted as $\Delta\mathrm{p}I$ *versus* electrophoretic pI values. They are remarkable; within a range of 0.8 pI units $\Delta\mathrm{p}I$ changes from $+0.5$ to -0.5, one complete unit upon the introduction

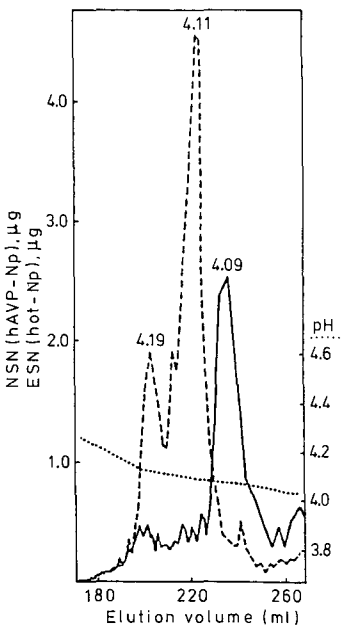

Fig. 4. Separation of neurophysins. For details see ref. 6.

TABLE II

ΔpI VALUES, OBSERVED AND CALCULATED

	pI_{app}	pI	ΔpI	φ	dZ/dpH	R_t	ΔpI_{calc}
Myoglobin[a]	9.05	8.25	+0.8	0.65	1.8	0.16	+0.85
Papain[b]	9.75	9.60	+0.15	0.65	5.0	0.15	+0.2
Papain[c]	9.15	9.60	−0.45	3.2	5.0	0.03	−0.5
Myoglobin[d]	8.35	8.25	+0.1	high	1.8	—	—

[a] Fig. 7a of ref. 2.
[b] Fig. 12a of ref. 2.
[c] Fig. 5 of ref. 7.
[d] Fig. 6 of ref. 7.

of from two to eight phosphate groups. Since neither φ nor dZ/dpH is known, no definite explanation can be given as yet.

In many of the few hundred preparative papers published so far, CF was used as the final step in a purification sequence. When applied at an early stage, a ten-fold purification is quite usual. The highest purification achieved was 50-fold (the profile was not shown)[9]. As many as 29 components of eye lens crystallin were distinguished in one CF experiment[10]. The elution buffer contained 6 *M* urea to prevent precipitation of some of the components. A non-ionic detergent was also used for dissolving (membrane) proteins[11].

CF has also invaded the patent literature. Kato *et al.*[12] separated two human interleukins-2. One of them carries alanine, the other methionine as the N-terminal amino acid, the methionine being a one-unit extension of the chain. The Ala-terminal interleukin emerged first, at pH 8.0, the Met-terminal protein second, at pH 7.9 (Fig. 6), indicating that the Ala variant is the slightly more basic one. This corresponds nicely with the p*K* values of an alanyl dipeptide (8.2) and of a methionine dipeptide

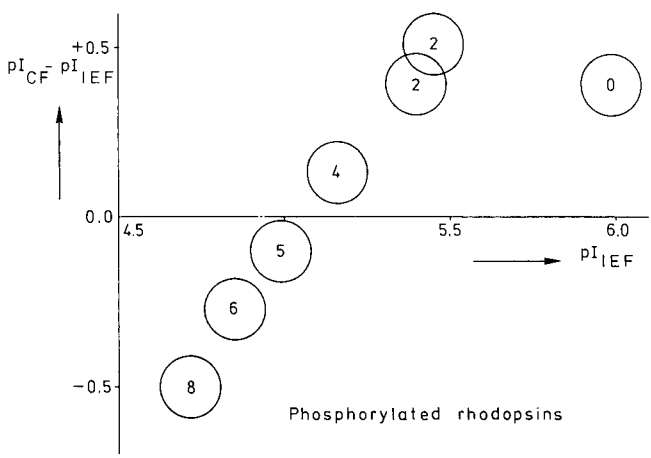

Fig. 5. Differences between p*I* values, determined by CF and by IEF, as a function of the values determined by IEF, for rhodopsins phosphorylated to different extents. The numbers indicate the number of phosphate groups per molecule. For details see ref. 8.

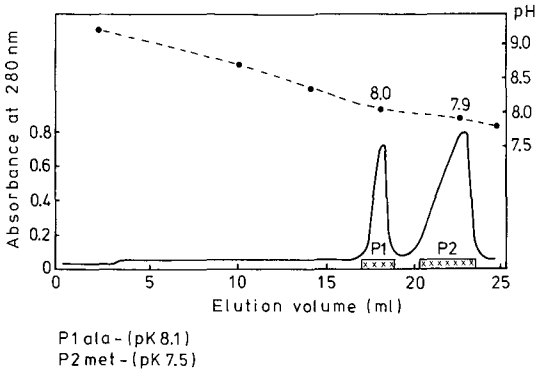

Fig. 6. The separation of two human interleukin-2 variants; pK values in parentheses indicate the values for related dipeptides.

(7.5), respectively. It is striking that such a small difference in the pK of one out of 34 charged groups in the two proteins permits their preparative separation.

DISCUSSION

It must be pointed out that eqns. 1 and 2 are equally applicable to all slowly-moving pH gradients, independent of whether they are produced with the aid of the buffering action of the column (CF) or entirely steered from the outside by appropriate gradient mixers (pH gradient ion exchange). Sometimes, a mixture of the two methods is used[13]. CF has the advantage of permitting the protein sample to be applied at the low pH of the range; no protein is subjected to a pH much higher than its pI value. Furthermore, CF allows an higher flow-rate[1].

The components of an ampholyte buffer behave much as proteins do, with the difference that a protein sample is added to the column only once and that the buffer is fed into it continuously. At the beginning of the separation, most of the components are strongly negative and are therefore gathered at the top of the column. When the pH in the column decreases, successive species lose most of their charge. All molecules of a particular species that had gathered that far move down and emerge as a single band. The approximate concentration of such just emerging ampholyte species in the fractions containing haemoglobin F_0 in Fig. 3 has been calculated (Appendix II). It was $3 \cdot 10^{-3}$ M, while the concentration of fixed charges at pH 7 in the last section of the column was 0.53 M[14]. The ratio is $6 \cdot 10^{-3}$, which is negligible; it is not possible that there is competition between protein and ampholyte species for such an abundance of fixed charges. It is therefore misleading to use the term displacement chromatography for this method. Displacement only starts after completion of CF. The elution volume between the end of CF and the start of the displacement is larger the lower is the concentration of negative buffer components in the elution buffer, *i.e.*, the nearer the terminal pH of the gradient is closer to the lower limit of the pH range covered by the ampholyte.

The concentration of an ampholyte species after its breakthrough point decreases to its level in the initial buffer. While more and more ampholyte species pass

TABLE III

CHANGE OF RESOLVING POWER DURING CF ON PBE 94 WITH POLYBUFFER 96, DILUTED 1:10, FROM pH 8.5 TO 6.0

Data from ref. 14.

pH	$[Cl^-]_m$ *(mM)*	P^+ *(mM)*	φ	$\sqrt{\varphi}$	*Ratio*
8.5	2.0	465	5.4	2.3	1.2
6.0	13.0	590	3.8	1.9	

through the column unretarded as positively charged molecules during CF, the concentration of counter ions in the emerging buffer increases gradually. Although the ion concentration in the mobile phase will affect the Donnan potential, the effect on the resolving power is small, as shown in Table III. The increase in chloride concentration is accompanied by an increase in charge inside the exchanger, P^+, as an increasing number of fixed amino groups is protonated with decreasing pH. Since $\varphi = \ln[Cl^-]_s/[Cl^-]_m$ and $[Cl^-]_s$ is virtually equal to P^+, φ can be calculated. It is found that φ does not change very much (Table III). Furthermore, ΔpH is inversely proportional to the square root of φ (see eqn. 1). Hence, the resolving power hardly changes in the range pH 8.5–6.

What improvements in resolving power might still be introduced? Increasing the maximum capacity of the exchanger three-fold would increase the buffering capacity three-fold and thus decrease dpH/dV three-fold. At the same time, φ would increase, but by no more than *ca.* 25%. Altogether, a nearly two-fold increase in resolving power would result. This is probably the most that can be obtained without reducing the pore size of the beads too much.

The non-uniformity of flow is quite limiting, but that is a general problem in chromatography. If diffusion were the only limiting factor (*cf.*, eqn. A3 of Appendix I), as in continuous gels, ΔpH for haemoglobin F_0 in Fig. 3B would theoretically have been *ca.* $1 \cdot 10^{-4}$[a]. This, of course, is unattainable, but even a few steps in that direction would be helpful.

APPENDIX I

Refinement of the equations describing bandwidth and ΔpI

In deriving eqn. 29 of ref. 1 it was tacitly assumed that the rate of movement of the pH gradient is negligible compared with the rate of the liquid flow. The equation can be made more general by introducing the ratio, R_t, of the two flows:

$$(dx/dt)_{pH} = R_t(dx/dt)_m \qquad (A1)$$

Inside the moving frame the liquid flow is equal to

$$(dx/dt)_{m,mf} = (dx/dt)_m - (dx/dt)_{pH} = (dx/dt)_m(1 - R_t)$$

[a] The following values were used: $r = 2$, diffusion coefficient $D = 7 \cdot 10^{-7}$ cm^2 s^{-1}, $\varphi = 4.9$[14], $dZ/dpH = 8.7$[15], $dV/dt = 22.5$ ml h^{-1} cm^{-2} (*cf.*, Fig. 3) and $dpH/dV = 0.0043$ (Table I). R_t was neglected.

R_t being variable between 0 and 1. The effect of the moving frame can therefore be introduced by multiplying eqn. 12 of ref. 1 by $(1 - R_t)$:

$$\left(\frac{dx}{dt}\right)_{p,mf} = \frac{1 - R_t}{1 + rK}\left(\frac{dx}{dt}\right)_m \tag{A2}$$

K denoting the partition coefficient of the compound. Utilizing eqn. A2 instead of eqn. 12 of ref. 1 yields eqn. A3 instead of eqn. 29 of ref. 1:

$$(\Delta pH)^2 = \frac{1 + rK_0}{rK_0(1 + r)^2(1 - R_t)}\left[\frac{D}{dV/dt} + (1 + r)^2 q\right]\frac{dpH/dV}{\varphi \cdot dZ/dpH} \tag{A3}$$

K_0 being the partition coefficient at the center of a protein band. Furthermore, comparison of eqn. A1 with eqn. 5 of ref. 1 yields:

$$R_c = \frac{1 - R_t}{R_t} \tag{A4}$$

Inserting eqn. A4 into eqn. 31 of ref. 1 yields:

$$K_0 = \frac{1 - R_t}{rR_t} \tag{A5}$$

Insertion of eqn. A5 into eqn. A3 and neglecting the diffusion component yields eqn. 1 of this paper.

In eqn. 1 another alteration has been incorporated. In eqn. A3, ΔpH is the bandwidth from the centre to 60% of the maximum[1]. If the total bandwidth is taken to 50% of the maximum, as is more convenient, the factor 2.35 is added.

Experimentally, R_t is equal to the ratio of the volume of the column, v, and the elution volume, V_t, when the terminal pH, pH_t, emerges from the column. This is true only when the pH gradient is strictly linear (Fig. A1A). When this is not the case (which occurs most frequently), every point on the pH curve has its own V_t value, equal to the intercept of the tangent to the curve at the pH of elution with the volume axis (Fig. A1B).

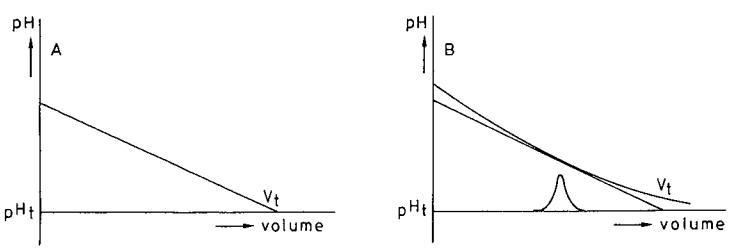

Fig. A1. Schematic representation of (A) an ideal pH gradient and (B) a non-linear pH gradient.

APPENDIX II

Calculation of the concentration of ampholyte species that are specifically eluted with a protein band

A protein is eluted at the elution volume, V_e, in a volume ΔV_e, that corresponds to $\Delta\text{pH} = (\text{dpH}/\text{d}V)\Delta V_e$. The amount of ampholyte specifically eluted with the protein can be derived as follows. The workable pH range of the ampholyte is i. It is assumed that the various buffer components are evenly distributed along this range. When they are arrayed in the order of their pI values, as in IEF, the interval ΔpH contains the fraction $\Delta\text{pH}/i$ of the total amount. The total amount of buffer introduced in the column is V_eM, where M denotes the molarity of the buffer solution. Hence, the interval ΔpH of the protein contains the amount of buffer $V_eM \cdot \Delta\text{pH}/i$. Since this amount is specifically eluted in the volume ΔV_e, its concentration, C_e, is:

$$C_e = \frac{V_eM}{i\Delta V_e} \cdot \Delta\text{pH} \approx \frac{V_eM}{i} \cdot \frac{\text{dpH}}{\text{d}V} \qquad \text{(A6)}$$

Taking again haemoglobin as an example (F_0 in Fig. 3B), V_e = 205 ml, $\text{dpH}/\text{d}V$ = 0.0043 (Table I). Polybuffer 96 appeared to contain 9.8% of dry weight material; the molecular weight was taken to be about 750 (ref. 16). The molarity of the undiluted buffer is therefore 0.13 M; after 1:13 dilution, 0.010 M. The workable pH range, i = 3 units. Inserted into eqn. A6, these data yield C_e = 3 mM.

Those components of the ampholyte that had already broken through the column are positively charged and do not enter the matrix.

ACKNOWLEDGEMENTS

The authors thank Dr. O. Elgersma, Philips, Eindhoven, The Netherlands, for discussing the alterations in the main equations.

REFERENCES

1 L. A. Æ. Sluyterman and O. Elgersma, *J. Chromatogr.*, 150 (1978) 17.
2 L. A. Æ. Sluyterman and J. Wijdenes, *J. Chromatogr.*, 150 (1978) 31.
3 L. Söderberg, T. Laao and D. Low, in H. Peeters (Editor), *Protides of Biological Fluids, Proceedings of the 29th Colloquium*, Pergamon, Oxford, 1982, p. 955.
4 *Chromatofocusing Handbook*, Pharmacia Fine Chemicals, Uppsala, 1981.
5 N. M. Alexander and W. E. Neeley, *J. Chromatogr.*, 230 (1982) 137.
6 J. G. Verbalis, *J. Chromatogr.*, 254 (1983) 309.
7 L. A. Æ. Sluyterman and J. Wijdenes, *J. Chromatogr.*, 206 (1981) 441.
8 B. R. Aton, B. J. Litman and M. L. Jackson, *Biochemistry*, 23 (1984) 1737.
9 M.-G. Yet and F. Wold, *J. Biol. Chem.*, 263 (1988) 118.
10 P. Body and H. Bloemendal, *FEBS Lett.*, 232 (1988) 39.
11 L. Wakefield, *J. Biochem. Biophys. Methods*, 9 (1984) 331.
12 K. Kato, T. Yamada and K. Kawahara, *Eur. Pat. Appl.*, 85,306,559.7 (1985).
13 T. H. J. Huisman and A. M. Dozy, *J. Chromatogr.*, 19 (1965) 160.
14 L. A. Æ. Sluyterman and C. Kooistra, unpublished results.
15 J. B. Matthew, G. I. H. Hanania and F. R. N. Gurd, *Biochemistry*, 18 (1979) 1919.
16 L. Söderberg, D. Buckley, G. Hagström and J. Bergström, *Protides Biol. Fluids*, 27 (1980) 687.

Journal of Chromatography, 470 (1989) 327–335
Elsevier Science Publishers B.V., Amsterdam — Printed in The Netherlands

CHROMSYMP. 1520

FIELD-FLOW FRACTIONATION OF MACROMOLECULES

J. CALVIN GIDDINGS
Department of Chemistry, University of Utah, Salt Lake City, UT 84112 (U.S.A.)

SUMMARY

Field-flow fractionation (FFF) is a versatile family of techniques, applicable to macromolecules, colloids, and cell-sized particles. This paper focuses specifically on the applicability of FFF to macromolecules. Following a brief description of the principles of FFF, the characteristics of FFF that bear on its efficacy in separating macromolecules are summarized. The basis of selectivity is established. The general applicability of FFF to macromolecules is then surveyed. For this purpose macromolecular substances are divided into four classes, distinguished by a molecular weight cutoff of 10^6 and by aqueous *versus* organic solubility. The capabilities of different FFF subtechniques in fractionating these classes of macromolecules is then discussed.

INTRODUCTION

The separation of macromolecular materials, both for preparative and analytical purposes, has become one of the most important and demanding activities for separation scientists worldwide. The needs in this area are driven not only by advances in medicine, biology, biotechnology, agriculture, and polymer science but also by increasingly stringent requirements by government regulatory bodies that constantly demand the improved characterization of complex materials of human relevance. Many of these complex materials, particularly in the biosciences, are laden with intricate mixtures of macromolecular components.

In response to the demands for better macromolecular separation and characterization techniques, scientists have responded with a battery of new and vastly improved techniques to separate macromolecules. These techniques include reversed-phase, ion-exchange, affinity, and size-exclusion chromatography; gel, two-dimensional, and capillary zone electrophoresis, along with isoelectric focusing; and the broad field-flow fractionation family of techniques including sedimentation, thermal, and flow field-flow fractionation (FFF). These various approaches are in some respects competitive but in most respects complementary, providing alternate mechanisms for unraveling the formidable complexity of macromolecular materials.

The most recent broad category of macromolecular separation techniques, FFF, is less than a quarter century old[1–3]. Thus, FFF is young relative to chromatography (over 80 years old) and electrophoresis (almost 60 years old). Because FFF is, in

0021-9673/89/$03.50

relative terms, a new methodology not yet in full stride, there is a smaller reservoir of practical experience to draw from than is available for other families of techniques. The level of development and applications work devoted to FFF is only a miniscule fraction of that devoted to the older and better-established groups of techniques. Nonetheless, sufficient work has been done to show that FFF is likely to have an important and substantial niche in the multifaceted repertoire of macromolecular separation tools.

For perspective, we note that FFF has not yet been found particularly effective for low-molecular-weight compounds. The effectiveness of FFF appears to begin at a molecular weight of somewhat less than 1000. From there, the capabilities of FFF, unlike those of most other techniques, improve as molecular mass increases. Thus, FFF is applicable over the entire macromolecular range which, in general terms, can be considered to extend across five or six orders of magnitude in molecular weight. While this mass range will constitute the primary focus of this article, we observe that FFF continues to increase in relative effectiveness beyond the macromolecular limit, proving applicable to colloidal and particulate materials extending over another nine or ten orders of magnitude of mass, extending up to a particle size of *ca.* 100 μm.

The high speed and resolving power of FFF in the separation of the relatively large particulate constituents of colloidal materials and cell-sized (*ca.* 1–50 μm) particles is one of the most important assets of FFF technology as it exists today. By comparison, the development of FFF techniques for the macromolecular range has been somewhat more limited. However, there has been a sufficient accumulation of experience to demonstrate that FFF should have an important role in this area as well.

The nature of FFF has been described on many occasions[2–6]. Briefly, FFF is an elution technique, like chromatography, in which separation occurs within the confines of a narrow tube or channel. There is no packing material and no stationary phase. In the absence of obstructing particles, flow in the tube assumes a uniform laminar profile, usually parabolic in shape. With parabolic flow, the velocity is highest at the channel center and drops to zero upon approaching the channel walls.

Quite obviously, if different species can be somehow placed in different streamlines in the FFF channel, they will be swept along at different velocities and separated. The difficult part in implementing this simple concept is that of finding the means for confining different components to localized regions of the flow cross-section. Such confinement is difficult because entropy-based processes (such as diffusion) are constantly at work distributing entrained components over the entire flow cross-section. Because the channels are thin, any initially confined material tends to spread out rapidly over all streamlines, thus obliterating all velocity differentiation.

In FFF, various driving forces are utilized to force different components to occupy narrow confines of the flow cross-section. These forces must be strong enough to dominate the ubiquitous entropic forces. The driving forces must be oriented perpendicular to flow because their objective is not to drive components along flow lines but rather across flow lines in such a way that they form a unique distribution over the flow cross-section.

For the above purposes many kinds of driving forces have been harnessed, including sedimentation, electrical, thermal (temperature gradient), crossflow, magnetic, and hydrodynamic forces[2–6]. Used singly or in combination, these driving forces are capable of generating different kinds of concentration distributions over the flow

cross-section. The different distributions underlie different operating modes of FFF, including normal FFF, steric FFF, hyperlayer FFF, secondary equilibria FFF, and so on.

The combination of different driving forces and different operating modes leads to a very large family of FFF techniques[7]. Among the prominent subtechniques applicable to macromolecules are those designated as sedimentation/normal FFF, thermal/normal FFF, thermal/hyperlayer FFF, and flow/normal FFF. By this nomenclature the first descriptor (sedimentation, thermal, etc.) refers to the driving force and the second descriptor (normal or hyperlayer) refers to the operating mode[7]. However, as a matter of common practice the word "normal" is usually omitted in describing the normal mode of operation.

The normal operating mode, which has been more widely used than the others, entails the formation of a simple exponential distribution of component molecules or particles against one wall (the accumulation wall) of the FFF channel. Since these exponential distributions are of different thickness for different components, the velocity at which each component is carried along the channel is unique, leading to the desired separation of components.

While the above description of the FFF process and its variations is brief and necessarily incomplete, it provides enough information on the nature of FFF to deduce some of its strengths and weaknesses in dealing with macromolecular materials. By discussing these characteristics, we are better able to deduce the potential role of FFF in macromolecular separations.

CHARACTERISTICS OF FFF

First of all, we recall that FFF, like chromatography, is an elution technique. Techniques based on elution are unusually simple and flexible in sample manipulation, detection, and in general operation. The flexibility of elution is particularly advantageous in the capability it provides for using flow-rate to control the speed of separation over wide limits with no structural changes (*e.g.*, changes in column length) in the separation system. These variations in separation speed generally involve a trade-off with resolution, but the operator has the freedom to choose, with no changes other than in flow-rate, the preferred conditions for separation. We note that some forms of electrophoresis have some quasi-elution characteristics by virtue of electroosmotic flow but these systems have not yet developed the flexibility of true elution systems.

Some differences between FFF and chromatography are centered on the different type of forces used to induce retention. In chromatography, these forces are highly localized at phase boundaries and surfaces. Such forces are highly selective but for macromolecules they tend to be very powerful and are capable of causing irreversible adsorption and structural disruption, including denaturation. The field-based driving forces of FFF and electrophoresis are, by contrast, much more diffuse and locally weak in nature; they rarely reach a level of intensity sufficient to alter molecular conformation.

As molecular size increases, the flow process itself is capable of exerting disruptive shear forces on macromolecules[8]. These forces are particularly harsh in the erratic flow occurring in packed chromatographic beds. By contrast, the shear forces

induced by the uniform laminar flow of FFF channels are relatively gentle.

Operating flexibility is a great asset in macromolecular separations, particularly in exploratory work intended to guage the limits of molecular parameters in a sample. FFF is exceptionally flexible by virtue of the ready variability of the factors underlying the FFF techniques. We have already noted the flow-based flexibility of elution systems, giving immediate access to a range of resolution levels, operating speeds, and sample handling options. Of perhaps even greater importance, retention in FFF is induced by externally controlled forces and gradients that can be altered quickly and precisely to suit experimental needs. Thus, with no change in the FFF channel or equipment, the driving forces can be "tuned" to optimize the separation of components of diverse properties and molecular weights. Not only can these forces be adjusted to maximize the separation of particular species, they can be gradually changed in the course of a run (a technique called field-programmed FFF) to accommodate widely differing sample components[9]. Changes in driving forces also influence (and can be used to control) resolution and speed.

We observe also that most FFF channels have solid, nonpermeable walls compatible with most solvents. Consequently, a given FFF apparatus can usually be adapted to many different solvent (carrier) compositions, thus making it possible to choose a solvent that will maximize the stability and separability of component species. The solvent composition can be rapidly changed for successive runs.

Another important characteristic of FFF is its theoretical tractibility. Because the form (generally parabolic) of the flow profile and the forces exerted on components are controllable and calculable, retention in such systems can be generally related by theory to component properties[2,4]. By linking system behavior and molecular properties, it is possible to control the separation closely. It is also possible to deduce relevant properties of the components from observed retention characteristics.

More difficult to assess is the relative ability of the different families of techniques in resolving macromolecular components. Resolution is related to both selectivity and efficiency[10], the latter reflecting the degree of band broadening in the system. Efficiency in macromolecular separation is generally higher for various electrophoretic techniques than it is for chromatography and FFF. Unfortunately, the high theoretical efficiency calculated for FFF[11] has not yet been realized.

In general, FFF is highly selective. Specifically, it is selective with respect to the particular properties of components that influence the force exerted by the external field. Since different external driving forces can be used, a wide range of selective parameters is available: molecular weight, density, Stokes radius, electrical charge, thermal diffusion coefficient, etc. Separation can be based on any of these parameters by properly choosing the FFF system.

We note that the selective properties of FFF are primarily physical in nature. For FFF, there is little direct selectivity based on chemical properties, which dominate selectivity in most forms of chromatography. (Nonetheless, we note that thermal FFF does show selectivity with respect to the composition of polymeric materials.) In some cases, physical properties (such as electrical charge) are modulated by chemical changes. Electrophoresis, of course, displays a more limited selectivity than FFF based only on electrophoretic mobility; the latter can sometimes be modulated to reflect chemical differences.

Selectivity provides an excellent example of the complementary relationship of different separation techniques. The enormous variation in the basis of selectivity made available by combining all the families of macromolecular separation methods illustrates the magnitude of the arsenal now available to attack macromolecular separation problems and clearly illustrates the complementary role of the different weapons in the arsenal.

FFF APPLICABILITY

Because the FFF family is so broad, it appears that one or more of the FFF subtechniques is potentially applicable to any soluble macromolecule (or suspendable colloid), irrespective of solvent type, presence or absence of electrical charge, random coil or globular conformation, etc. However, in order to examine systematically which of the FFF subtechniques is applicable to any particular macromolecular material, it is necessary to divide the almost infinite variety of macromolecular substances into a few broad categories. It is then possible to specify the FFF subtechniques applicable or partially applicable to each category.

For the above purposes we divide macromolecular components into four classes, as specified below.

(1) Water-soluble macromolecules (WSM) of molecular weight $M < 10^6$.

(2) Water-soluble macromolecules (WSM) with $M > 10^6$.

(3) Organic solvent-soluble macromolecules (OSM) with $M < 10^6$.

(4) Organic solvent-soluble macromolecules (OSM) with $M > 10^6$.

The four categories listed here are not intended to divide all types of macromolecules into rigid compartments. Clearly, many families of macromolecules will span across categories with little regard for either the arbitrary molecular weight cutoff at 10^6 or the solubility criterion that divides one category from another. Nonetheless, most proteins fall cleanly in category 1 while most DNAs fall in category 2. A majority of industrial polymers fall in category 3, and a special group, consisting of ultrahigh-molecular-weight polymers, falls in category 4. Thus, these categories provide a rough grouping of prominent macromolecular materials and make it possible to examine FFF applicability without reference to each of the enormous variety of important macromolecular substances.

Table I provides a summary of the major FFF subtechniques that have been found applicable to each of the four categories of macromolecules. This table is limited to the normal operating mode of FFF. Other operating modes, particularly steric and hyperlayer, are primarily applicable to larger particles, although recent work has shown that a high-speed hyperlayer technique (thermal/hyperlayer FFF) is applicable to category 4 and potentially to category 2 (ref. 12).

Below we describe each of the four subtechniques listed in Table I. We then discuss more specifically the applicability of each subtechnique to the four categories of macromolecules with emphasis on the factors controlling selectivity.

Thermal FFF

The thermal FFF subtechnique is one in which the driving force derives from a strong temperature gradient established between two highly conductive (*e.g.*, copper) bars[4,5]. The temperature drop ΔT between bars, usually 20–80°C, is responsible for

TABLE I

APPLICABILITY OF DIFFERENT FFF SUBTECHNIQUES (IN THE NORMAL OPERATING MODE) TO FOUR CLASSES OF MACROMOLECULAR SUBSTANCES: WATER-SOLUBLE MACROMOLECULES (WSM) AND ORGANIC SOLVENT-SOLUBLE MACROMOLECULES (OSM) OF MOLECULAR WEIGHT, M, EITHER LESS THAN OR GREATER THAN 10^6

× = is or should be fully applicable; + = applicable to some members of class; − = not applicable.

Subtechnique	*1* *WSM* *($M<10^6$)*	*2* *WSM* *($M>10^6$)*	*3* *OSM* *($M<10^6$)*	*4* *OSM* *($M>10^6$)*
Thermal FFF	+	+	×	×
Sedimentation FFF	−	×	−	+
Flow FFF	×	×	×	×
Electrical FFF	+	+	−	−

extremely high temperature gradients, since it is applied over a very thin gap only *ca.* 100 μm in thickness. Gradients up to *ca.* 10 000°C per centimeter are realized. Changes in the gradient are used to control retention. Commercial instrumentation has recently become available (FFFractionation, Salt Lake City, UT, U.S.A.).

The strong temperature gradients of thermal FFF give rise to a thermal diffusion effect in which components are driven along the temperature gradient, thus sideways across the channel. The driving force of thermal diffusion is particularly strong for nonpolar macromolecules in categories 3 and 4 (ref. 10). However, limited applicability has also been found for the water-soluble species in categories 1 and 2 (ref. 13).

FFF theory has shown that retention in thermal FFF is dependent upon the ratio of D_T/D, where D_T is the thermal diffusion coefficient and D is the ordinary diffusion coefficient[5]. Unfortunately, D_T is one of the most poorly characterized physicochemical properties. However, D_T values can be measured in the course of thermal FFF operation, and a large data base of D_T values has been compiled in our laboratory. As a result, the basis of polymer selectivity in thermal FFF is now fairly well understood[14].

We note that molecular weight is a property of central importance in the characterization of most industrial polymers falling in categories 3 and 4. Thermal FFF provides high selectivity with respect to polymer molecular weight. This selectivity does not originate in D_T, which has been found to be independent of molecular weight, but in D, which varies inversely with molecular weight. We note that size-exclusion chromatography (gel permeation chromatography) also separates macromolecular components on the basis of molecular weight. Somewhat surprisingly, the molecular weight sensitivity of both the FFF and chromatographic techniques originates in the same factor, the hydrodynamic radius or diffusion coefficient[14]. However, the thermal FFF subtechnique is far more selective with respect to molecular weight than is size-exclusion chromatography[10].

The thermal diffusion coefficient D_T, while free of dependence on molecular weight, is sensitive to the chemical composition of both polymer and solvent. Thus, separations can be carried out on the basis of differences in polymer composition. This holds considerable promise for the characterization of copolymers and polymer blends. A dependence of retention on solvent type is also observed, analogous to the

case of liquid chromatography, where the choice of solvent has become useful in enhancing selectivity.

Sedimentation FFF

In sedimentation FFF, the thin separation channel is wrapped around the inside circumference of a centrifuge basket such that the flow axis is everywhere perpendicular to the sedimentation force, as is generally required for FFF operation. The channel assembly can then be spun at different rotation rates in order to control retention in the system[2].

Sedimentation FFF is now the most widely used of all FFF subtechniques. There are presently two commercial instruments available (Du Pont Instruments, Wilmington, DE, U.S.A. and FFFractionation). A vast majority of the applications of sedimentation FFF are in the colloid and particle fields[15].

The application of sedimentation FFF to macromolecules is subject to a basic limitation: the driving force, proportional to molecular mass, is too weak to induce the retention of low-molecular-weight macromolecules. At the highest spin rates available, some retention begins to appear at a molecular weight of about 10^6. Above this transition value, sedimentation FFF becomes a highly selective technique, in theory applicable to most macromolecular materials having large molecular components. However, only a few macromolecular systems in category 2 have been examined. Schallinger *et al.*[16] have separated both DNA species and polyacrylamide by sedimentation FFF. Preliminary work on DNA has also been carried out in our laboratories.

In principle, sedimentation FFF is also applicable to the more massive organic solvent-soluble macromolecules in category 4. However, most sedimentation FFF instrumentation developed to date relies on a rotating seal, subject to damage by organic solvents. Consequently, sedimentation FFF has not yet been applied to this important category of macromolecular materials.

The driving force in sedimentation FFF is, as noted above, directly proportional to molecular mass. Consequently, sedimentation FFF displays a high selectivity with respect to molecular weight. Since the driving force is also dependent upon the difference between the density of the retained component and the carrier liquid (solvent), this technique also displays some density selectivity. This has been demonstrated for colloidal particles and is presumably also valid for macromolecules. The density effect can be modulated by changes in the carrier density.

Flow FFF

The subtechnique of flow FFF is implemented by using a channel having permeable walls. The wall elements are made up of porous or membrane layers. The permeable walls allow fluid to be driven into and across the channel, creating a perpendicular flow of carrier liquid superimposed on the normal axial flow of FFF. The perpendicular flow serves to drive entrained components from one wall of the channel to the other[5].

Flow FFF has the advantage of being the most universal of all FFF subtechniques and perhaps the most universal of all separation techniques. This is because all macromolecules, no matter what category they occupy, are fractionated by virtue of the fact that every imaginable species is displaced by simple flow. The strength

of the driving force is determined by the cross-flow rate, which is controlled, like other FFF driving forces, to adjust retention levels[17]. The fact that flow FFF is shown in Table I to be applicable to all four categories of macromolecules reflects the wide range of applicability of the subtechnique. In our laboratory, we have shown flow FFF to be applicable to protein aggregates, viruses, cells, and a variety of water-soluble polymers. Wahlund and Litzen[18] have recently shown that flow FFF can be applied to the fractionation of DNA and other biological macromolecules.

The principal disadvantage of flow FFF is that thin channels, meeting the rigorous uniformity requirements of FFF systems, are difficult to fabricate with permeable wall materials. Because of this, and also because of some interaction of macromolecules with membranes, the performance of flow FFF systems has not yet reached its theoretical potential. This subtechnique should become increasingly important in the future.

Selectivity in the normal mode of flow FFF is determined by differences in component diffusion coefficients which, in turn, are determined by the Stokes (or hydrodynamic) radius of the macromolecules. Since the Stokes radius is essentially a measurement of molecular size, the flow FFF subtechnique is, above all, size-selective. However, as found in size-exclusion chromatography and thermal FFF, size in a homologous class of macromolecules is merely a reflection of molecular weight; in this sense, flow FFF can be considered to display molecular-weight selectivity. The magnitude of the selectivity is about the same as that of thermal FFF, a value considerably higher than that of the best size-exclusion chromatography column.

Electrical FFF

The electrical field of electrical FFF is applied not only across the FFF channel but also across permeable membrane and porous elements that allow the electrode compartments to be isolated from the FFF channel[5]. Because of wall permeability, the system somewhat resembles that used for flow FFF. However, it has been difficult to achieve effective separations in electrical FFF systems, largely because inadequate attention has been paid to the development of the necessary technology. Earlier work in our laboratories showed that electrical FFF is applicable to proteins; applicability should extend to other charged species as well. The limitation of electrical FFF to charged components is reflected in Table I where electrical FFF is shown as applicable to only some members of the water-soluble macromolecule categories.

Selectivity in electrical FFF is based on differences in the effective electrical charge on a species or, considered in another way, it is dependent upon the ratio of electrophoretic mobility to ordinary diffusion coefficient. Thus, selectivity has some resemblance to that exhibited by electrophoresis, but the two are not identical in nature. Like electrophoresis, selectivity in electrical FFF can be modulated by pH and presumably by chemical factors that influence electrical charge.

ACKNOWLEDGEMENT

This work was supported by grant GM10851-31 from the National Institutes of Health.

REFERENCES

1 J. C. Giddings, *Sep. Sci.*, 1 (1966) 123.
2 J. C. Giddings, *Anal. Chem.*, 53 (1981) 1170A.
3 J. C. Giddings, *C&E News*, 66 (1988) 34.
4 J. C. Giddings, *Pure Appl. Chem.*, 51 (1979) 1459.
5 J. C. Giddings, M. N. Myers, K. D. Caldwell and S. R. Fisher, in D. Glick (Editor), *Methods of Biochemical Analysis*, Vol 26, Wiley, New York, 1980, pp. 79–136.
6 J. C. Giddings, *Sep. Sci. Technol.*, 19 (1984) 831.
7 J. C. Giddings, X. Chen, K.-G. Wahlund and M. N. Myers, *Anal. Chem.*, 59 (1988) 119.
8 P. Leopairat and E. W. Merrill, *J. Liq. Chromatogr.*, 1 (1978) 21.
9 J. C. Giddings and K. D. Caldwell, *Anal. Chem.*, 56 (1984) 2093.
10 J. J. Gunderson and J. C. Giddings, *Anal. Chim. Acta*, 189 (1986) 1.
11 J. C. Giddings, *Sep. Sci.*, 8 (1973) 567.
12 J. C. Giddings, S. Li, P. S. Williams and M.E. Schimpf, *Makrol. Chem. Rapid Commun.*, 9 (1988) 817.
13 J. J. Kirkland and W. W. Yau, *J. Chromatogr.*, 353 (1986) 95.
14 M. E. Schimpf and J. C. Giddings, *Macromolecules*, 20 (1987) 1561.
15 J. C. Giddings, G. Karaiskakis, K. D. Caldwell and M. N. Meyers, *J. Colloid Interface Sci.*, 92 (1983) 66.
16 L. E. Schallinger, W. W. Yau and J. J. Kirkland, *Science (Washington, D.C.)*, 225 (1984) 434.
17 K.-G. Wahlund, H. S. Winegarner, K. D. Caldwell and J. C. Giddings, *Anal. Chem.*, 58 (1986) 573.
18 K.-G. Wahlund and A. Litzen, *J. Chromatogr.*, submitted for publication.

Journal of Chromatography, 470 (1989) 337–350
Elsevier Science Publishers B.V., Amsterdam — Printed in The Netherlands

CHROMSYMP. 1600

CHARGE HETEROGENEITY OF RECOMBINANT PRO-UROKINASE AND URINARY UROKINASE, AS REVEALED BY ISOELECTRIC FOCUSING IN IMMOBILIZED pH GRADIENTS

PIER GIORGIO RIGHETTI and BARBARA BARZAGHI
Chair of Biochemistry, Faculty of Pharmacy, and Department of Biomedical Sciences and Technologies, University of Milano, Via Celoria 2, Milan 20133 (Italy)
EDOARDO SARUBBI and ADOLFO SOFFIENTINI
Merrell Dow Research Institute, Lepetit Research Centre, Via R. Lepetit 34, 21040 Gerenzano (Varese) (Italy)
and
GIOVANNI CASSANI*
Tecnogen SpA, Via Ampère 56, Milan 20131 (Italy)

SUMMARY

When analysing homogeneous preparations of recombinant pro-urokinase and urinary urokinase by isoelectric focusing (IEF) in immobilized pH gradients, an extreme charge heterogeneity was detected (at least ten major and ten minor bands in the pH range 7–10). This extensive polydispersity was not caused by different degrees of glycosylation, or by IEF artefacts, such as binding to carrier ampholytes or carbamylation by urea. A great part of this heterogeneity could be traced back to the existence of a multitude of protein molecules containing Cys residues at different oxidation levels (–SH, –S–S–, even cysteic acid). Owing to the very large number of Cys residues in pro-urokinase (24 out of a total of 411 amino acids) and to the relatively high p*I* of its native forms (p*I* 9.5–9.8; the native form is believed to contain all Cys residues as –S–S– bridges), the presence of SH or cysteic acid residues would increase the negative surface charge, as even SH groups would be extensively ionized. In pro-urokinase, part of the heterogeneity was also due to spontaneous degradation to urokinase and possibly also to cleavage into lower-molecular-mass fragments. When all these causes of heterogeneity were removed, the p*I* spectrum was reduced to only four, about equally intense, bands. The cause of this residual heterogeneity is unknown.

INTRODUCTION

Urokinase plasminogen activator (u-PA) is the factor responsible for the fibrinolytic activity of human urine. The enzyme is a serine protease that can convert, via a specific proteolytic clip, the zymogen plasminogen into the active form, plasmin, which in turn degrades the fibrin clots. For this property u-PA is widely used as

0021-9673/89/$03.50

fibrinolytic agent in thrombolytic therapy.

u-PA is a glycoprotein[1], present in human urine in two active forms: high-molecular-weight urokinase (HMW u-PA), consisting of two polypeptide chains, A and B, of 20000 and 30000 Da, respectively, connected by a disulphide bridge (also called two-chain urokinase or tcu-PA), and low-molecular-weight urokinase (LMW u-PA), of *ca.* 33000 Da, which contains the entire B chain and a short fragment (about 20 amino acids) of the A-chain. LMW u-PA is generally considered to be a degradation product, which retains catalytic activity, generated by the loss of an 18000 Da amino terminal fragments (ATF) from the A-chain of HMW u-PA. In urine the proenzyme is also present in the form of a single-chain urokinase (pro-urokinase or scu-PA[2]), which can be activated by plasmin to tcu-PA by proteolytic cleavage at the Lys-158 residue[3]. scu-PA is the most abundant form found in the culture media of different cell lines[2,4–8], and it is probably the only u-PA secreted by cells *in vivo*[9].

Although the primary structure of u-PA has been completely elucidated, some important biochemical features of the enzyme. such as glycosylation, amidation, phosphorylation and in general post-translational modifications, still require a more extensive investigation. For instance, although u-PA has been purified to homogeneity and shown to behave as a single band by sodium dodecyl sulphate polyacrylamide gel electrophoresis (SDS-PAGE), some heterogeneity has been observed by isoelectric focusing (IEF), with a variable number of bands in the pH range 8–9.6[10–13]. Similar results have also been obtained for other, related proteins, such as plasminogen[14], but to date not general explanation has been proposed.

In this work, we investigated the behaviour in IEF (both conventional and in immobilized pH gradients) of u-PA in the glycosylated and neuraminidase-treated forms and extended our study to scu-PA and to molecular fragments of u-PA. It will be shown that the charge heterogeneity of u-PA is independent of the source of u-PA (be it urinary; from cell culture supernatant or from recombinant-DNA sources).

EXPERIMENTAL

Immobiline, Repel- and Bind-Silane, Ampholines, Gel Bond PAG, the Multiphor 2 chamber, the Multitemp thermostat and the Macrodrive power supply were from LKB (Bromma, Sweden) and Pharmalytes, activated Sepharose and the electrophoresis calibration kit for low-molecular-mass (M_r) proteins were purchased from Pharmacia (Uppsala, Sweden). Acrylamide, N,N′-methylenebisacrylamide (Bis), N,N,N′,N′-tetramethylethylenediamine (TEMED), ammonium persulphate, Affi-Gel 10, sodium dodecylsulphate (SDS) and Coomassie Brilliant Blue R-250 were from Bio-Rad Labs. (Richmond, CA, U.S.A.). Dithiothreitol (DTT) and urea were from Merck (Darmstadt, F.R.G.) and 5,5′-dithiobis-2-nitrobenzoate (DTNB) was purchased from Serva (Heidelberg, F.R.G.). Iodoacetamide was from BDH (Poole, U.K.). Neuraminidase (*Clostridium perfringens*) was from Boehringer (Mannheim, F.R.G.). Commercially available, therapeutic-grade urinary u-PA was isolated from urine by Lepetit (Gerenzano, Italy). Human scu-PA was extracted from recombinant LB6 cell supernatant[15] by immunoaffinity and ion-exchange chromatography, essentially as described for A431 scu-PA[6]. LMW u-PA and ATF were purified from auto-catalytically degraded u-PA by chromatography on Sephadex G-100, as described previously[16].

Conventional isoelectric focusing (IEF)

IEF in carrier ampholyte buffers (CA) was performed in 0.5-mm thick gels, supported by a gel Bond PAG plastic film[17]. The gel had a 4%T, 4%C composition (%T = total amount of monomers; %C = grams of Bis per 100 grams of total monomers). The gels were polymerized as "empty" matrices, in the absence of CA; after two washing steps in distilled water (30 min each) they were dried and reswollen in a mixture of 2% CA in the pH range 5–10 and 8 *M* urea. In some experiments, this mixture also contained 5 m*M* DTT. The sample size was 100 μg for Coomassie Brilliant Blue and 2 μg for silver staining (in both instances in a 30-μl volume). The running conditions were 5 W limiting, with a final voltage of 1500 V, for a total of 5 h, at 10°C. Staining was with Coomassie Brilliant Blue–Cu^{2+} according to Righetti and Drysdale[18] and with silver according to Merril *et al.*[19].

Immobilized pH gradients (IPG)

IEF in IPG was performed in 4%T, 4%C, 0.5-mm thick matrices, according to Bjellqvist *et al.*[20]. After standard polymerization (1 h at 50°C)[21], the gels were washed twice in distilled water (20 min each) and then for an additional 20 min in 1% glycerol. After drying, they were reswollen in 8 *M* urea and 1% CA in the pH range 3.5–10 (in some experiments, 5 m*M* DTT was added to the reswelling mixture). Most IPG experiments were performed in the pH range 5.0–10.0; in some pH 5.0–10.5 was utilized. The recipe for the IPG pH 5–10 range was as follows: acidic dense solution (3.8 ml final volume), 143 μl of p*K* 3.6, 117 μl of p*K* 4.6, 75 μl of p*K* 6.2, 69 μl of p*K* 7.0, 57 μl of p*K* 8.5 and 32 μl of p*K* 9.3 Immobilines; basic, light solution (3.8 ml final volume), 5 μl of p*K* 3.6, 15 μl of p*K* 4.6, 8.5 μl of p*K* 6.2, 106 μl of p*K* 7.0, 79 μl of p*K* 8.5 and 69 μl of p*K* 9.3 Immobilines (for IPG recipes, see also ref. 22). The above recipe was also used for the IPG pH 5–10.5 range, except that the basic solution was titrated to pH 10.5 with a p*K* 10.3 Immobiline. The samples were applied in pockets, precast at the anodic side (same amounts and volumes as described under conventional IEF). Electrophoresis was performed for the first 4 h at 400 V, followed by overnight at 2000 V at 10°C (the initial low-voltage period is necessary to prevent sample denaturation before entry into the gel[23]).

IPG in alkaline pH ranges

For IPG in strongly alkaline ranges (pH 10–11) the gel must be supported on silanized glass plates (with Bind-Silane)[24] and must contain a pH 8.0 plateau for sample loading. For the recipe and gel handling, see ref. 25. During electrophoresis, adsorption of carbon dioxide is minimized by alkali traps (filter-paper strips impregnated with 1 *M* sodium hydroxide solution, deposited on the empty surface of the cooling block of the Multiphor II chamber) and by covering the gel surface (except in the region of the pockets for sample application) with a plastic foil (Gel Bond PAG, hydrophobic surface facing the gel). Staining is carried out with Coomassie Brilliant Blue, as very dark background results with silver staining.

SDS-PAGE

SDS-PAGE was carried out in the discontinuous system according to Laemmli[26]. The stacking gel was 5%T–4%C–125 m*M* Tris–HCl (pH 6.8)–0.1% SDS and the running gel was a 10–15%T gradient–4%C–374 m*M* Tris–HCl (pH 8.8)–0.1% SDS.

The sample and marker proteins were denatured in 50 m*M* Tris–HCl (pH 6.8), containing 2% SDS–1% DTT–6 *M* urea–30% glycerol. The denaturating solution can be kept frozen for several months, but DTT is always added at the last moment, just prior to use. Electrophoresis is carried out at a constant 300 V, until the Bromophenol Blue front begins to leach out at the anode.

SH group alkylation

Alkylation of SH groups is performed according to Crestfield *et al.*[27] at room temperature. A 500-μg amount sample is dissolved in 500 μl of 8 *M* urea–1 *M* Tris–10 m*M* EDTA and titrated to pH 8.5 with acetic acid under nitrogen and with continuous stirring. After 15 min, the solution is made 10 m*M* in DTT. After 2 h, monoiodoacetamide is added and the reaction is allowed to continue in the dark for 20 min. The reaction is terminated with an excess of 2-mercaptoethanol.

Titration of free SH groups with DTNB

A 10 m*M* solution of DTNB in 300 m*M* Tris–HCl (pH 8) was prepared in the dark just prior to use. For the assay, 100 μl of DTNB solution and 100 μl of sample solution are added to 2.8 ml of the above buffer. The sample is composed from the major isoelectric bands of u-PA, isolated from excized gel portions in an IPG gel, in amounts calculated to contain up to 10 nmol of cysteine residues (see Fig. 7). The absorbance at 410 nm is measured immediately against blank tubes. The calibration graph is constructed with standards of glutathione (0–10 nmol). The molar absorption coefficient of reduced DTNB is taken as 13600, according to Ellman[28].

RESULTS

Size homogeneity of different urokinases

When recombinant scu-PA and tcu-PA were analysed by SDS-PAGE they were found to be essentially homogeneous (Fig. 1A). The same gel also shows the position of LMW u-PA (track C) and the pattern given by ATF (track D). When the same experiment was repeated in the presence of an excess of 2-mercaptoethanol, scu-PA still exhibited a single band while tcu-PA was split into two bands, corresponding to the B-chain (30000 Da) and to the A-chain (20000 Da), respectively. The present data clearly indicate that all species isolated are free from contaminant polypeptides of different molecular mass.

Charge heterogeneity of different urokinases

However, when the above tcu-PA, purified from human urines, was analysed by IEF in IPG in the pH range 5–10, it was found to be extensively heterogeneous, exhibiting at least ten major and ten minor isoelectric bands, with p*I* values covering the pH range 7–10 (Fig. 2). This most pronounced polydispersity prompted us to study its possible causes. It is in general believed that one of the most frequent causes of charge heterogeneity is post-synthetic glycosylation of the polypeptide chains, producing a series of charge variants due to the different content of sialic acid or other charged sugars. To verify this, scu-PA was subjected to treatment with neuraminidase, and then analysed by conventional IEF. As seen in Fig. 3, the train of bands in the control (at least six major zones) is shifted to higher p*I* values, indeed suggesting

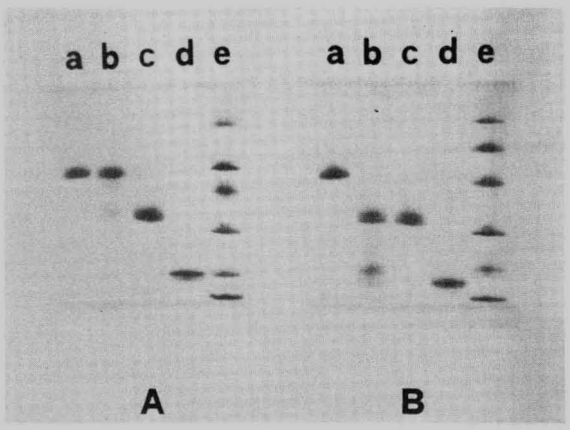

Fig. 1. Analysis of different urokinase preparations by SDS-PAGE was performed in the discontinuous system according to Laemmli[26] in a 10–15%T porosity gradient under (A) non-reducing and (B) reducing conditions. Lanes: (a) recombinant single-chain urokinase plasminogen activator (scu-PA); (b) two-chain u-PA (tcu-PA); (c) low-molecular-mass urokinase (LMW-UK); (d) amino-terminal fragment (ATF) of urokinase; (e) molecular-mass standards (Pharmacia), from top to bottom phosphorylase B (M_r 94 000), bovine serum albumin (M_r 67 000), ovalbumin (M_r 43 000), carbonic anhydrase (M_r 30 000), trypsin inhibitor (M_r 20 100) and β-lactalbumin (M_r 14 400). SDS-PAGE was performed in Phast-gel apparatus (Pharmacia). 2-Mercaptoethanol was used as reducing agent. Staining: Coomassie Brilliant Blue R-250.

the presence of sialic acid, but the heterogeneity is not reduced, although the relative band intensity seems to be altered in favour of the most alkaline components.

In a search for other possible sources of heterogeneity, we hypothesized that some of it could be produced by the presence of 8 *M* urea in the gel, as electrophoresis occurs at alkaline pH values, which could favour degradation of urea to cyanate and the subsequent carbamylation of deprotonated amino groups in proteins. However, when electrophoresis was repeated in the presence of 50% dimethyl sulphoxide, as a substitute for urea, essentially the same pattern was obtained (not shown), thus ruling out modifications due to the presence of urea.

Another possible cause of heterogeneity could be potential binding to the carrier ampholytes, admixed with the IPG gel. We therefore repeated the experiment in an IPG pH 5–10 gel in the absence of CA chemicals. As shown in Fig. 4, urokinase exhibits essentially the same polydisperse spectrum, although the bands are more diffuse, possibly owing to adsorption on the IPG matrix. This also rules out potential artefacts due to binding to the CA buffers.

In search for other possible causes of such extensive heterogeneity, we noticed that pro-urokinase contains a very large number of Cys residues (a total of 24, all of them believed to be in the form of –S–S– bridges) in the native molecule. If the fully oxidized molecule were in equilibrium with partially reduced species (containing SH groups), this could greatly contribute to the charge heterogeneity, as these groups, at the pH prevailing during IEF, would be extensively ionized to $-S^-$, thus automatically generating lower -p*I* components. Evidence for such a mechanism comes from Fig. 5; here, the same IPG gel was divided into two sections and reswollen either in the presence (left) or in the absence (right) of DTT. It is seen that "native" urokinase

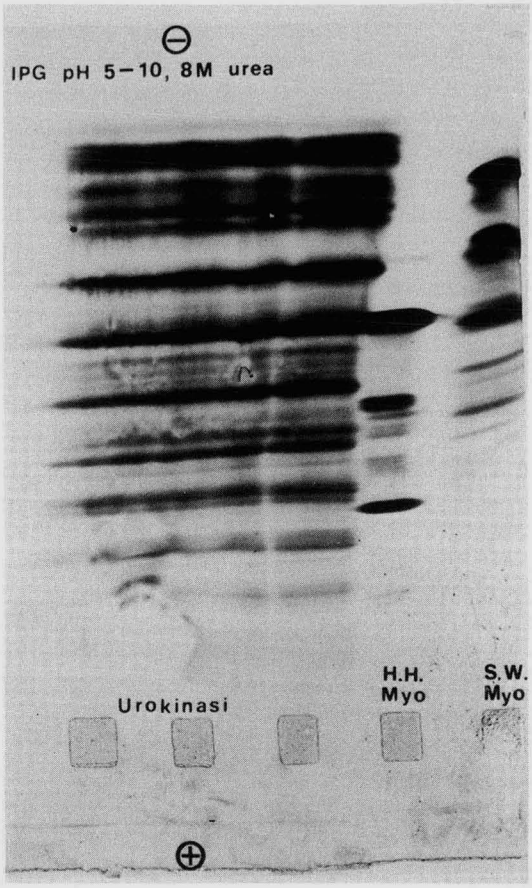

Fig. 2. Analysis of urokinase by IEF in IPG. A 4%T–4%C polyacrylamide gel was prepared, containing a pH 5–10 immobilized gradient. The gel was washed, dried and reswollen in 8 *M* urea–1% CA in the same pH 5–10 range. Samples were applied in pockets, precast at the anodic side. Electrophoresis: overnight at 2000 V, 10°C. The three urokinase lanes contained a total of 100 μg of protein and the two pH indicators were 20 μg each. HH Myo and SW Myo: horse heart and sperm whale myoglobins, respectively. Staining: Coomassie Brilliant Blue R-250 in the presence of copper sulphate.

consists of a major group of tightly packed species with high p*I* values (pH range 9.5–9.8) followed by a number of minor bands with lower p*I* values (pH 7–9). In the presence of DTT (left panel) (added also to the sample zone) the high-p*I* components almost disappear and the lower-p*I* components are strongly reinforced. Note that the major lower-p*I* components of reduced urokinase coincide, in isoelectric points, with the minor lower-p*I* species present in "native" urokinase, suggesting a precursor–product relationship. In order to prove this hypothesis, the IPG gel was used in a small-scale preparative version, by applying a single sample to an anodic trench. A lateral gel segment was stained, for detecting the band position, while leaving the remainder of the gel under voltage. By aligning the stained with the unstained gel

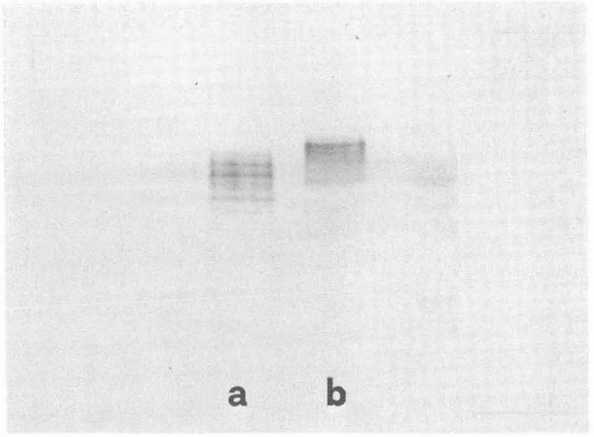

Fig. 3. Conventional IEF (in CA buffers) in the pH range 7–10 of recombinant scu-PA, (a) before and (b) after treatment with neuraminidase (from *Clostridium perfringens*). IEF was in a 1-mm thick, 6%T polyacrylamide gel, containing 6 *M* urea and 0.5% Nonidet P-40. scu-PA was incubated with neuraminidase in 50 m*M* acetate buffer (pH 5), containing 15 m*M* sodium chloride–0.01% bovine serum albumin–10 m*M* benzamidine, for 18 h at 37°C. Electrophoresis: 5 h at 1500 V, 10°C. Staining as in Fig. 2.

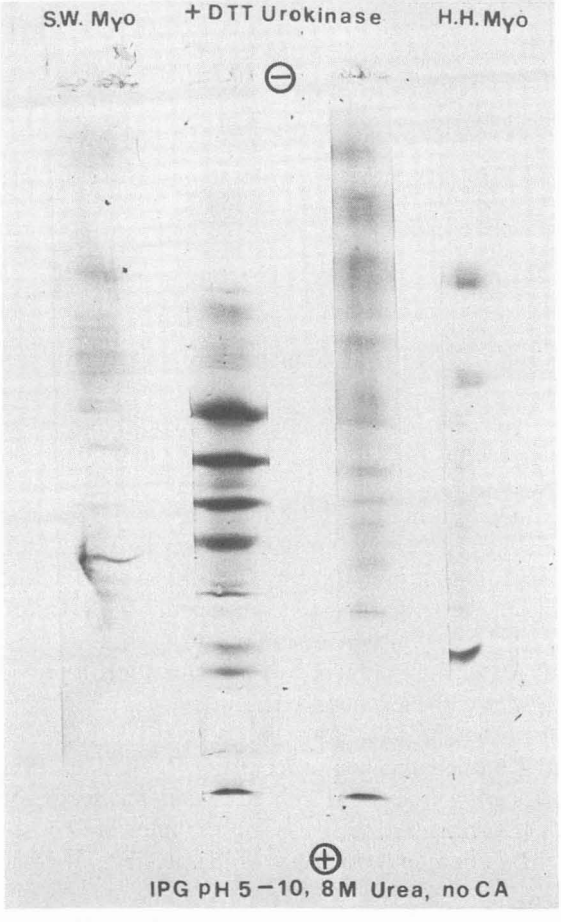

Fig. 4. IEF in IPG of urokinase. Conditions as in Fig. 2, except that the gel contained no carrier ampholytes. Of the two urokinase tracks, that on the right is in the absence and that on the left in the presence of dithiotreitol (DTT; 5 m*M* final concentration in sample and gel). p*I* markers as in Fig. 2.

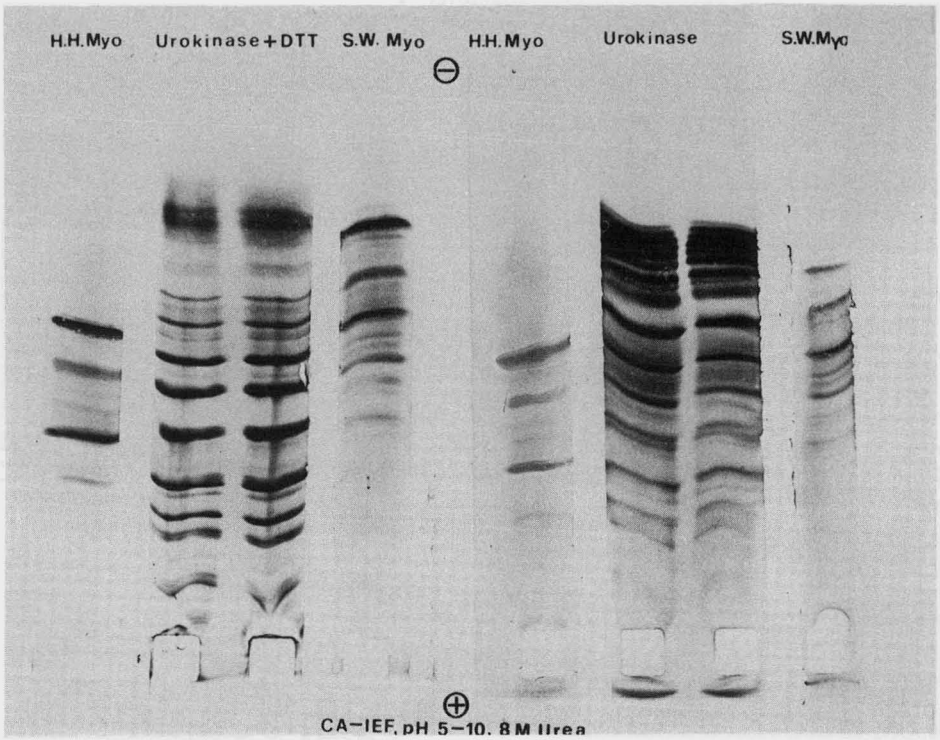

Fig. 5. IEF in IPG of urokinase in the presence (left) and in the absence (right) of reducing agents (DTT). Other conditions as in Fig. 2. Two gels were prepared; the left one was reswollen in 1% CA–8 *M* urea–5 m*M* DTT, while the right one contained the same reswelling mixture without DTT. Note the disappearance of the very alkaline urokinase bands in the DTT gel.

portions, a group of six bands (see Fig. 7) were excized, eluted and assayed for free SH groups.

As shown in Fig. 6, on a molar basis, the lower-p*I* components contain progressively higher amounts of titratable SH groups than the native high-p*I* components, in which less than 1 mol of SH per mole of protein can be evidenced. However, even the low-p*I* group (*ca.* pH 7.5) is far from exhibiting the full number of 24 SH groups, which should be present in a completely reduced pro-urokinase (see the Discussion for this phenomenon). It therefore appears that preparations of urokinase are indeed a mixture of molecules in equilibrium, with the high-p*I* components representing "native" species and the lower-p*I* species typifying conversion products with progressively broken –S–S– bridges. As this pattern is exhibited by all preparations that we analysed (scu-PA and tcu-PA), it appears to be a general phenomenon. It remains to be seen how this happens.

Some evidence for the genesis of these bands comes from Fig. 7. Here, an IPG gel containing "native" molecules (in the absence of DTT) is cut again into six major zones, as described above. These gel segments (labelled 1–6) are immediately reloaded on to two IPG gels, one in the absence and the other in the presence of DTT

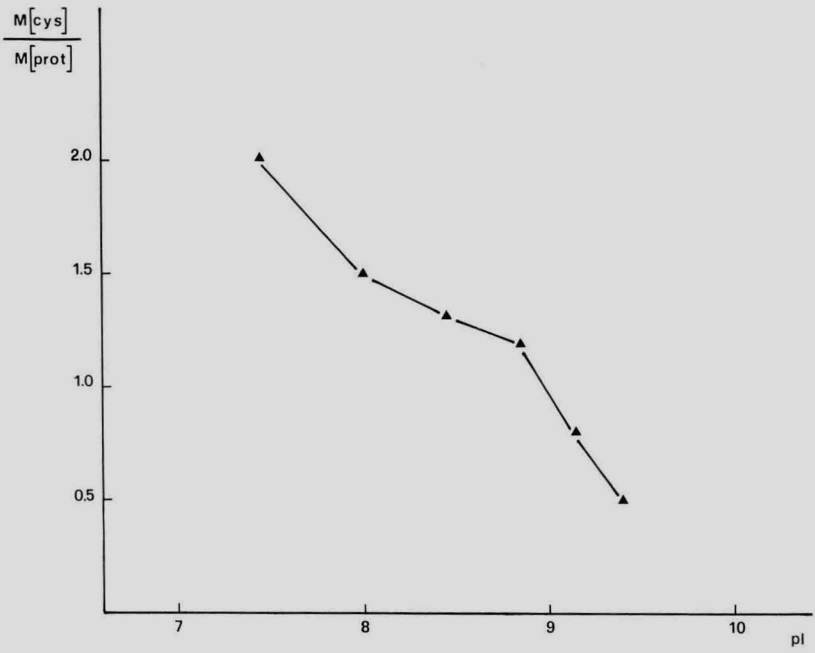

Fig. 6. Titration of free SH groups in urokinase bands of different isoelectric points. A preparative gel was run and six urokinase zones with p*I* values ranging from 7.5 to 9.5 were excized and eluted from the polyacrylamide gel (the IPG pattern with the six labelled zones is shown on the extreme right of Fig. 7). The supernatant was assayed for protein and for free SH groups, as described under Experimental, and the results were expressed in mol Cys/mol protein as a function of the observed p*I* values in the IPG gel.

at the anodic side, and re-focused as such. It is seen that, whereas the bands in the DTT gel give the usual spectrum of reduced, lower-p*I* components (four major plus a number of minor zones; *cf.*, Fig. 5), surprisingly, in the native gel (in the absence of DTT) all the components run again to the original position of the six groups of zones, while simultaneously forming the entire spectrum of lower-p*I* components, typical of the DTT gel (left panel). The group of bands labelled No. 6 appears to be the final conversion product, as its position does not change upon re-running. Hence it appears that the lower-p*I* components are formed spontaneously, possibly even in the test-tubes, on storage, and definitely during IPG (at least 30% conversion during an overnight run).

The situation is further complicated by the fact that, *e.g.*, in the case of pro-urokinase, the molecule could be spontaneously activated by proteolytic cleavage to form urokinase. We therefore analysed, side-by-side, pro-urokinase and urokinase in an IPG pH 5–10 gel in the absence of DTT. As shown in Fig. 8, pro-urokinase indeed gives a major, strongly alkaline band (p*I* 9.8), followed by a multitude of lower-p*I* components (rendered visible only by silver-staining this portion of the gel). It would appear that all these minor components are shared by preparations of urokinase, which, in fact, lacks only the strongly alkaline species. At this point, we took all the possible interconversion products and analysed them in the same gel. As shown in

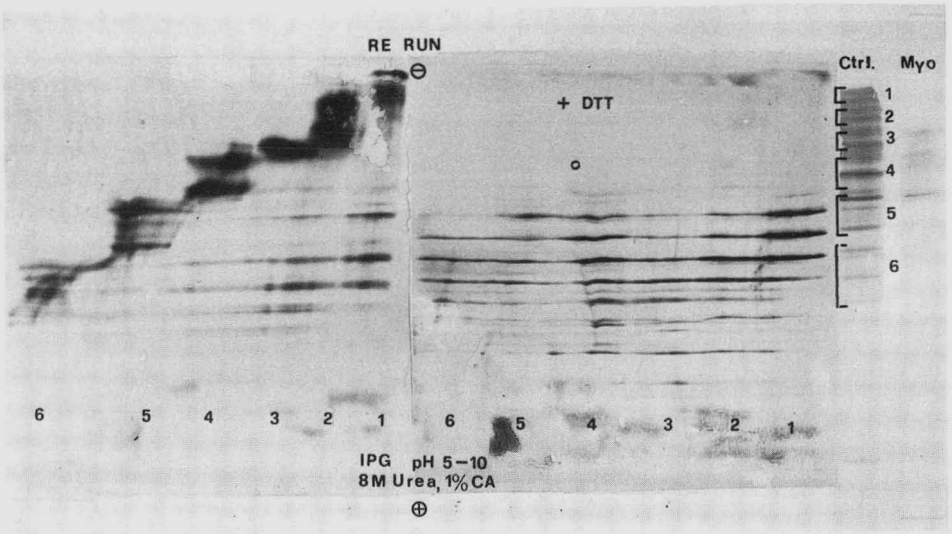

Fig. 7. IEF in IPG of urokinase. Gel and running conditions as in Fig. 2. After electrophoresis, a lateral segment was cut and stained in Coomassie Brilliant Blue, while leaving the remaining of the gel under voltage. Six major zones of urokinase were selected (see the right lane marked Ctrl., control), the bands excized and applied directly at the anodic side, on the gel surface, of two different gels, both reswollen in 8 *M* urea and 1% CA, one in the presence and the other in the absence (left portion) of DTT. These two gels were subjected to a second overnight focusing, run at 2000 V. Note that the "native" bands rerun in the left gel focus again at their original p*I* position, but forming a substantial amount of lower-p*I* components (*ca.* 30% during an 18-h run). Myo: horse heart myoglobin marker.

Fig. 9, pro-urokinase gives, as expected, a major alkaline zone, followed by a fine spectrum of lower-p*I* components. Urokinase, run in DTT, reproduces this spectrum of low-p*I* species, which is essentially identical, in position and intensity, with the bands produced by LMW u-PA. In contrast. ATF gives only two or three very faint bands, coincident with some minor bands in the LMW u-PA track. As the amount of ATF loaded is the same as that of LMW u-PA, there is clearly something missing. As the ATF fragment, on the basis of its amino acid composition, should have a very high p*I*, we repeated the run in an IPG in the pH 10–11 range. Now ATF was found to give two intense bands, the major one with a p*I* of *ca.* 10.4 and the minor one of *ca.* 10.2; however, owing to the very poor stainability of these alkaline bands, they could be revealed only by visual inspection and could not be reproduced photographically.

DISCUSSION

These studies reveal an often overlooked source of charge heterogeneity for protein molecules, *viz.*, coexistence among species in the SH, –S–S– and SO_3^{2-} states. This equilibrium could remain undetected in most instances, as two thirds of the known proteins have isoelectric points falling in the acidic portion of the pH scale. Given the mildly alkaline p*K* of the SH group of Cys (p*K* = 8.3), the presence of an SH rather than an –S–S– group would remain unnoticed in acidic proteins, as neither

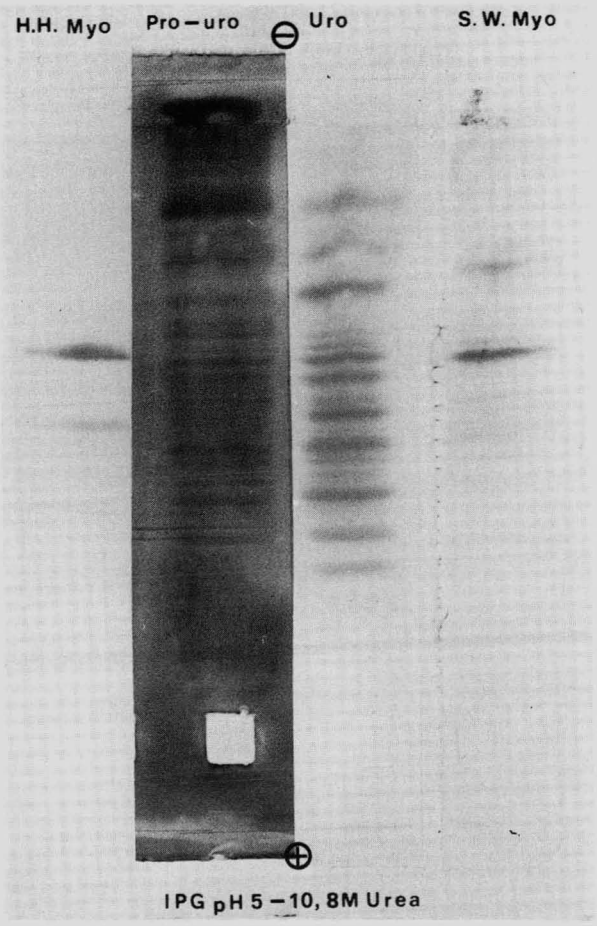

Fig. 8. IEF in IPG of pro-urokinase (pro-uro) and of urokinase (uro). Conditions as in Fig. 2. Owing to the small amount present, the pro-uro track was stained with silver, while the others were dyed with Coomassie Brilliant Blue. Note the strongly alkaline major band in the pro-uro preparation.

would contribute to the surface charge. However, in urokinase-like molecules, owing to the high isoelectric point of the "native" forms and to the presence of an unusually large number of Cys (24 out of a total of 411 amino acid residues), an equilibrium between SH and –S–S– states would be immediately visible by producing a series of charge-altered species. For example, the rupture of any single –S–S– bridge, with the formation of two SH groups, would produce species with a net increment of *ca.* two negative charges because at the high p*I* of the "native" protein molecules (p*I* 9.8), such groups would be extensively ionized. It is a fact that the high-p*I* species were found to have almost no titratable SH groups (less than 1 mol per mole of protein), in agreement with literature data, whereas the lower-p*I* components had a larger number of available SH groups. It could be asked, however, why this number (see Fig. 6) is much lower than the theoretically expected number of 24 SH groups per mole of

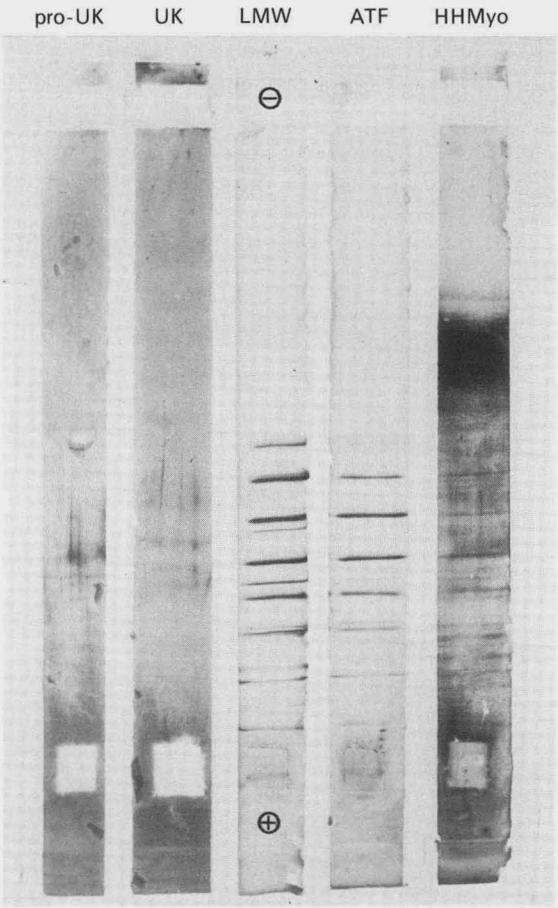

Fig. 9. IEF in IPG of pro-urokinase (pro-UK), urokinase (UK), low-molecular-weight urokinase (LMW) and amino-terminal-fragment (ATF). HH Myo: horse heart myoglobin. Conditions as in Fig. 2, except that all tracks were stained with silver. The gel was reswollen in 8 *M* urea–1% CA–5 m*M* DTT.

protein. The answer could be that at high pH values, in the presence of atmospheric oxygen and under an electric field (the anode is a strongly oxidizing compartment), oxidation of Cys could proceed to an irriversible state, *i.e.*, cysteic acid. From the point of view of charge, high-p*I* molecules carrying a free SH group or its fully oxidized cysteic acid derivative should be indistinguishable, as both would carry a net negative charge. However, titration with Ellman reagent would reveal only the former and ignore Cys residues transformed to cysteic acid. Indeed, this phenomenon was reported so long ago that is has probably been forgotten. Thus, as early as 1971, Jacobs[29,30] first reported the partial modification of Cys and Met to cysteic acid and methionine sulphoxide, upon prolonged IEF, in bovine ribonuclease (also an alkaline protein). These oxidation phenomena could be largely suppressed by removal of oxygen from the IEF column (at that time most IEF experiments were run in a vertical column in a sucrose density gradient) and by addition of antioxidants, such as thiodiglycol and ascorbic acid. With the advent of open-face IEF gels, both of these

remedies were abandoned as impractical (thiol groups are inhibitors of gel polymerization). However, with IPG technology, such remedies can easily be exploited again, as IPG gels are routinely washed and dried and can be reswollen in the solvent of choice (including any desired reducing agent).

Another possible source of heterogeneity comes from the nature of the protein itself. Pro-urokinase can be spontaneously cleaved with the formation of urokinase, which can further split into LMW u-PA and ATF. The former has a p*I* spectrum similar to that of urokinase. while the latter produces two major strongly alkaline bands ($I > 10$) and only a few, very faint zones in the pH 7–8 region. However, it is surprising that, under strongly reducing conditions (addition of DTT), one can dramatically reduce the enormous p*I* spectrum (ten major and at least 10 minor p*I* components) without obtaining a single p*I* band. The best that can be achieved, in fact, is the reduction of this multiple spectrum to a set of four bands of about equal intensity. Having ruled out different extents of glycosylation, the other possible cause of this residual heterogeneity would be the existence in the molecule of residues in the Asp–Asn or Glu–Gln states. Further work is needed to elucidate these more elusive aspects. It is nevertheless hoped that this work will be of help in understanding the enormous complexity of urokinase-type molecules, when analysed by surface-charge-dependent methods, and that it will offer some guidelines to scientists purifying recombinant-DNA products and having to meet the stringent requirements of FDA regulations.

ADDED NOTE

After this paper had been accepted, on continuing our studies on IPG matrices, we have now obtained proof that alkaline IPG ranges indeed have a strong oxidizing power. This residual oxidizing power is typical of IPG matrices, and remains even on prolonged washing of the gel and electrophoretic removal of any residual persulphate. Thus, considering that native urokinase molecules contain essentially only cystine residues, the only possibility left is that their further oxidation produces cysteic acid. This is in agreement with our hypothesis and with the experimental evidence given (Fig. 6) that the low-p*I* species exhibited only a modest increment in free, titratable SH groups.

ACKNOWLEDGEMENT

This work was supported in part by a grant from the Italian Space Agency, Progetto Biomedicina Spaziale.

REFERENCES

1 W. L. McLellan, D. Vetterlein and R. Roblin, *FEBS Lett.*, 115 (1980) 181–184.
2 D. C. Stump, M. Thienpont and D. Collen, *J. Biol. Chem.*, 261 (1986) 1267–1273.
3 S. Kasai, H. Arimura, M. Nishida and T. Suyama, *J. Biol. Chem.*, 260 (1985) 12382–12389.
4 V. Gurewich, R. Pannell, S. Louie, P. Kelley, R. L. Suddith and R. Greenlee, *J. Clin. Invest.*, 73 (1985) 1731–1739.
5 D. Stump, H. R. Lijnen and D. Collen, *J. Biol. Chem.*, 261 (1986) 1274–1378.
6 A. Corti, M. L. Nolli, A. Soffientini and G. Cassani, *Thromb. Haemostas.*, 56 (1986) 219–224.

7 L. Skriver, L. S. Nielsen, R. Stephen and K. Dano, *Eur. J. Biochem.*, 124 (1982) 409–412.
8 J. D. Vassali, J. M. Dayer, A. Wohlwend and D. Belin, *J. Exp. Med.*, 159 (1984) 1653–1668.
9 V. Kielberg, P. A. Andreasen, J. Grondhal-Hansen, L. S. Nielsen, L. Skiver and K. Dano, *FEBS Lett.*, 182 (1985) 441–445.
10 N. Ogawa, H. Yamamoto, T. Katamine and H, Tajima, *Thromb. Diath. Haemorrh.*, 34 (1975) 194–209.
11 M. E. Soberano, E. B. Ong, A. J. Johnson, M. Levy and G. Schoellman, *Biochim. Biophys. Acta*, 445 (1976) 763–773.
12 M. Nobuhara, M. Sakamachi, H. Ohnishi and Y. Suzuki, *J. Biochem.*, 90 (1981) 225–232.
13 J. Schaller, H. Nick, E. E. Rickli, D. Gillessen, W. Lergier and R. O. Studer, *FEBS Lett.*, 179 (1982) 251–257.
14 L. Summaria, L. Arzadon, P. Bernabe and K. C. Robbins, *J. Biol. Chem.*, 247 (1972) 4691–4702.
15 M. L. Nolli, E. Sarubbi, A. Corti, F. Robbiati, A. Soffientini, F. Parenti, F. Blasi and G. Cassani, *Fibrinolysis*, 3 (1989) in press.
16 M. P. Stoppelli, A. Corti, A. Soffientini, G. Cassani, F. Blasi and R. K. Assoian, *Proc. Natl. Acad. Sci. U.S.A.*, 82 (1985) 4939–4943.
17 P. G. Righetti, *Isoelectric Focusing: Theory, Methodology and Applications*, Elsevier, Amsterdam, 1983.
18 P. G. Righetti and J. W. Drysdale, *J. Chromatogr.*, 98 (1974) 271–321.
19 C. R. Merril, D. Goldman and M. L. van Keuren, *Electrophoresis*, 3 (1982) 17–23.
20 B. Bjellqvist, K. Ek, P. G. Righetti, E. Gianazza, E. Görg, W. Postel and R. Westermeier, *J. Biochem. Biophys. Methods*, 6 (1982) 317–339.
21 P. G. Righetti, K. Ek and B. Bjellqvist, *J. Chromatogr.*, 291 (1984) 31–42.
22 E. Gianazza, S. Astrua-Testori and P. G. Righetti, *Electrophoresis*, 9 (1985) 113–117.
23 P. G. Righetti, M. Chiari and C. Gelfi, *Electrophoresis*, 9 (1988) 65–73.
24 A. Bosisio, C. Loeherlein, R. S. Snyder and P. G. Righetti, *J. Chromatogr.*, 189 (1980) 317–330.
25 C. Gelfi, M. L. Bossi, B. Bjellqvist and P. G. Righetti, *J. Biochem. Biophys. Methods*, 15 (1987) 41–48.
26 U. K. Laemmli, *Nature (London)*, 227 (1970) 680–685.
27 L. Crestfield, J. Moore and S. Stein, *J. Biol. Chem.*, 238 (1963) 622–630.
28 G. L. Ellman, *Arch. Biochem. Biophys.*, 82 (1959) 70–77.
29 S. Jacobs, *Protides Biol. Fluids Proc. Colloq.*, 19 (1971) 499–502.
30 S. Jacobs, *Analyst (London)*, 98 (1973) 25–33.

Journal of Chromatography, 470 (1989) 251–367
Elsevier Science Publishers B.V., Amsterdam — Printed in The Netherlands

CHROMSYMP. 1586

HAS IMMUNOBLOTTING REPLACED ELECTROIMMUNOPRECIPITATION?

EXAMPLES FROM THE ANALYSIS OF AUTOANTIGENS AND TRANSGLUTAMINASE-INDUCED POLYMERS OF THE HUMAN ERYTHROCYTE MEMBRANE

OLE J. BJERRUM*
ImmunoTechnology, Novo Industri A/S, DK-2880 Bagsvaerd (Denmark)
and
NIELS H. H. HEEGAARD
The Protein Laboratory, University of Copenhagen, Sigurdsgade 34, DK-2200 Copenhagen N (Denmark)

SUMMARY

The virtues and drawbacks of immunoblotting and electroimmunoprecipitation in the characterization of macromolecules in crude mixtures are presented. Interactions between autoantibodies and human erythrocyte membrane proteins were studied by means of crossed-affinoimmunoelectrophoresis with autologous immunoglobulins incorporated into the first dimension gel and by immunoblotting of sodium dodecyl sulphate-polyacrylamide gel electrophoresis separated erythrocyte membrane proteins with autologous immunoglobulins as primary antibodies. Substrates for transglutaminase in calcium-activated human erythrocyte membranes were examined by immunoelectrophoretic and immunoblotting methods. The experiments concerning autoantibodies complemented each other and showed that epitopes on Band 3 protein, spectrin and ankyrin are recognized by circulating immunoglobulin autoantibodies in normal individuals. The polymer experiments showed the presence of spectrin, ankyrin, Band 3, Band 4.1, glucose transporter, actin and haemoglobin epitopes in the polymer (M_r $3 \cdot 10^6$–$5 \cdot 10^6$). It is concluded that the two techniques complement each other. The most evident advantage of immunoblotting is its sensitivity and applicability while electroimmunoprecipitation in some instances allows an easier identification of distinct protein species and still has a rôle for quantification and certain monitoring purposes.

INTRODUCTION

In the immunochemical analysis of proteins the replacement of immunodiffusion procedures[1,2] with the rocket[3,4] and crossed-immunoelectrophoretic[5,6] techniques represented a significant step forward. Their appearance introduced the era of immunoelectrophoretic procedures, where electrophoresis and detection based on

0021-9673/89/$03.50

precipitation in agarose are the common denominators. Through numerous modifications and combinations of the basic procedures, techniques like the fused-rocket immunoelectrophoresis and tandem and intermediate-gel crossed-immunoelectrophoresis, specific monitoring of chromatographic procedures, characterization of crude mixtures of macromolecules in solution and quantification of both antigens and antibodies can be accomplished[7]. The reactivity and estimation of affinity constants of non-precipitating antibodies and other ligands can be achieved with the crossed-affinoimmunoelectrophoretic procedures[8,9], and it is also possible to characterize microheterogeneity of glycoproteins[7,10] and to identify amphiphilic molecules[7,11,12]. Combinations of a second-dimension immunoelectrophoresis with separations by isoelectric focusing or sodium dodecyl sulphate-polyacrylamide gel electrophoresis (SDS-PAGE) have also been used[15,16]. The antigen characteristics that can be determined by such means are summarized in Table I.

As a solid-phase hybrid between electroimmunoprecipitation and enzyme-linked immunosorbent techniques, the immunoblotting procedure[34] combines the high resolving powers of different analytical separation methods with the specificity of immunodetection. As for the immunoelectrophoretic techniques, many modifications of the basic principle have emerged[14,19,35–37]. Blotting can be performed in many types of separations and in principle all ligand–acceptor systems can be utilized for visualization. The technique allows a very sensitive characterization of molecules in

TABLE I

FEASIBILITY OF IMMUNOBLOTTING *VERSUS* CROSSED-IMMUNOELECTROPHORETIC METHODS FOR DETERMINING VARIOUS SELECTED CHARACTERISTICS OF ANTIGENS IN CRUDE MIXTURES

Abbreviations: IB = immunoblotting; CIE = crossed-immunoelectrophoresis; t.s. = this study; + = feasible; − = not feasible; (+) = feasible in special cases.

Feature	*Method*		*References*	
	IB	*CIE*	*IB*	*CIE*
Amino acid sequence	+	−	13	−
Size, quaternary structure	+	(+)	14	15
Degradation	+	+	14	17
Charge, p*I*	+	+	18	7
Glycosylation (microheterogeneity)	+	+	19	7
Glycolipids	+	(+)	20	21
Enzymatic activity	(+)	+	22	7
Amphiphilicity	(+)	+	23	7
Membrane topography	+	+	24	25
Protein–protein interaction	+	(+)	t.s.	t.s.
Ligand binding (receptor, transporter)	+	+	26	27
Substrate identification	+	−	28	−
Cell binding	+	−	19	−
Complex formation	+	+	t.s.	t.s.
Derivatization	+	−	29	−
Epitope type (denaturation)	+	(+)	30	31
Epitope mapping	+	−	32	−
Quantification	(+)	+	33	7

complex mixtures[14]. It is useful for antibody characterization, irrespective of the precipitating abilities of the antibody, and it has also been employed in micro-preparative work[38,39]. However, the technique is not yet optimally suited for quantifying purposes. The relative advantages of the two techniques in the determination of selected protein characteristics are listed in Table I.

As a model system, the study of the relationship between ageing phenomena and human erythrocyte membrane proteins illustrates the advantages and drawbacks of these two approaches to the immunochemical characterization of crude antigen preparations. Thus, autoantigenic determinants on the erythrocyte membrane[40] and on the membrane polymer, formed in response to an increase in intracellular Ca^{2+} (refs. 41 and 42), are characterized.

MATERIALS AND METHODS

Proteins and reagents

Human albumin, human transferrin and Ionophore A23187 were obtained from Calbiochem. Behring Corp. (San Diego, CA, U.S.A.), Triton X-100 [polyoxyethylene (9-10) *p-tert.*-octylphenol] scintillation grade from BDH (Poole, Dorset, U.K.), Lubrol PX [polyoxyethylene (10) palmitoyl-stearoyl ester], iodoacetamide, dithiothreitol, phenylmethylsulphonyl fluoride, 3-amino-9-ethylcarbazole, 5-bromo-4-chloro-3-indolyl phosphate and Nitroblue tetrazolium from Sigma (St. Louis, MO, U.S.A.), Amidoblack, Pyronin G and Tween 20 (polyoxyethylene sorbitan ester) from Merck, (Darmstadt, F.R.G.), SDS from Aldrich-Chemie (Steinheim, F.R.G.), aprotinin from Bayer (Leverkusen, F.R.G.), acrylamide and bisacrylamide from Bio-Rad (Richmond, CA, U.S.A.), agarose from FMC Bio Products (Rockland, ME, U.S.A.) (Type LF) and Litex (Copenhagen, Denmark) (Types HSA and HSB). Pepstatin was obtained through courtesy of the United States/Japan Cooperative Cancer Research Program. Stock solutions of the ionophore (5 m*M*) and pepstatin (200 m*M*) were prepared in dimethyl sulphoxide. Nitrocellulose sheets (HAWP, 304 Fo, 0.45 μm) were from Millipore (Bedford, MA, U.S.A.); pore size 0.22 μm was from Schleicher & Schuell (Dassel, F.R.G.); Sepharose 4B and protein A–Sepharose CL4B were from Pharmacia (Uppsala, Sweden) and divinyl sulphone-activated agarose (Minileak medium) was from Kem-En-Tec (Copenhagen, Denmark).

Erythrocyte membranes and lysate

Human erythrocytes were prepared as described[40,42] in a buffer containing 100 m*M* KCl, 60 m*M* NaCl, 10 m*M* glucose and 5 m*M* Tris–HCl (pH 7.4). For the calcium-loading experiments, the cells were suspended at a haematocrit value of 20% and incubated with Ionophore A 23187 at a final concentration of 20 μM. After 15 min, either $CaCl_2$ or $MgCl_2$ was added to a final concentration of 2 m*M*. The cell suspension was then incubated at 37°C for 3 h. Red blood cells were pretreated with 1 m*M* pepstatin by adding the inhibitor to the suspended cells 30 min before addition of ionophore. After addition of Na_2EDTA to a final concentration of 5 m*M*, the cells were washed in the above-mentioned buffer without Ca^{2+}. This wash and the following step were performed at 5°C. Lysis of the cells was performed 20 min after the addition of EDTA by diluting 10 times in 5 m*M* phosphate buffer pH 8, containing 0.5 m*M* phenylmethylsulphonyl fluoride and 1 m*M* iodoacetamide. Membranes were

then isolated according to Dodge *et al.*[43] and were kept frozen at −20°C at a protein concentration of 5 mg/ml, as determined spectrophotometrically at 280 nm[42].

Isolation of polymers

High-molecular-weight material from calcium-loaded erythrocytes, stripped for S–S linked or non-covalently bound proteins, was isolated by means of sucrose gradient centrifugation, as previously described[42]. Isolation of polymers was also performed by chromatography on Sepharose 4B. A 1-mg amount of membrane protein was solubilized in 2% (w/v) SDS in the presence of 2.5 m*M* EDTA and 40 m*M* dithiothreitol and separated at 4°C on a 100 cm × 0.9 cm column (volume, 78 ml) equilibrated with 0.01 *M* potassium phosphate buffer (pH 7.4), 0.1% (w/v) SDS and 1 m*M* EDTA. Fractions of 1.4 ml were collected every 20 min.

Antibodies

The immunoglobulin (IgG) fraction of human plasma was obtained by means of Protein A chromatography followed by dialysis against electrophoresis buffer, as described in ref. 40. The final concentration of IgG was 5–10 mg/ml.

Swine antibodies against rabbit immunoglobulin, peroxidase-conjugated (P 217) or alkaline-phosphatase-conjugated (D 306), rabbit antibodies against human albumin (A 119), human transferrin (A 061), human haemoglobin (A 118) and human erythrocyte membranes (A 104) and alkaline phosphatase-conjugated rabbit antibodies against human IgG (D 336) were obtained from Dakopatts (Copenhagen, Denmark).

The following rabbit antisera against individual erythrocyte membrane proteins were generous gifts: anti-glycophorin [En(a-)absorbed] from C. G. Gahmberg, Helsinki University; anti-band 4.1 from S. E. Lux, Children's Hospital Medical Center, Boston; anti-actin (Band 5) from R. Hynes, Massachusetts Institute of Technology; anti-glucose transporter (Band 4.5) from M. Kasahara and P. Hinkle, Cornell University and anti-band (4.1 + 4.2) from V. T. Marchesi, Yale University. The anti-human haemoglobin antibody was absorbed with completely white ghosts, prepared according to ref. 44. The antibody solution (0.1 ml) was absorbed with 12 mg ghost protein [suspended in 1.32 ml 0.66% (w/v) SDS] overnight at 4°C, followed by centrifugation (35 000 g_{av} for 1 h). The treatment with SDS exposed hidden epitopes of the native proteins, which otherwise were recognized by the unabsorbed antibody on the blot[14]. This incubation time and centrifugation were used for the subsequent absorptions as well.

Immunoabsorption with isolated human erythrocyte membrane polymer (150 μg/ml) was performed by adding 0.6 ml and 0.2 ml polymer per 0.1 ml of the anti-ghost antibody (A104) and the anti-band (4.1 + 4.2) antiserum, respectively.

The antibodies described below were raised in rabbits. For each antigen at least two animals were immunized, using the immunization procedure and schedule recommended by Harboe and Ingild[45]. The early bleedings (6–12 weeks) were found to be most suitable for immunoblotting, whereas the later bleedings were the best for immunoprecipitation. The immunoglobulin fraction (about one-third of the serum volume) was dissolved in 100 m*M* NaCl, containing 15 m*M* NaN_3, with 300 kallikrein units of aprotinin added per ml.

Anti-spectrin antibodies (Anti-band 1 and Anti-band 2). Immunoprecipitates

were used as immunogens[46]. These were cut out from the agarose gels of a line-immunoelectrophoresis of EDTA-extractable human erythrocyte membrane proteins[47], using a polyspecific rabbit anti-ghost antibody. During the electro-immunoprecipitation, the spectrins were partially degraded by plasmin present in the antibody preparation[48]. The specificity of the antibodies was ensured by absorption with spectrin-depleted erythrocyte membranes, which had been repeatedly washed with phosphate buffer, pH 11 and with 6 *M* urea[12,49]. Finally, it was found necessary to absorb with small amounts of washed normal ghosts too small to cause an appreciable reduction in the anti-spectrin titre.

Anti-ankyrin antibody (Anti-band 2.1). The ankyrin-specific immunoprecipitate was excised from a crossed-immunoelectrophoresis of human erythrocyte membrane proteins, solubilized and separated in the presence of 1% (w/v) Berol EMU-043 in Tris–glycine buffer, (pH 8.7)[12]. Under these conditions, the ankyrin precipitate appears in the gel free from other precipitates[12]. Before excision the plates were washed in 100 m*M* NaCl for 20 min and pressed with filter-paper three times. Each rabbit was immunized with the material, obtained from two crossed-immuno-electrophoresis plates, loaded with 40 μg of protein. It was not necessary to absorb this antiserum.

Anti-glycophorin antibody. This was raised against a glycophorin preparation, obtained by the procedure of Marchesi and Andrews[50]. The specificity of the antibody was assured by absorption with EDTA-extracted erythrocyte membrane proteins. Finally absorption with a small amount of washed ghosts was performed, as mentioned for spectrin.

Anti-band 3 protein antibody. That was obtained by immunization with the proteins eluted from the Band 3 region, following SDS-PAGE of erythrocyte ghosts[51]. The purified antibody, which had an equally high titre against Band 3 protein and glycophorin[15], was sequentially absorbed with intact erythrocytes (1 ml compacted erythrocytes per ml antibody solution[48]), a small amount of purified glycophorin and finally with EDTA-extractable membrane proteins[47]. For immunoblotting the two last steps were replaced by absorption with erythrocyte membrane proteins extractable with 6 *M* urea[49]. Before the absorption took place, the membrane proteins were bound to a sheet of nitrocellulose.

Electrophoretic methods

SDS-PAGE was carried out in 1.5 mm thick slab gels (18 cm × 16 cm, Protean apparatus, Bio-Rad, Richmond, CA, U.S.A.). Two gel systems were employed: 5% (w/v) gels with 2.6% cross-linking (bis), prepared according to the method of Steck and Yu[52], and a composite polyacrylamide–agarose gel, consisting of 2% (w/v) polyacrylamide with 5% cross-linking (bis) and 0.5% (w/v) agarose (Type HSB). This gel was cast according to the methods of Peacock and Dingman[53] with 0.2% (w/v) SDS, using the buffer and catalyst formulation given by Steck[54]. The lower 5 cm of the gel consisted of 2% (w/v) HSB agarose. Application slits were made with a specially designed comb, forming six slits 0.8 cm wide. Each tooth could be removed separately to avoid cracks in the gel because of the low gel strength. Gels overlaid with electrophoresis buffer were left to stand overnight before use. Samples (15 μl) of membrane proteins (125 μg) were applied after solubilization in 2% SDS and 40 m*M* dithiothreitol (15 min, 56°C). Electrophoresis at a controlled buffer temperature of

12°C was performed, applying 40 mA per gel side. The electrophoresis was terminated when the tracking dye pyronin had migrated 7.2 cm.

Definitions and procedures for fused-rocket, line and crossed-immunoelectrophoresis, crossed-immunoelectrophoresis with an intermediate gel and crossed-immunoelectrophoresis with interaction in first dimension electrophoresis are given by Bjerrum and Bøg-Hansen[46]. The 1% (w/v) agarose gels contained 0.1 or 0.5% (v/v) of Triton X-100. Solubilization of erythrocyte membrane to a protein concentration of 2 mg/ml was performed as described in ref. 12. Staining for esterase was performed according to ref. 55.

A combination of SDS polyacrylamide (5%, w/v) and agarose (1%, w/v) crossed-immunoelectrophoresis was carried out as described by Bjerrum *et al.*[12,16]. SDS-PAGE was performed as described above. After electrophoresis, the polyacrylamide slab was trimmed to a width of 0.75 cm and was washed for 15 min at 22°C in a buffer containing 38 m*M* Tris, 100 m*M* glycine (pH 8.7) and 1% (w/v) Lubrol PX. The slice was then placed 2 cm above the cathodic edge of the 10 cm × 7 cm plate used for crossed-immunoelectrophoresis, on top of a 2 mm thick and 4 cm wide agarose layer, which contained 3.5% (w/v) of Lubrol PX. The two layers were then sealed by application of a few drops of warm agarose (with 2%, w/v, Lubrol PX) at the cathodic side. The antibody-containing agarose with 2% (w/v) Lubrol PX was cast as a 6 cm wide and 1.5 mm thick layer on the anodic side of the plate. To spare costly antibodies, they were applied in smaller "windows", corresponding to the expected appearance of the corresponding antigens of the SDS gel. Electrophoresis was carried out at 2 V/cm for 16 h, using the Tris–glycine buffer of pH 8.7. The polyacrylamide gel was removed prior to pressing, washing and staining of the agarose.

For immunoblotting, the procedure originally described by Towbin *et al.*[34] was followed, using the modifications of Heegaard and Bjerrum[56]. For the polymer analysis, electrotransfer to nitrocellulose in a buffer tank was performed[56]. The positions of the lanes on the nitrocellulose sheet were indicated by the dye Pyronin G, which was added to the slits at the start and the end of the electrophoresis. The amount of protein transferred was visualized by Amidoblack staining[56].

Blocking was performed at room temperature by incubation in 40 ml of washing buffer (50 m*M* Tris–HCl, 150 m*M* NaCl and 5 m*M* NaN_3, pH 10.2), containing 2% (v/v) Tween 20 for 2 min giving rise to a completely white background[56]. After washing with peroxidase staining buffer (50 m*M* acetate buffer, pH 5.5), incubation with the peroxidase-conjugated swine anti-rabbit antibody preparation (1 μl/ml) took place for 2 h with gentle shaking. Aminocarbazole was used for peroxidase staining[56].

For the autoantigen experiments, the semi-dry electroblotting procedure was employed[40]. After electrotransfer, the blots were washed and probed with different concentrations of the Protein A-purified autologous immunoglobulin fractions (5–10 mg/ml) or rabbit anti-erythrocyte membrane protein antibodies diluted (1:2000) in washing buffer (pH 10.2)[56]. Colloidal gold was used for general protein staining[56]. Bound human or rabbit IgG was visualized after incubations with alkaline phosphatase-conjugated rabbit anti-human IgG or swine anti-rabbit immunoglobulin antibodies, respectively using Nitroblue tetrazolium and 5-bromo-4-chloro-3-indolyl phosphate as the substrate[40].

RESULTS

Identification of autoantigens

Crossed immunoelectrophoresis was employed for the study of possible autoantibodies directed against erythrocyte membrane proteins, which might be responsible for the removal of aged erythrocytes[40]. With a polyspecific rabbit anti-ghost antibody preparation, the reference precipitation pattern of erythrocyte membrane proteins, solubilized in non-ionic detergent, shown in Fig. 1A, was established[12]. A modification of the technique, where a free ligand is present in the first-dimension electrophoresis, can reveal interactions with high sensitivity[9,57]. Binding is revealed as migrational differences of the interacting protein(s), measured as the position of the precipitate in question relative to an internal marker protein. The marker in this case is albumin, which has been added to the membrane preparation and which is precipitated by anti-albumin antibodies present in the anti-erythrocyte membrane antibody preparation.

Fig. 1 shows that incorporation of Protein A-purified autologous immunoglobulin in increasing amounts in the first dimension selectively affects the migration of the cytoskeletal proteins ankyrin (2.1), spectrin (1, 2) and the integral membrane protein band 3[7,10,57]. The shifts in mobility are likely to be due to binding of almost non-migrating immunoglobulin molecules in the first dimension, while glycophorin

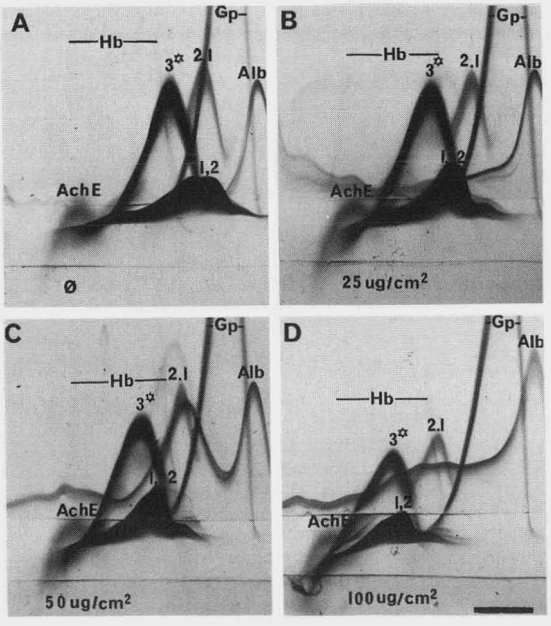

Fig. 1. Crossed-immunoelectrophoresis of Triton X-100-solubilized human erythrocyte membrane proteins with increasing amounts of autologous Protein A-purified immunoglobulin fraction of serum in a volume of 1 ml, incorporated into the first-dimension gels of B, C and D. A is the reference. The anti-ghost antibody content of the second dimension gel was 6 μl/cm^2. The following precipitates are indicated: 1 and 2 (spectrin), 2.1 (ankyrin), 3* (Band 3 protein complex), Gp (glycophorin), Alb (albumin), AchE (acetylcholinesterase, separately stained[52]), and Hb (haemoglobin)[12]. The albumin precipitate shows various degrees of tailing due to the presence of albumin in the Protein A-eluate. Bar = 1 cm.

(Gp), acetylcholinesterase (AchE) and haemoglobin (Hb) are unaffected.

A comparable activity was present in an autologous IgG preparation, purified by means of immunosorbent chromatography of the Protein A eluate on columns with immobilized rabbit anti-human IgG[40].

The presence of autoantibodies can also be studied by means of immunoblotting procedures[19,33,35,36,58]. Fig. 2 shows the outcome of an immunoblot of SDS-solubilized and dithiothreitol-reduced erythrocyte membrane proteins subjected to SDS-PAGE and incubation with autologous immunoglobulin after electroblotting. Visualization of IgG binding was performed by means of alkaline-phosphatase-labelled anti-human IgG antibodies. Reactivity with most of the protein bands present on the blot is apparent (Fig. 2, lane b). This binding ability was not influenced by absorption of the autoantibody preparation with intact erythrocytes, while immunoabsorption with crude erythrocyte membrane preparations removed the activity (Fig. 2, lane c). Thus the anti-human IgG alkaline conjugate did not react with the erythrocyte proteins. These experiments indicate that the majority of epitopes recognized by the circulating autoantibodies are situated inside the erythrocyte, *i.e.*, on cytoskeletal proteins and on intracellulary parts of the integral membrane protein band 3.

In conclusion, these experiments illustrate the value of the crossed-immunoelectrophoretic technique, where a combination of precipitate morphology, migration and immunoreactivity gives information in addition to the high resolution and sensitivity of the immunoblotting procedure itself.

Isolation of polymer materials generated in erythrocytes

Erythrocytes contain an γ-glutamyl-ε-lysine transglutaminase[41], which upon activation with Ca^{2+} cross-links the membrane proteins. The physiological rôle of this enzyme is not known, although it has been suspected to be involved in the removal of

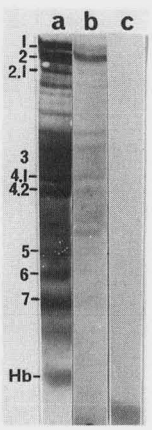

Fig.2. Immunoblots of human erythrocyte membrane proteins (30 μg in each lane), separated by SDS-PAGE (anode at the bottom) and electroblotted on nitrocellulose. (a) Gold-stained transfer; (b) incubation with 1:180 dilution of Protein A-purified autologous immunoglobulin fraction; (c) as in (b) but absorbed with crude erythrocyte ghosts. Visualization by means of an alkaline-phosphatase-conjugated rabbit anti-human IgG antibody, followed by staining with Nitroblue tetrazolium with 5-bromo-4-chloro-3-indolyl phosphate as a substrate[56]. Band assignments according to Steck and Yu[52].

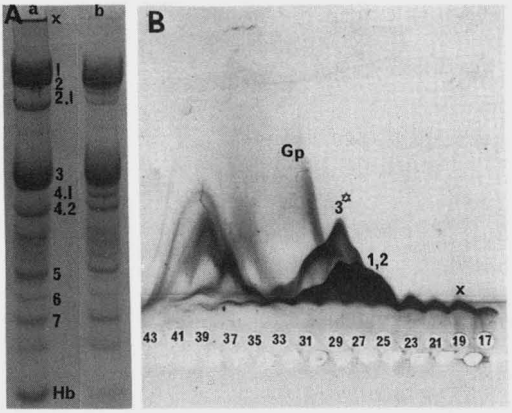

Fig. 3. (A) Effect of Ca^{2+} on the membrane profile in intact human erythrocytes. Lanes: a, SDS-PAGE pattern of membrane material from cells exposed to 2 m*M* Ca^{2+} for 3 h at 37°C at 20% haematocrit with 20 μM ionophore; b, corresponding control incubated with 2 m*M* Mg^{2+}. Note the disappearances of Band 2.1 and Band 4.1 and the production of high-molecular-weight membrane protein polymer (X). (B) Fused-rocket immunoelectrophoresis in the presence of 2% Lubrol PX of an SDS-solubilized membrane material from calcium-incubated cells, separated by means of Sepharose CL4B chromatography. The immunoprecipitated material in fractions 17–20 represents high-molecular-weight material, corresponding to X of lane a in (A). The anti-ghost antibody content of the gel was 6 μl/cm^2. To avoid interference from the SDS in the samples, 5 μl 20% (w/v) Lubrol PX was added to each well before electrophoresis. Designations correspond to those of Fig. 2.

aged erythrocytes[41,59,60]. However, the intracellular free calcium levels occurring physiologically are by far lower than those employed in the present study.

The polymer is generated upon incubation with Ca^{2+} in the presence of the Ionophore A23187 and is visible on top of the gel in SDS-PAGE (Fig. 3A, X). The polymer can be isolated by gradient ultracentrifugation in the presence of a non-ionic detergent[42] or by gel chromatography. The fused-rocket immunoelectrophoresis profile of the latter experiment is shown in Fig. 3B and illustrates the separation obtained in the presence of 0.1% SDS of the high-molecular-weight polymeric material from the normal membrane proteins. Interference of SDS with the immunoprecipitation was avoided by the presence of the non-ionic detergent in the wells and gel. Only fractions 17–20 were used as the source of the polymer whereby contamination of the spectrin was avoided.

Immunoelectrophoretic epitope analysis of the polymers

With the crossed-immunoelectrophoretic pattern of normal human erythrocyte membrane antigens as a reference, the effect of absorbing the polyspecific anti-ghost antibody with isolated polymers was examined (Fig. 4).

When the absorbed antibody was included in the intermediate gel (as in Fig. 4A) rather than the original antibody (as in Fig. 4B), an upward displacement in the heights of the precipitation lines for spectrin (1 and 2), ankyrin (2.1) and Band 3 proteins (only to a small degree) was observed. This is consistent with the idea that these protein components are present in the polymeric material, as the titre against the rest of the precipitated components including haemoglobin was undisturbed[42].

Since no precipitates corresponding to the Band 4.1 and 4.2 polypeptides were

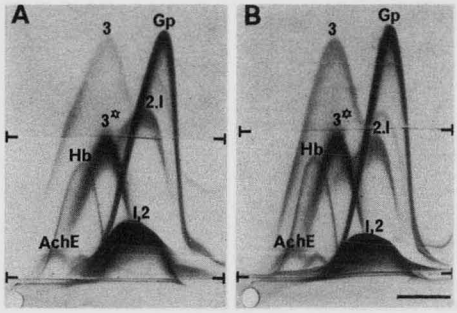

Fig. 4. Crossed-immunoelectrophoresis with an intermediate gel containing anti-human erythrocyte membrane antibody absorbed with isolated membrane polymer. For details of absorption, see Materials and Methods. Normal human erythrocyte ghost (8 μg of protein), solubilized in Triton X-100 at pH 10^{12}, was applied for electrophoresis. The absorbed antibody (3 μl/cm^2) was included in the intermediate gel (between the markings) in (A). The intermediate gels for (B) contained the unabsorbed antibody (3 μl/cm^2). The upper gels in both experiments contained unabsorbed antibody (5 μl/cm^2). Designations correspond to those of Fig. 1.

identified in the precipitation pattern, the presence of such epitopes was investigated in a separate experiment, in which an oligospecific anti-band 4.1 and 4.2 antibody was used. Since the antiserum was raised against material cut from SDS-PAGE gels, it did not react with Triton X-100-solubilized material[15]. The specificity of the Anti-band 4.1 and 4.2 antiserum was therefore first tested by SDS-PAGE crossed-immunoelectrophoresis (Fig. 5). Upon incorporation of the antibody preparation in an intermediate window (Fig. 5A), two immunoprecipitates were observed at the bottom line of the gel. Also, the glycophorin precipitate was slightly affected, as an extension of its legs appeared in the intermediate gel (compare Fig. 5A, B and C). That these two lower precipitates corresponded to Band 4.1 and Band 4.2, respectively, was established as follows. Upon incubation of erythrocytes with Ca^{2+}, Band 4.1 disappeared from the SDS-PAGE pattern[41,60] and so did the cathodic precipitate (Fig. 5B). Furthermore, the positions of the two precipitates strictly correlate with Band 4.1 and Band 4.2, as measured relatively to the markers, human transferrin and albumin (Fig. 5C and D), both of which retain their immunoreactivity after SDS-PAGE.

The Anti-band 4.1 and 4.2 antiserum was absorbed with purified polymer and applied in SDS-PAGE crossed-immunoelectrophoresis of normal erythrocyte membrane proteins (Fig. 6B). By comparison with the control (unabsorbed antiserum) (Fig. 6A) it appeared that the precipitate corresponding to Band 4.1 disappeared, indicating the presence of this protein in the polymer. The precipitate of band 4.2 appeared larger but less strongly stained, and by absorption with a triple amount of polymer material this precipitate also disappeared. This may indicate that the polymer also contains some epitopes of Band 4.2. A similar dilution of the antibody employed by buffer from a blank sucrose gradient did not have this effect.

Immunoblotting analysis of the constituents of the polymer

The immunoblotting technique is very sensitive and the demand for monospecificity of the antibodies employed is equivalently high. It was therefore found necessary to perform extensive absorption of the available antibodies. Fig. 7 shows the

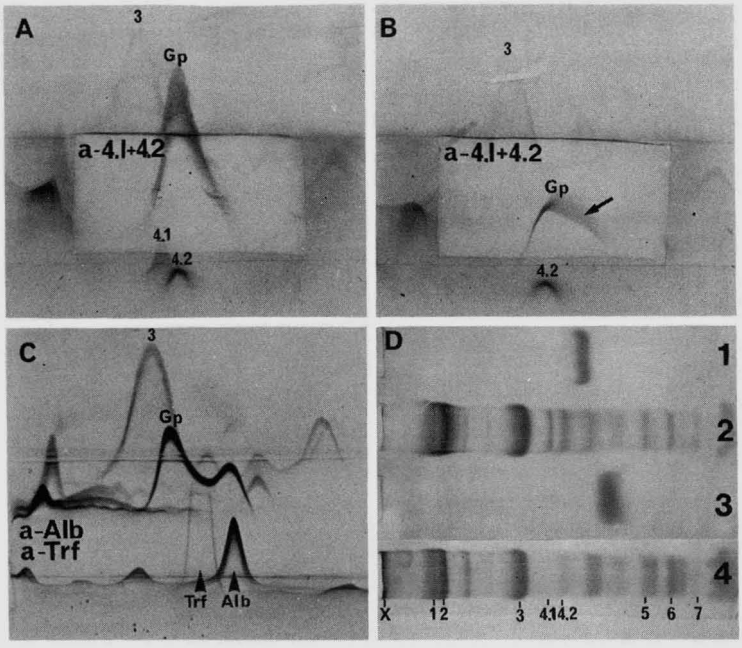

Fig. 5. Identification of Band 4.1 and Band 4.2 precipitates in SDS-PAGE crossed-immunoelectrophoresis. Immunoelectrophoretic analysis of 40 μg membrane proteins from normal erythrocytes (A and C) and of membrane proteins from 3-h calcium-incubated cells (B). Note that glycophorin is degraded (arrow). In (C) the proteins were mixed with 1.5 μg human albumin and 0.5 μg human transferrin prior to electrophoresis. The intermediate gel contains in (A) and (B) Anti-band (4.1 + 4.2) antiserum (20 μl/cm^2), applied in a "window". In (C) it contains 4 μl/cm^2 of anti-human albumin (a-Alb) and 4 μl/cm^2 of anti-human transferrin (a-Trf). The upper gels contain antibodies against normal human erythrocyte membranes: 9 μl/cm^2 in (A) and (B), 15 μl/cm^2 in (C). (D) The resolution obtained by first-dimension SDS-PAGE (anode to the right). The albumin and transferrin markers are shown in lanes 1 and 3, respectively. Erythrocyte membrane proteins from normal cells and from 3-h calcium-loaded cells are shown in lanes 2 and 4, respectively. On incubation with Ca^{2+}, Band 4.1 is missing. Designations and other conditions correspond to those of Fig. 2.

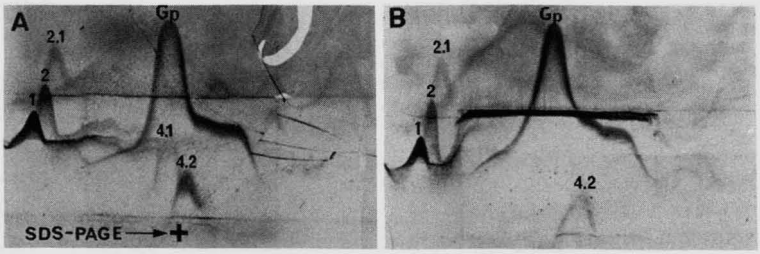

Fig. 6. Analysis for epitopes of Band 4.1 and Band 4.2 on purified polymer. SDS-PAGE crossed-immunoelectrophoresis of normal erythrocyte membrane proteins with an intermediate gel, containing, in (B), 21 μl/cm^2 of Anti-band (4.1 + 4.2), absorbed with 15 μg SDS-isolated polymer, and in (A) the corresponding control with unabsorbed antiserum (21 μl/cm^2). Both antibodies were applied in a "window". Other conditions and designations correspond to those of Fig. 5.

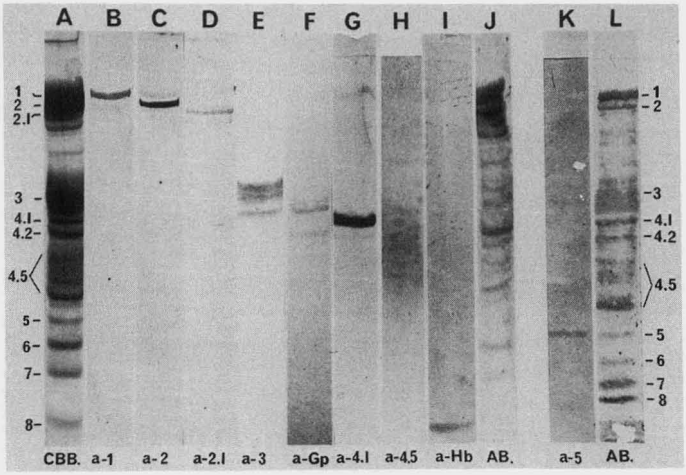

Fig. 7. Antibody specificity, tested by immunoblotting. Human erythrocyte membrane proteins were separated by SDS-PAGE (A–J), according to Steck and Yu[52] and (K, L) according to Laemmli[63]. Anode at the bottom. Lane A shows a Coomassie brilliant blue (CBB)-stained gel (50 μg protein); lanes B–L are nitrocellulose strips with electrophoretically transferred proteins, stained (J, L) with Amidoblack (AB) (50 μg protein) and (B–I, K) for peroxidase activity (10 μg protein) after incubation with monospecific rabbit antibodies, followed by a peroxidase-conjugated swine anti-rabbit immunoglobulin. The primary rabbit antibody was Anti-band 1 (diluted 1 + 666) (B), Anti-band 2 (1 + 333) (C), Anti-band 2.1 (1 + 333) (D), Anti-band 3 (1 + 200) (E), Anti-glycophorin (1 + 500) (from Dr. Gahmberg) (F), Anti-band 4.1 (1 + 2000) (an artefactual staining is seen in the spectrin region) (G), anti-glucose transporter (a-4.5) (1 + 2500) (H), anti-haemoglobin (a-Hb) (1 + 200) (I) and anti-actin (a-5) (1 + 25) (K). Designations as in Fig. 2.

resulting specificity of these antibodies in immunoblotting. Antibodies against Band 1, Band 2, Band 3, haemoglobin and actin give one band in the blots. Where several bands are seen, it can be explained by molecular-weight heterogeneity, as for glycophorin[61], glucose transporter[62] and probably also for Band 3 protein. Proteolytic cleavage may be the reason for the two bands seen with the Anti-band 2.1 antibody[12]. The high-molecular-weight polymeric material can be analysed in the same way, because this material migrates in an SDS-containing composite gel, consisting of 2% acrylamide and 0.5% agarose. The polymer is separated from the rest of the erythrocyte membrane proteins (Fig. 8, lane A) and appeared under these conditions as a symmetrically distributed polydisperse band with a molecular weight between $3 \cdot 10^6$ and $5 \cdot 10^6$ (Fig. 8, X).

The polymeric material can easily be transferred from the electrophoresis gel to the nitrocellulose sheet, as demonstrated by subsequent staining with Amidoblack (Fig. 8, lane L). When the absorbed monospecific antibodies, used in the same concentrations as in Fig. 7, were applied to such transferred proteins, a staining of the polymer band was observed for all antibodies employed, except that directed against glycophorin (Fig. 8, lanes B–J). Two different anti-glycophorin antibody preparations showed consistent results. The reaction of the anti-actin antiserum (lane I) with the polymer was weak, but clearly visible in the freshly stained immunoblots. Furthermore, in the concentration range applied, sera and IgG preparations from non-immunized rabbits did not react with the blotted erythrocyte membrane protein material (Fig. 8, lane K).

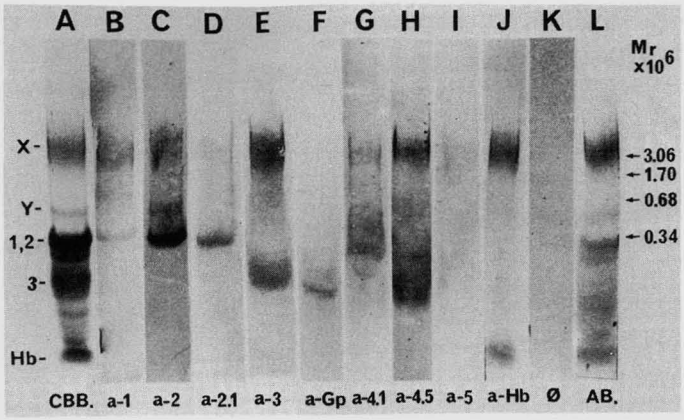

Fig. 8. Demonstration by immunoblotting of the presence of epitopes of individual membrane proteins on the polymeric protein material, generated in calcium-loaded human erythrocytes in the presence of pepstatin. The proteins were separated on SDS-containing composite gels of 2% polyacrylamide and 0.5% agarose. Molecular-weight markers are indicated on the right on the basis of transglutaminase mediated cross-linked fibrin oligomers. Lane A shows the Coomassie brilliant blue-stained gel, loaded with 125 μg protein. The polymeric material appeared as a broad band X in the molecular-weight range of $3 \cdot 10^6$–$5 \cdot 10^6$ well separated from the spectrins, $M_r \approx 2.2 \cdot 10^5$ (1, 2) and as a new, discrete band with $M_r \approx 5 \cdot 10^5$ (Y). Lanes B–K are nitrocellulose strips with electrophoretically transferred proteins (125 μg), stained (K) with Amidoblack and (B–L) for peroxidase activity. The primary monospecific antibodies, used in the same concentrations as in Fig. 7, were applied as stated on the Figure. Lane K served as a control where a non-immune rabbit serum was employed (1 + 1000) (Ø). Other conditions and designations as in Fig. 7.

The specificity of the antibody binding to the polymer was further evidenced by the simultaneous binding to the corresponding individual antigens of lower molecular weight. In this respect, the behaviour of the Anti-band 4.1 antibody was abnormal. Aside from its reaction with the polymer, it also reacted with normal membrane material of higher molecular weight than expected (Fig. 8, lane G). This observation

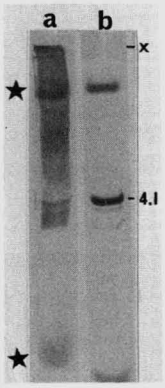

Fig. 9. Demonstration by immunoblotting of the distribution of Band 4.1 epitopes after SDS-PAGE, performed according to Steck and Yu[52], of erythrocyte membrane protein from (a) calcium-loaded cells in the presence of pepstatin and (b) magnesium-loaded cells (control). The primary antibody was Anti-band 4.1 (1 + 2000). Note the continuous distribution of immunoreactivity from the position of Band 4.1 to the top of the gel. The asterisks indicate the transferred track of the marker stain Pyronin G. Conditions and other designations as in Fig. 7.

was verified in a separate immunoblotting experiment, where polymer-containing erythrocyte membrane material was separated by conventional SDS-PAGE (Fig. 9).

Thus, the two immunochemical approaches employed for epitope analyses of the transglutaminase-generated polymers in the erythrocyte membrane complement each other. Both techniques show that spectrin, ankyrin, Band 3 protein and Band 4.1 participate in the polymer formation. Immunoblotting gave further evidence for the incorporation of both spectrins (Band 1 and 2), haemoglobin, glucose transporter (4.5) and actin in the polymer. The crossed-immunoelectrophoresis approach seems not to be sensitive enough to demonstrate a decrease in the titre of antibody against haemoglobin after absorption (*cf.*, Fig. 3) but is capable of showing that Band 4.2 epitopes probably are also involved.

DISCUSSION

The demonstration of circulating IgG autoantibodies against human erythrocyte membrane proteins illustrates how the techniques of crossed-affinoimmunoelectrophoresis and immunoblotting complement each other. By the former technique, interactions with cytoskeletal and integral membrane proteins, excluding glycophorin, were observed. Immunoblotting experiments with absorbed antibodies then showed that the autoantibodies reacted mainly with epitopes on the inside of the cell membrane. Immunoblotting requires only small amounts of reagents and the experiment with absorbed antibodies would have been cumbersome to perform by means of immunoelectrophoretic techniques.

A further advantage of immunoblotting in this connection is that the class and specificity of the interacting molecules are demonstrated directly by the visualization step. The crossed affinoimmunoelectrophoresis, on the other hand, gives a clearer impression of which proteins are involved in the interaction.

Glycophorin, which is also an integral membrane protein and which is easily identifiable in the precipitation pattern, is evidently non-reacting (Fig. 1). Thus, these techniques give results which, taken together, are easier to interpret than the results of either of these techniques alone. In the experiments on polymer formation, glycophorin was further demonstrated not to participate in the cross-linking events. This series of experiments (Figs. 3–9) shows how connoisseur modifications of basic procedures make it possible to extract approximately the same amount of information by both techniques, although immunoblotting in most instances represents the quickest and less difficult approach. Special problems arose when the antibodies precipitated only SDS-treated material (the Anti-band 4.1 and 4.2 antibody preparation) but this was circumvented by means of special modifications of the crossed-immunoelectrophoresis procedure (Fig. 5). Immunoblotting did not demand any special modifications to show the presence of Band 4.1 epitopes on the polymer (Fig. 8), and the presence of Band 4.1 epitopes in a wide range of molecular weights was further demonstrated (Fig. 9). This observation, together with the early disappearance from the SDS pattern after addition of Ca^{2+}, points to the Band 4.1 protein as an important substrate for the enzyme. Unfortunately, the electrophoresis system employed did not separate Band 4.1 in 4.1a and 4.1b. The ratio between these bands differs with age[64]. Immunoblotting requires a very high degree of monospecificity of the primary antibodies, which ideally is accomplished by means of monoclonal antibodies.

Furthermore, immunoelectrophoresis allows direct demonstration of antigens with catalytic activities. Thus, the polymer has been shown to possess catalase activity, whereas acetylcholinesterase activity was shown to be completely independent of the polymer entities[65].

For quantification of antigens and antibodies, immunoelectrophoresis also takes the lead, while the sensitivity, high resolving power, broad applicability, independence of precipitating abilities of the employed antibodies and low consumption of reagents constitute the main advantages of immunoblotting. In addition, studies of interactions by means of immunoblotting techniques can be performed with an high degree of freedom in the selection of ionic strength, pH and other buffer manipulations. This is in contrast to the immunoelectrophoretic techniques, which are much more restricted in this respect. On the other hand, in certain instances the latter techniques will, as illustrated by the experiments with autoantibodies against human erythrocyte membrane protein components, give more information about the identity of the interacting macromolecules than the immunoblots. Also, the positions and other characteristics (shape and stainability) of precipitates can offer additional information for identification which is not given by ordinary immunoblotting procedures as the use of the oligospecific antibody preparation in the experiment shown in Fig. 5 illustrates. Finally, for quantification, including monitoring of column chromatography experiments (*cf.*, fused-rocket immunoelectrophoresis in Fig. 3), and for the study of glycosylation microheterogeneity the electroimmunoprecipitation methods are valuable.

In conclusion, the two immunochemical methods complement each other. For antigen characterization (Table I) the two methods are almost equally suited. However, as immunoblotting normally relies on SDS-PAGE methods, which are part of the standard protein analysis armament of most laboratories, while crossed-immunoelectrophoresis methods often are regarded as troublesome, it may be said that immunoblotting in general is the easier method of the two. As an extension of routine protein analyses, immunochemical characterization by means of immunoblotting is thus the straightforward choice. As mentioned, the flexibility and versatility of the immunoblotting principle is greater than that of the electroimmunoprecipitation techniques. Therefore, the latter will most likely in many instances in the future be replaced by immunoblotting procedures as the almost exponential growth of publications on immunoblotting methods nicely illustrates[36].

ACKNOWLEDGEMENTS

The financial support of Lundbeckfonden, The Danish Foundation for the Advancement of Medical Science, and the Danish Hospital Foundation (Region of Copenhagen, the Faroe Islands and Greenland) is gratefully acknowledged. A portion of this work was carried out in the Department of Biochemistry, Molecular and Cell Biology, Northwestern University, Evanston, IL 60208, with the support of a grant from the National Institutes of Health, U.S. Public Health Service (AM-25412).

REFERENCES

1 O. Ouchterlony, *Acta Path. Microbiol. Scand.*, 25 (1948) 186.
2 G. Mancini, J.-P. Vaerman, A. O. Carbonara and J. F. Heremans, *Protides Biol. Fluids*, 11 (1964) 373.
3 N. Ressler, *Clin. Chim. Acta*, 5 (1960) 359.
4 C.-B. Laurell, *Anal. Biochem.*, 15 (1966) 45.
5 C.-B. Laurell, *Anal. Biochem.*, 10 (1965) 358.
6 H. G. M. Clarke and T. Freeman, *Protides Biol. Fluids*, 14 (1967) 503.
7 N. H. Axelsen (Editor), *Handbook of Immunoprecipitation-in-Gel Techniques*, Blackwell, Oxford, 1983.
8 K. Takeo and E. A. Kabat, *J. Immunol.*, 121 (1978) 2305.
9 J. Breborowicz, J. Gan, J. Klosin, K. Gryska, P. Majewski, D. Breborowicz and P. Waliszewski, *Electrophoresis*, 8 (1987) 313.
10 T. C. Bøg-Hansen, O. J. Bjerrum and J. Ramlau, *Scand. J. Immunol.*, 4 Suppl. 2 (1975) 141.
11 S. Bhakdi, B. Bhakdi-Lehnen and O. J. Bjerrum, *Biochim. Biophys. Acta*, 470 (1977) 35.
12 O. J. Bjerrum, P. J. Bjerrum, K. P. Larsen, B. Norrild and S. Bhakdi, in O. J. Bjerrum (Editor), *Electroimmunochemical Analysis of Membrane Proteins*, Elsevier, Amsterdam, 1983, p. 173.
13 N. LeGendre and P. Malsudaira, *BioTechniques*, 6 (1988) 154.
14 O. J. Bjerrum and N. H. H. Heegaard (Editors), *Handbook of Immunoblotting of Proteins*, Vol. 1, CRC Press, Boca Raton, FL, 1988.
15 O. J. Bjerrum, in O. J. Bjerrum (Editor), *Electroimmunochemical Analysis of Membrane Proteins*, Elsevier, Amsterdam, 1983, p. 30.
16 O. J. Bjerrum and S. Bhakdi, in N. H. Axelsen (Editor), *Handbook of Immunoprecipitation-in-Gel Techniques*, Blackwell, Oxford, 1983, p. 289; *Scand. J. Immunol.*, 17, Suppl. 10 (19xx) 289.
17 O. J. Bjerrum and T. C. Bøg-Hansen, *Scand. J. Immunol.*, 4, Suppl. 2 (1975) 89.
18 A. Kinzkofer-Peresch, N. P. Patestos, M. Fauth, F. Kögel, R. Zok and B. J. Radola, *Electrophoresis*, 9 (1983) 497.
19 O. J. Bjerrum and N. H. H. Heegaard (Editors), *Handbook of Immunoblotting of Proteins*, Vol. 2, CRC Press, Boca Raton, FL, 1988.
20 W. C. Bradbury, S. D. Mills, MA. Preston, L. J. Barton and J. L. Penner, *Anal. Biochem.*, 137 (1984) 129.
21 O. J. Bjerrum, J. H. Gerlach, T. C. Bøg-Hansen and J. B. Hertz, *Electrophoresis*, 3 (1982) 89.
22 B. G. Ohlsson, B. R. Weström and B. W. Karlsson, *Electrophoresis*, 9 (1987) 415.
23 G. M. Small, T. Imanaka and P. B. Lazarow, *Anal. Biochem.*, 169 (1988) 405.
24 J. Jarausch and B. Kadenbach, *Eur. J. Biochem.*, 146 (1985) 219.
25 P. Owen, in O. J. Bjerrum (Editor), *Electroimmunochemical Analysis of Membrane Proteins*, Elsevier, Amsterdam, 1983, p. 56.
26 J. M. Gershoni, *Electrophoresis*, 7 (1987) 428.
27 C. Mattsson, E. Heilbron, J. Ramlau and E. Bock, *J. Neurochem.*, 32 (1979) 309.
28 L. Lorand, S. N. P. Murthy, P. T. Velasco and F. Kamsh, *Biochem. Biophys. Res. Commun.*, 134 (1986) 685.
29 E. A. Bayer, M. Safars and M. Wilchek, *Anal. Biochem.*, 161 (1987) 262.
30 O. J. Bjerrum, J. C. Selmer and A. Lihme, *Electrophoresis*, 8 (1987) 388.
31 C. Schäfer-Nielsen and O. J. Bjerrum, *Scand. J. Immunol.*, 4, Suppl. 2 (1975) 73.
32 J. P. Luzio and P. Jackson, in O. J. Bjerrum and N. H. H. Heegaard (Editors), *Handbook of Immunoblotting of Proteins*, Vol. II, CRC Press, Boca Raton, FL, 1988, p. 13.
33 J. Hald, S. Naaby-Hansen, J. Egense, T. Hjort and O. J. Bjerrum, *J. Reprod. Immunol.*, 10 (1987) 15.
34 H. Towbin, T. Staehelin and J. Gordon, *Proc. Natl. Acad. Sci. U.S.A.*, 76 (1979) 4350.
35 U. Beisiegel, *Electrophoresis*, 7 (1985) 1.
36 O. J. Bjerrum (Editor), *Papersymposium on Proteinblotting*, *Electrophoresis*, 8 (1987).
37 G. Bers and D. Garfin, *BioTechniques*, 3 (1985) 276.
38 J.-C. Hsieh, F.-P. Lin and M. F. Tam, *Anal. Biochem.*, 170 (1988) 1.
39 Q.-Y. Xu and J. E. Shively, *Anal. Biochem.*, 170 (1988) 19.
40 N. H. H. Heegaard and O. J. Bjerrum, in C. Shafer-Nielsen (Editor), *Electrophoresis '88*, VCH Verlag, Weinheim, 1988, p. 424.
41 L. Lorand, L. B. Weissmann, D. L. Epel and J. Bruner-Lorand, *Proc. Natl. Acad. Sci. U.S.A.*, 73 (1973) 4479.
42 O. J. Bjerrum, M. Hawkins, P. Swanson, M. Griffin and L. Lorand, *J. Supramol. Struct. Cell. Biochem.*, 16 (1981) 289.

43 J. T. Dodge, C. Mitchel and D. J. Hanahan, *Arch. Biochem. Biophys.*, 100 (1963) 119.
44 P. J. Bjerrum, *J. Membr. Biol.*, 48 (1979) 43.
45 N. M. G. Harboe and A. Ingild, in N. H. Axelsen (Editor), *Handbook of Immunoprecipitation-in-Gel Techniques*, Blackwell, Oxford, 1983, p. 345; *Scand. J. Immunol.*, 17, Suppl. 10 (1983) 345.
46 O. J. Bjerrum and T. C. Bøg-Hansen, in A. H. Maddy (Editor), *Biochemical Analysis of Membranes*, Chapman & Hall, London, 1976, p. 378.
47 J. A. Reynolds and H. Trayer, *J. Biol. Chem.*, 246 (1971) 7337.
48 O. J. Bjerrum, J. Ramlau, I. Clemmensen, A. Ingild and T. C. Bøg-Hansen, *Scand. J. Immunol.*, 4, Suppl. 2 (1975) 81.
49 O. J. Bjerrum and E. Gianazza, in O. J. Bjerrum (Editor), *Electroimmunochemical Analysis of Membrane Proteins*, Elsevier, Amsterdam, 1983, p. 127.
50 V. T. Marchesi and E. P. Andrews, *Science (Washington, D.C.)*, 174 (1972) 1247.
51 H. Knüfermann, S. Bhakdi and D. F. H. Wallach, *Biochim. Biophys. Acta*, 389 (1975) 464.
52 T. L. Steck and J. Yu, *J. Supramol. Struct.*, 1 (1973) 220.
53 A. C. Peacock and C. W. Dingman, *Biochemistry*, 7 (1968) 226.
54 T. L. Steck, *J. Mol. Biol.*, 66 (1972) 295.
55 O. J. Bjerrum, P. Lundahl, C.-H. Brogren and S. Hjertén, *Biochim. Biophys. Acta*, 394 (1975) 173.
56 N. H. H. Heegaard and O. J. Bjerrum, in O. J. Bjerrum and N. H. H. Heegaard (Editors), *Handbook of Immunoblotting of Proteins*, Vol. 1, CRC Press, Boca Raton, FL, 1988, p. 1.
57 H. S. Platt, B. M. Sewell, T. Feldman and R. L. Souhami, *Clin. Chim. Acta*, 46 (1973) 419.
58 S. Naaby-Hansen and O. J. Bjerrum, *J. Reprod. Immunol.*, 7 (1985) 41.
59 L. Lorand and S. M. Conrad, *Mol. Cell. Biochem.*, 58 (1984) 9.
60 L. Lorand, V. Zappia, P. Galletti, R. Porta and F. Wold, *Adv. Exp. Med. Biol.*, 231 (1988) 79.
62 T. J. Wheeler, I. A. Simpson, D. C. Sogin, P. C. Hinkle and S. W. Cushman, *Biochem. Biophys. Res. Commun.*, 105 (1982) 89.
63 U. K. Laemmli, *Nature (London)*, 227 (1970) 680.
64 J. T. Mueller, C. W. Jackson, M. E. Dockter and M. Morrison, *J. Clin. Invest.*, 79 (1987) 492.
65 O. J. Bjerrum, M. Hawkins, M. Michalska and L. Lorand, *Fed. Proc., Fed. Am. Soc. Exp. Biol.*, 42 (1983) 604, abstr. 1828.

Journal of Chromatography, 470 (1989) 369–376
Elsevier Science Publishers B.V., Amsterdam — Printed in The Netherlands

CHROMSYMP. 1518

RECYCLING ISOELECTRIC FOCUSING AND ISOTACHOPHORESIS

M. BIER*, G. E. TWITTY and J. E. SLOAN
Center for Separation Science, University of Arizona, Building 20, Tucson, AZ 85721 (U.S.A.)

SUMMARY

A new apparatus for large scale preparative isoelectric focusing in free solution is described. Its main characteristic is rapid fluid recirculation with but short residence times in the electric field. For the first time the recycling principle was also applied to preparative isotachophoresis, by incorporating into the system a computer controlled leader counterflow. The rapid recirculation permits application of unusually high electrical power for rapid resolution, as it suppresses fluid flow instabilities arising from electrohydrodynamic effects.

INTRODUCTION

Isoelectric focusing is a particularly appealing method for scaling-up of protein purification because of its exceptional resolution. Several preparative instruments[1–5] were developed over the last few years based on a novel recycling principle and are gaining increasing acceptance. One of the advantages of recycling is that it permits dissipation of Joule heat outside of the fractionation apparatus. The general usefulness of recycling was also recently demonstrated by Righetti *et al.*[6] in an innovative manner. The diversity of instruments is welcome as it allows the selection of the most appropriate instrument for the problem at hand.

Isotachophoresis has also the potential of high resolution[7], but has received as yet far less attention as a preparative method and no high throughput apparatus was available. Isotachoporesis has an advantage over focusing in lending itself to greater flexibility in the choice of operating pH, thus avoiding the problem of protein precipitation ocasionally seen in focusing.

In this paper we wish to describe our latest recycling apparatus, equally well suited for focusing and isotachophoresis. It provided the first demonstration that the principle of recycling operation is also applicable to separation by isotachophoresis[8,9]. This was not evident *a priori*, as the two methods differ significantly in the characteristics of their final steady state. In isoelectric focusing, the final steady state is stationary, all components becoming virtually immobilized within the pH gradient at their isoelectric point. In such a situation the final state is independent of the route taken, *i.e.*, the recycling of the process fluid does not impede the establishment of the pH gradient or the focusing of the components.

In the steady state of isotachophoresis, to the contrary, all components migrate

0021-9673/89/$03.50

at the same velocity as a train of adjacent components, sorted according to their mobilities[10]. It was not obvious that such an ordering of components would occur also in a recycling mode of operation, where, in effect, only a relatively small part of the total volume (3–10% as a rule) is exposed to the electric current at any one time, the bulk of the fluid being in the external fluid circuitry loops. Moreover, counter-flow of leader ions is essential to provide sufficient migrating distance for the achievement of the steady state.

In common with other researchers interested in scaling up of electrophoretic methodology[11], we use free solutions without any supporting media such as gels or packed granular beds. Gels are essential for analytical separations and granular beds are convenient for micropreparative purposes, but they impose serious problems in scale up. Operating in free solutions, of course, necessitates rigorous control of fluid flow. Drawing analogies with gel electrophoresis, it was axiomatically assumed that best separations will be achieved in nearquiescent fluids. Several "curtain type" continuous flow instruments with fluid confinement to a narrow channel between parallel plates utilize this approach[12].

To our great surprise, we have discovered that in our instrument far better fluid stability is obtained at rapid rates of fluid flow, rather than in near stationary fluids[8]. The fluid instabilities seen at low flow-rates or in stationary fluid were attributed to certain electrohydrodynamic effects not previously associated with electrophoresis[13]. Electrohydrodynamic mixing, droplet deformation and other effects have been extensively studied by Melcher and Taylor[14] and Arp *et al.*[15], but only in two-phase systems, such as formed by immiscible fluids or fluid-air interfaces. The importance of these electrohydrodynamic factors for conventional continuous flow electrophoresis was recently clarified in an elegant manner by Rhodes and co-workers[16,17]. Their discovery merits attention from all workers in free fluid electrophoresis and is fully consonant with our results.

EXPERIMENTAL

Instrumentation

One of the best known methods for the control of fluid flow was pioneered by Hannig[12]. A thin film of flowing buffer is contained between two parallel plates, at least one of which is cooled. Fluid viscosity helps to maintain laminarity of buffer flow and the electric field is applied perpendicularly to the flow direction. The sample is introduced as a narrow stream within this curtain of flowing buffer and its components separate tangentially. Such separating chambers were incorporated into several commercially available instruments and a prototype has also been experimented with in the microgravity of orbiting spacecraft by NASA and McDonnell Douglas. Residence time in such instruments are typically relatively long, of the order of minutes, as separation has to be achieved in a single pass.

These instruments have been mainly used for zone electrophoresis, where separations are obtained as a function of relative mobilities in a background of homogeneous buffer composition. Fawcett[18] and others have also explored their usage for isoelectric focusing, but the results were rather disappointing. Low voltages only could be applied, resulting in residence times of the order of 30 min and correspondingly low throughput. Increase of voltage resulted in "feathering", a breakdown of the flow lines into feather-like structures.

The separation chambers we have used in the present studies of focusing and isotachophoresis use the same principle of a thin buffer film confined between two parallel plates. The chamber design is different, however, as it incorporates a symmetrical arrangement of an (arbitrary) number of inlet and outlet ports at the opposite ends of the chamber. These outlets and inlet ports are connected by closed circuitry loops for process fluid recirculation by means of a multichannel peristaltic pump. The recycling loops can be provided with UV, pH or other sensors, as well as with bubble traps and heat exchanger reservoirs. The latter provide for a changeable volume capacity of the instrument and avoid the necessity of cooling the focusing chamber itself. Recycling loops are also provided for the electrode compartments, separated from the chamber by either ion-exchange membranes for focusing, or by dialyzing membranes for isotachophoresis.

Five different chamber designs were implemented, with various overall length and width, the number of the closely spaced ports varying from 12 to 48. Two instruments had refrigerated chambers, the other three relied only on the heat exchanger reservoirs for Joule heat dissipation. Fig. 1 shows the simplicity of the

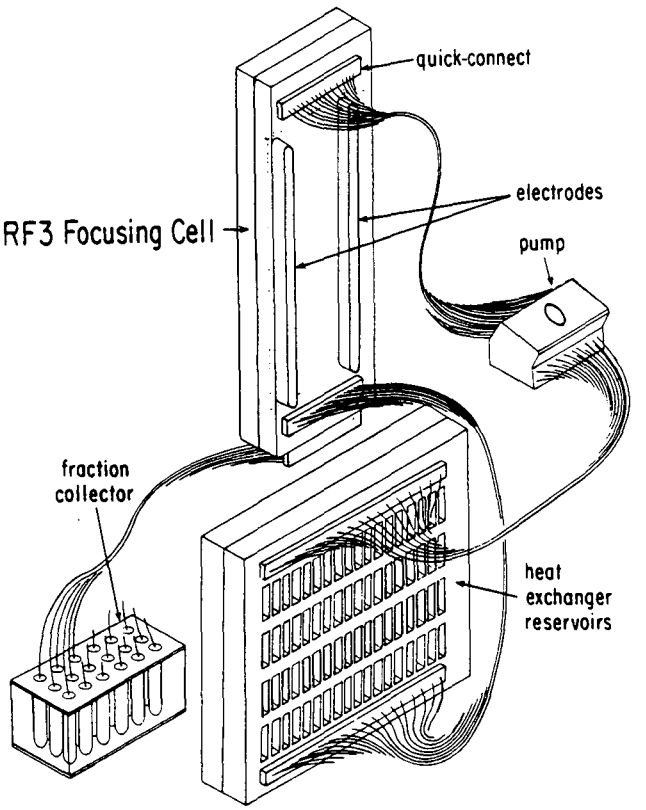

Fig. 1. Schematic presentation of the recycling flow pattern in the RF3 apparatus. Several different designs of the focusing apparatus and the heat exchanger were implemented, all exhibiting the same overall concept. In all of them, connecting the tubing set to the focusing cell, the pump, and the heat exchanger is facilitated by molded quick-connectors, only one of which is identified.

recycling loop in the 48-channel instrument, with a refrigerated focusing cell and heat-exchange reservoirs. All parts of the tubing set terminate in specially developed molded quick-connects, thereby greatly facilitating the apparatus assembly. A transfer of one of the quick-connects to the fraction collector allows for the simultaneous pumping out and collection of the separated fractions.

As in our other recycling instruments, the performance of the apparatus is rather independent of most operational factors, such as apparatus dimension, applied field, etc. Resolution, of course, mainly depends on the pH range of the carrier ampholyte. Two additional factors were found to be critical: the thickness of the fluid film and the rate of recycling. We discovered, indeed, that successful implementation of either focusing or isotachophoresis requires a narrow gap, of the order of 0.5–1 mm, with sufficiently fast flow-rates to give residence times of seconds only in the separation chamber[8]. The higher the applied voltage, the faster must be the recycling rate, if fluid instabilities are to be avoided. The cause of these fluid instabilities were attributed to electrohydrodynamics. Temperature or gravity were eliminated as major factors, as similar instabilities were observed with cooled or uncooled chambers, or with chambers operated in vertical or horizontal direction.

To implement leader counterflow, essential for isotachophoresis, several modifications were necessary. The advancing protein sample boundary was registered by inserting a UV sensor (2138 Uvicord S, LKB, Bromma, Sweden) into an appropriate recycling channel. For anionic isotachophoresis, this channel was somewhere between three and six channels in front of the anode (in a 30-channel apparatus). The counterflow was provided by a Sage Instruments syringe pump, feeding its leader buffer into the recycling channel adjacent to the anode membrane. Excess fluid was allowed to discharge from the last recycling channel, closest to the cathode. For cationic systems, only the polarity of the field needs to be reversed.

The syringe pump was toggled between on and off positions by a microcomputer (Commodore 64) interfaced with the UV sensor. Computer–UV sensor interface comprised an analog-to-digital/digital-to-analog (A-D/D-A) converter, a 12-V d.c. power supply and a relay. The computer was also utilized for data acquisition, treatment and storage. A specially written program provided visual graphic demonstration on the computer screen of the progress of separation, showing the preselected pump-triggering UV absorbance level, the actual absorbance registered by the sensor and the operation of the pump, as a function of time.

Operation

For isoelectric focusing, a batch mode of operation is simplest. The sample to be fractionated is mixed with the desired pH range ampholine or other carrier buffer and the apparatus filled to capacity. Recycling is initiated at a flow-rate of *ca.* 5–15 ml/min per channel. Power is applied to a maximum of 100–200 W, depending on the tolerance of the sample to temperature rise in the apparatus. At the lower power level, the temperature rise is less than 5°C, while at higher levels, the rise may be as much as 15°C. The bulk of the solution is maintained close to 0°C in the heat-exchange reservoir.

Recycling is continued until the amperage decreases to a stable minimum and for a "decent time" interval thereafter. Focusing of colored proteins has demonstrated that with a broadly based pH range, focusing of volumes of the order of 150 ml is completed within 40–60 min. With shallower pH gradients it is advisable to prolong the focusing time.

Three different modes of operation are possible. With a broad distribution of isoelectric points of the sample, the use of a broad pH range of carrier buffer will fractionate the mixture into step-pH fractions with some overlap between fractions. If one knows the isoelectric point of the desired protein, one can also select a narrow pH range carrier buffer, which will expand the resolution in the selected pH range, compressing the other proteins into the side compartments. Highest resolution is obtained in a third mode of operation, where the selected fractions of a first prefocusing, containing the desired protein, are submitted to a second fractionation, without addition of any other carrier buffer. This yields the narrowest pH range and optimizes resolution.

For isotachophoresis, batch or continuous flow operations are possible. The performance of the apparatus was mainly tested with dyes and with colored proteins, hemoglobin and blue-stained albumin. As protein fractions are adjacent in the isotachophoretic train, resolution is greatly enhanced by the choice of appropriate "spacers", non-protein components such as amino acids of intermediate mobilities[7]. Sharply focused protein boundaries were registered, using chloride ions as leader and ε-amino caproic acid as terminator. The choice of leader, terminator and spacers is critical and it is highly advisable that it be optimized by means of preliminary capillary isotachophoresis runs. Several such analytical instruments are available. Our computer programs[19] are also most useful in testing the separability of leader–spacer(s)–terminator. Glycine was an effective spacer to separate the two proteins. In either case, the leader is utilized to fill the chamber and one of the electrode compartments, the terminator being used in the other electrode compartment. The sample can be introduced through one of the channels close to the terminator as a single batch or in a continuous manner. A detailed account of this work is in preparation[24].

It is a characteristic of isotachophoresis that sample concentration is self-adjusting to the concentration of the leader, as a function of the Kohlrausch relation. For proteins, this results in their concentration to 1–10%. Thus, isotachophoresis is a convenient method for concentation of large volumes of dilute protein solutions with simultaneous fractionation. In fact, we have managed to fill virtually the whole contents of the apparatus with a desired protein in such a manner.

RESULTS AND DISCUSSION

Isoelectric focusing is gaining attention as a preparative method for protein purification[20,21]. Two instruments are commercially available, the older Rotofor (Bio-Rad Labs., Richmond, CA, U.S.A.)[3,4] and the present apparatus, dubbed recycling free-flow focusing (RF3) (Protein Technologies, Tucson, AZ, U.S.A.)[8] to differentiate it from our earlier recycling isoelectric focusing (RIEF) apparatus[1,2]. In the RIEF apparatus, fluid flow is stabilized by means of screen spacers, subdividing the focusing chamber. In the Rotofor, a combination of rotation around its horizontal axis and the partitioning of the annular space by the screen spacers stabilizes fluid against unwanted convections. The RF3 avoids some of the complications inherent in the presence of screen elements, simplifies the assembly and permits easy *in situ* cleaning. In addition, the rapid recirculation permits application of higher power for faster focusing.

The underlying concept of conventional continuous flow electrophoresis is that

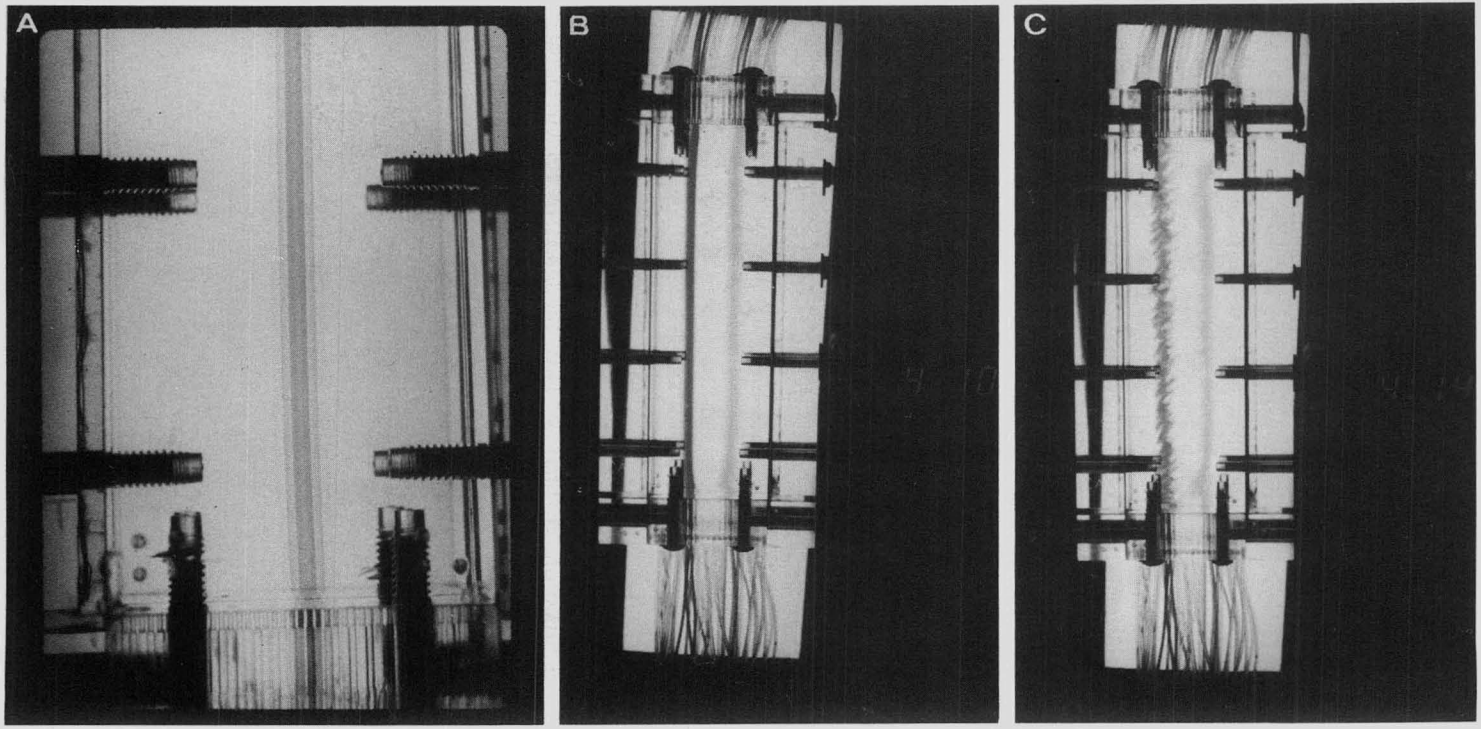

Fig. 2. Photographs of the streamlines of fluid flow in the RF3 apparatus. (A) Close-up of the remarkably sharp streamlines of focused hemoglobin. (B) RF3 cell with focused hemoglobin (left) and blue-stained albumin, rapid flow. (C) Dramatic disruption of the flow lines obtained within 4 s of flow stoppage.

a thin film of fluid, contained between two parallel plates, will provide the best medium for electrophoretic separations. At first appearance, this arrangement bears similarity to fractionation in a thin gel film. Unfortunately, this analogy is incorrect, as operation of such devices is subject to well known distortions of fluid flow caused by: the parabolic nature of flow through narrow gaps, the effect of Joule heating, gravitational slumping, if any, and electroosmosis[22]. Mathematical models seem to predict reasonably well the behavior of these instruments for zone electrophoresis[23].

In our type of recycling operation, none of the above factors seem to be of importance, the key consideration being the high rate of recycling. The parabolic flow of fluid is obviously of no concern, and there is no noticeable electroosmosis within the short residence times. Fig. 2 shows the remarkable sharpness of fluid flow lines obtained at fast recycling rates and the near explosive breakdown caused by electrohydrodynamic effects.

The only electrically driven fluid convection previously recognized was electroosmosis, resulting from the zeta potential of the walls of the vessel. In a homogeneous buffer, such as present in zone electrophoresis, electroosmosis is predictable and measurable by various methods. Rhodes and co-workers[16,17] have recently demonstrated that even in zone electrophoresis there can be a second kind of electrically driven convection, provided there is a significant conductivity or dielectric constant gradient within the otherwise uniform buffer system. Such gradients can arise through the use of high concentration (or conductivity) sample solutions.

These electrohydrodynamic effects have been previously observed[14,15] only when electric fields were imposed across immiscible water–solvent phase boundaries, giving rise there to feather-like disturbances as seen in our apparatus or to distortion of droplets. It is easy to differentiate between electroosmosis and the socalled electrohydrodynamic effect: electroosmosis is proportional to the field strength E, and thus requires d.c. currents. The electrohydrodynamic effect is proportional to E^2 and is equally responsive to direct or alternating currents. Thus, as a fringe benefit of our research, we have provided a confirmation of this effect in aqueous systems. In isoelectric focusing, of course, conductivity gradients are more prominent than in most other electrophoretic systems and the effect is more pronounced. As with gravity driven natural convection, a certain time element is necessary for the instabilities to develop and the rapid recycling is sufficient to avoid this in our case.

ACKNOWLEDGEMENTS

We wish to acknowledge the assistance of Craig Fisher and Terry Long in the testing of the apparatus, and of Drs. Wolfgang Thormann and Richard Mosher in the selection of isotachophoretic systems. This work was supported in part by NASA grant NAGW-693.

REFERENCES

1 M. Bier, *U.S. Pat.*, 4 362 612 (1982).
2 M. Bier *et al.*, in E. Gross and J. Meienhofer (Editors), *Peptides: Structure and Biological Function*, Pierce, Rockford, IL, 1979, pp. 35–48.
3 M. Bier, *U.S. Pat.*, 4 588 492 (1986).

4 N. B. Egen, W. Thormann, G. E. Twitty and M. Bier, in H. Hirai (Editor), *Electrophoresis 83*, Walter de Gruyter, Berlin, 1984, pp. 547–550.
5 M. Bier, in J. A. Asenjo and J. Hong (Editors), *Separation, Recovery and Purification in Biotechnology (ACS Symposium Series* 314), American Chemical Society, Washington, DC, 1986, pp. 185–192.
6 P. G. Righetti *et al.*, *J. Biochem. Biophys. Methods*, 15 (1987) 189.
7 M. Bier, R. M. Cuddeback and A. Kopwillem, *J. Chromatogr.*, 132 (1977) 437.
8 M. Bier and G. E. Twitty, *Process and Apparatus for Recycling Isoelectric Focusing and Isotachophoresis*, patent pending.
9 J. E. Sloan, *Master Thesis*, University of Arizona, Tucson, AZ, 1987.
10 M. Bier and T. Allgyer, in P. G. Righetti, C. J. van Oss and J. W. Vanderhoeff (Editors), *Electrokinetic Separation Methods*, Elsevier, Amsterdam, New York, 1979, pp. 443–469.
11 P. Mattock, G. F. Aitchison and A. R. Thomson, *Sep. Purif. Methods*, 9 (1980) 1.
12 K. Hannig, in M. Bier (Editor), *Electrophoresis*, Vol. II, Academic Press, New York, 1967, pp. 423–472.
13 J. R. Melcher, personal communication.
14 J. R. Melcher and G. I. Taylor, *Annu. Rev. Fluid Mech.*, 1 (1969) 111.
15 P. A. Arp, R. T. Foster and S. G. Mason, *Adv. Colloid Interface Sci.*, 12 (1980) 295.
16 P. H. Rhodes and R. S. Snyder, *NASA Technical Paper 2777*, NASA, Washington, DC, 1987.
17 P. H. Rhodes, R. S. Snyder and G. O. Roberts, *J. Colloid Interface Sci.*, in press.
18 J. S. Fawcett, *Ann. NY Acad. Sci.*, 200 (1972) 112.
19 M. Bier, O. A. Palusinski, R. A. Mosher and D. A. Saville, *Science (Washington, D.C.)*, 219 (1983) 1281.
20 K. G. Tibbits, *BioPharm Manufacturing*, 1 (1988) 12.
21 R. Kosecki, *BioPharm Manufacturing*, 1 (1988) 28.
22 A. Strickler, *Sep. Sci.*, 2 (1967) 335.
23 D. A. Saville, *Annu. Rev. Fluid Mech.*, 9 (1977) 321.
24 J. E. Sloan, W. Thormann, G. E. Twitty and M. Bier, *J. Chromatogr.*, in press.

Journal of Chromatography, 470 (1989) 377–383
Elsevier Science Publishers B.V., Amsterdam — Printed in The Netherlands

CHROMSYMP. 1588

SEPARATION OF LARGE DNA MOLECULES BY PULSED-FIELD GEL ELECTROPHORESIS

A REVIEW OF THE BASIC PHENOMENOLOGY

MAYNARD V. OLSON
Department of Genetics, Campus Box 8031, Washington University School of Medicine, St. Louis, MO 63110 (U.S.A.)

SUMMARY

Pulsed-field gel electrophoresis is a method of separating large DNA molecules. The distinctive feature of this method is that the direction of the electric field is changed periodically. During the five years since Schwartz and Cantor introduced this technique, there has been dramatic progress in pulsed-field instrumentation and in associated electrophoretic methods. Progress has been driven by practical experience with little guidance from theory. In this review, the basic phenomenology of pulsed-field gel electrophoresis is summarized and some speculations are advanced about possible molecular mechanisms.

INTRODUCTION

Pulsed-field gel electrophoresis (PFGE) is a method of separating large DNA molecules that was introduced by Schwartz and Cantor in 1983[1]. In its usual forms, it involves alternately applying two electric fields that differ in direction. Electrophoretic conditions are otherwise similar to those normally used to separate double-stranded DNA molecules ranging in size up to tens of thousands of base-pairs. By the simple device of periodically alternating the electric field direction, the size range for separations can be extended to several millions of base-pairs. The time scale of the alternations is typically in the range of seconds to minutes, increasing with the sizes of the molecules that are to be separated.

Under typical PFGE conditions, the mobilities of small DNA molecules (*i.e.* those ranging in size up to 10 000–15 000 base-pairs) are not affected by the switching events. These molecules simply migrate in accordance with the time-averaged electric field. However, larger DNA molecules behave quite differently. During continuous electrophoresis, they adopt an elongated conformation and their long axes become aligned with the electric field. The motion of such molecules through the gel has been referred to as "reptation" since it resembles the forward motion of a snake. In continuous electric fields, the mobilities of reptating molecules larger than a threshold size (typically, 20 000–30 000 base-pairs) are independent of size. In PFGE, however, the mobilities of these molecules are diminished compared to the continuous-field case.

0021-9673/89/$03.50

Because the magnitude of this effect is a sensitive function both of the size of the molecules and the frequency of the switching events, molecules that are altogether inseparable by continuous electrophoresis can have dramatically different mobilities in PFGE.

During its short history, PFGE has been carried out on a succession of apparatuses that differ primarily in the shapes and relative orientations of the two alternately applied electric fields. The first successful separations employed an apparatus in which at least one of the alternately applied electric fields was spatially non-uniform. Because of the field inhomogeneity and the orientation of the wells relative to the applied fields the molecules migrated along curved trajectories[1,2]. In order to emphasize the presence of large gradients in the applied fields, the method was referred to as pulsed-field-gradient (PFG) electrophoresis. Carle and Olson[3] introduced an apparatus in which —at least in the central lanes— the molecules migrated in a straight line. However, this line was defined by the time-averaged direction of two symmetrically applied, inhomogeneous fields; consequently, trajectories were still sharply curved towards the edges of the gel, albeit in a symmetric pattern. The name orthogonal-field-alternation gel electrophoresis (OFAGE) was suggested to accentuate the spatial relationship between the alternately applied fields.

A number of perplexing features of the phenomenology were described in these early papers, particularly the apparent need for inhomogeneous electric fields. Nonetheless, the observations were basically consistent with a "corner-turning" model. In this model, the dramatic size-dependence of the mobilities of large DNA molecules on pulsed-field gels was thought to occur because large molecules take longer to turn corners in the gel than do small molecules.

The first indication that neither inhomogeneous electric fields nor corner-turning were central to the pulsed-field effect came with the discovery that periodic inversion of a uniform electric field also gives rise to strongly size-dependent mobilities[4]. In field-inversion gel electrophoresis (FIGE), net forward migration is achieved either by employing longer switching intervals or higher field strengths in the forward than in the reverse direction. The optimum switching intervals for separating molecules in a particular size range are strikingly similar to those observed in the earlier experiments with transverse alternating fields, an observation that suggests that the molecules are undergoing similar types of rearrangement in the two cases.

The most recent phase of instrumental development involves a field geometry similar to OFAGE, but featuring uniform fields. The key to success in achieving OFAGE-style separations with uniform fields —and, thus, straight-line migration all the way across the gel— was the recognition of a requirement that the fields intersect at a markedly obtuse angle[4–6]. Earlier unsuccessful experiments with transverse homogeneous fields had all evidently been carried out at 90°, which any simple corner-turning model would predict to provide the greatest effect. In actuality, there is a strong requirement for an obtuse angle. Several types of instrumentation, such as the contour-clamped homogeneous electric field (CHEF) system[6], which is based on a closed hexagonal array of electrodes, and table-turning apparatuses[7,8], in which the gel rotates in the presence of a stationary electric field, can provide uniform alternating electric fields that intersect at an obtuse angle. The angle does not appear to be particularly critical, as long as it is significantly greater than 90°; a value of approximately 120°, as in the CHEF system, is highly effective.

In summary, two basic electrophoretic geometries arose during the early years of PFGE, and they continue to dominate current practice. In one of these geometries (FIGE), the alternating electric fields and the net movement of the molecules are all colinear. The other geometry involves two alternating fields that are transverse to one another and also to the direction of net migration. Systems of the latter type will be referred to here by the generic acronym TFAGE for transverse-field-alternation gel electrophoresis. As this acronym suggests, the basic geometry of TFAGE systems is similar to that of OFAGE. However, OFAGE was a misnomer, since it is known that an important feature of the OFAGE geometry was that the fields were not orthogonal: as in all successful TFAGE systems, they intersected at an angle greater than 90°.

DNA molecules behave quite similarly in all TFAGE systems. Although instrumental advances have been of great practical importance, particularly in providing straight lanes, they have not revealed any basically new electrophoretic effects. FIGE, on the other hand, does involve electrophoretic behavior that is qualitatively different from that observed with TFAGE. The most notable FIGE-specific effect is the presence of a sharply double-valued relationship between size and mobility[4]. Molecules of some intermediate size, which can be selected by tuning the frequency of the field inversions, typically have zero mobility. The mobilities of smaller molecules are inversely related to their sizes (as on a conventional gel), while the mobilities of larger molecules actually increase with increasing size. The latter phenomenon is weakly displayed on TFAGE[9] —and has been observed even on ordinary agarose gels under extreme conditions[10]— but it is a dominant feature of FIGE separations over a broad range of sizes, field strengths, and switching conditions[4,11].

Several efforts have been made to analyze PFGE from a theoretical perspective. These efforts span a wide range of formalisms, ranging from extensively developed theories based on the statistical mechanics of macromolecules[11] to entirely heuristic models[7]. Although these treatments offer a variety of insights into molecular processes that may be important in PFGE, they all have severe limitations. For example, the adaption of the "biased reptation" theory to FIGE by Lalande *et al.*[11] fails to explain the sharp minimum in FIGE mobility as a function of DNA size and also incorrectly predicts that the FIGE effect will disappear when the forward and reverse field strengths are equal. The heuristic model of Southern *et al.*[7] provides a possible explanation of the need for obtuse angles in TFAGE, but does so in a way that offers no insight at all into FIGE.

UNIFIED VIEW OF PFGE PHENOMENOLOGY

Given the complexity of the problem, progress towards a powerful, unified theory of PFGE is likely to be slow. In the absence of such a theory, it would at least be useful to have a systematic way of thinking about pulsed-field phenomenology, particularly if all the prominent features of both TFAGE and FIGE could be accomodated. Starting with ideas that were briefly developed in the original description of FIGE by Carle *et al.*[4], an effort will be made here to develop a highly simplified, but unitary, view of TFAGE and FIGE phenomenology.

The starting point is the concept that DNA adopts a directional conformation during ordinary steady-state electrophoresis. That is, an electrophoresing DNA molecule that is much larger than the size of the pores in the gel should not be regarded as

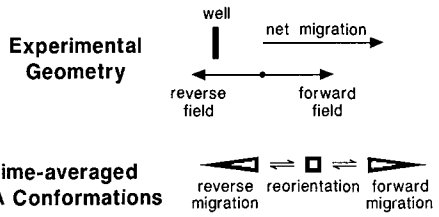

Fig. 1. Field-inversion gel electrophoresis (FIGE). The top of the diagram indicates the simple electrophoretic geometry. Note that the forward and reverse fields can be of equal strength with longer forward than reverse switching intervals, the switching intervals can be equal with a higher forward than reverse field, or some combination of inequalities in the field strengths and the switching intervals can be used to achieve net forward migration. The bottom of the diagram presents a simple three-state model for the conformational changes that accompany the field-inversion events.

a symmetric rod. A closer approximation would be a cone, represented in two dimensions as a wedge. While a rod would be expected to slide easily back and forth in an inverting field —responding only to the net forward impulse— the wedge is unable to change directions without undergoing a conformational change, which will be referred to as wedge inversion. The rate of wedge inversion is hypothesized to be slow and strongly size-dependent, the rate decreasing monotonically as the size of the molecules increases. Consequently, the simplest possible model for FIGE would involve three states, two of which are physically identical but oppositely oriented wedges (Fig. 1). Under particular electrophoretic conditions, the interconversions between the three states are assumed to be first-order kinetic processes. Furthermore, the mobility of the intermediate conformation, represented as a square, is assumed to be zero in either direction, while the mobility of an inappropriately oriented wedge is also assumed to be zero.

This simple formalism is adequate to explain basic FIGE phenomenology, particularly the dramatic double-valuedness of the size–mobility curve. When the time scale of the switching is closely matched to the rate of conformational interconversion, the molecules spend most of their time in the intermediate, zero-mobility conformation. We have previously described this phenomenon as "resonance" since it is a singularity that arises when the frequency of a driving force (the electric field) is tuned to a basic molecular parameter (the rate of conformational interconversion)[4]. Molecules much smaller than those at resonance have high mobility, since they can respond instantaneously to the field inversions: the ratio of time spent in the forward conformation to that spent in the reverse conformation is simply the ratio of the forward to the reverse switching intervals. On the other hand, molecules much larger than those at resonance are unable to respond significantly to the field inversions. In a strict three-state model, these molecules would nearly all become trapped in the high-mobility forward conformation under a typical FIGE switching regime. In a more realistic model, with a larger number of intermediates, they would accumulate in conformations intermediate between the fully forward state and the zero-mobility intermediate. In either case, they would be expected, as is observed, to have much higher mobility than the resonant molecules.

This discussion has deliberately not adopted any detailed view of the wedged conformation. The wedge is simply intended to symbolize the directionality of DNA conformations during steady-state electrophoresis. Molecular directionality is un-

doubtedly a property of all macromolecules undergoing steady-state electrophoresis under conditions such that the molecules are much longer than the effective sizes of the gel pores. Experiments employing intermittent unidirectional fields also provide evidence for conformational directionality[12,13]. Recent computer simulations of the chain dynamics of electrophoresing DNA molecules may provide some insight into the nature of the wedges[14]. These simulations suggest that, on a time average, the leading edge of the chain is relatively extended and under tension while tailing segments are increasingly likely to be hooked around obstacles in the gel. On the whole, these simulations are consistent with our earlier supposition that "the farther a segment is from the leading end of the molecule, the more likely it is to be penetrating the gel matrix along a path that is counterproductive to overall translocation of the molecule, and the larger the radius from which such counterproductive paths can be selected"[4]. However, the simulations emphasize that the concept of a wedge is, at best, a time-averaged description and that wedge collapse occurs relatively frequently[14].

This view of FIGE is readily extended to the more complex TFAGE geometry. Most particularly, it provides a simple explanation for the requirement that the transverse field in TFAGE intersect at an obtuse angle. This point is developed in Fig. 2 by comparing the expected behavior of rod-shaped (non-directional) and wedge-shaped (directional) conformations under TFAGE with field-intersection angles of 120 and 60°. The same considerations apply for any pair of angles chosen symmetrically about 90°. The key point is that a rod-shaped molecule can become realigned with the electric field after either a 60 or a 120° change in field direction simply by undergoing a 60° reorientation. To achieve this result, the molecule keeps the same leading segment in the 60° case, while it changes leading segments in the 120° case. Since, by definition,

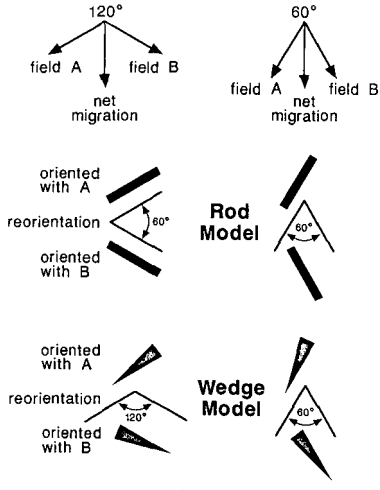

Fig. 2. Transverse-field-alternation gel electrophoresis (TFAGE). This diagram shows the geometric factors that apply when either rod- or wedge-shaped molecules become realigned with electric fields whose directions have been changed by 120 of 60°. The key point is that rod-shaped molecules can become realigned in either case with a 60° reorientation, while wedge-shaped molecules cannot. The particularly important case of the realignment of a wedge-shaped molecule following a 120° change in field direction is discussed in the text.

the two ends of a rod are considered equivalent, a rod-shaped molecule should be able to respond with equal ease to 120 and 60° changes in field direction.

In contrast, if the molecules are taken to be wedge-shaped, the nature of the molecular reorientation required when the field direction changes by 120° is fundamentally different from that required by a 60° change. If a wedge-shaped molecule is to keep the same leading segment, then it must undergo the full 120° reorientation. More plausibly, such molecules would be expected to undergo an end-to-end conformational change, as in FIGE, while also becoming reoriented by 60°. Since 60° reorientation, by itself, gives rise to size-independent migration, a reasonable hypothesis is that most of the size-dependence in TFAGE comes from essentially the same end-to-end conformational change that is central to the FIGE effect[4].

However, there is an important difference between the molecular motions involved in the response to a 120° TFAGE switching event, as opposed to a field-inversion event. This difference arises because a molecule that is undergoing an end-to-end conformational change in TFAGE is initially out of alignment with the electric field by 60°. Consequentiy, at the same time that the wedge is inverting, there is a large cross section for motions in the new field direction by local segments along the wedge. Most of these motions will be counterproductive with respect to overall molecular translocation. As a new path through the gel develops, these motions will give rise to added friction because many local segments will be hooked around components of the gel matrix that are obstacles with respect to the new path. The number of such segments will increase with the size of the molecules; consequently, the effect of this initial misalignment of an inverting wedge would be to introduce a drag on mobility that increases with molecular lengths and is uniquely associated with TFAGE rather than FIGE. This additional penalty for being large is likely to explain the absence in TFAGE of the dramatic double-valuedness of the size–mobility curve that is a prominent feature of FIGE.

CONCLUSION AND FUTURE PROSPECTS

Although heuristic and lacking in molecular detail, this view of pulsed-field phenomenology has the virtue of providing a unified perspective towards the diverse forms of PFGE. In particular, the following key points are accomodated:

(1) Large DNA molecules develop a high-mobility conformation during steady-state electrophoresis, which relaxes with time once the field is turned off[12,13]. This conformation is presumably the wedge itself, which although highly dynamic may represent an adequate description of the time-averaged structure[14].

(2) FIGE displays spectacularly size-dependent mobilities, even with equal forward and reverse field strengths, a result that is not predicted by any standard reptation theory[10,14].

(3) In contrast to the expectations of simple corner-turning models, 90° is an ineffective angle for TFAGE separations. Obtuse angles, which require the same type of wedge inversion featured in FIGE, are required.

(4) Size is a dramatically double-valued function of mobility in FIGE, while it is a largely single-valued function in TFAGE. Detailed consideration of the constraints on wedge inversion suggests that there is an additional penalty for being large in TFAGE that does not apply in FIGE.

Future progress in understanding the molecular basis of PFGE is likely to come from several directions. Biophysical studies of electrophoresing molecules should provide direct evidence of molecular conformations[15]. More advanced molecular dynamic simulations show promise of avoiding the oversimplifications inherent in formal statistical-mechanical theories[14]. In practical terms, it is possible to develop kinetic models of the type suggested in Fig. 1 into parameterized equations that relate mobilities to size and switching intervals, much in the way that enzyme kinetic measurements are treated. Finally, there is a great need for more systematic experimentation. The problem of developing pulsed-field instrumentation has been adequately solved in the context of present knowledge of electrophoretic behavior. Further advances depend on refining our knowledge of that behavior by a fruitful combination of theory and experiment.

REFERENCES

1 D. C. Schwartz, W. Saffran, J. Welsh, R. Haas, M. Goldenberg and C. R. Cantor, *Cold Spring Harbor Symp. Quant. Biol.*, 47 (1983) 189.
2 D. C. Schwartz and C. R. Cantor, *Cell*, 37 (1984) 67.
3 G. F. Carle and M. V. Olson, *Nucleic Acids Res.*, 12 (1984) 5647.
4 G. F. Carle, M. Frank and M. V. Olson, *Science (Washington, DC)*, 232 (1986) 65.
5 C. L. Smith, P. E. Warburton, A. Gaal and C. R. Cantor, *Genet. Eng.*, 8 (1986) 45.
6 G. Chu, D. Vollrath and R. W. Davis, *Science (Washington, DC)*, 234 (1986) 234.
7 E. M. Southern, R. Anand, W. R. A. Brown and D. S. Fletcher, *Nucleic Acids Res.*, 15 (1987) 5925.
8 P. Serwer, *Electrophoresis*, 8 (1987) 301.
9 G. F. Carle and M. V. Olson, *Methods Enzymol.*, 155 (1987) 468.
10 M. Lalande, J. Noolandi, C. Turmel, R. Brousseau, J. Rousseau and G. W. Slater, *Nucleic Acids Res.*, 16 (1988) 5427.
11 M. Lalande, J. Noolandi, C. Turmel, J. Rousseau and G. W. Slater, *Proc. Natl. Acad. Sci. U.S.A.*, 84 (1987) 8011.
12 T. Jamil and L. S. Lerman, *J. Biomol. Struct. Dynam.*, 2 (1985) 963.
13 J. C. Sutherland, D. C. Monteleone, J. H. Mugavero and J. Trunk, *Anal. Biochem.*, 162 (1987) 511.
14 J. M. Deutsch, *Science (Washington, DC)*, 240 (1988) 240.
15 G. Holzwarth, C. B. McKee, S. Steiger, G. Crater, *Nucleic Acids Res.*, 15 (1987) 10031.

Journal of Chromatography, 470 (1989) 385–389
Elsevier Science Publishers B.V., Amsterdam — Printed in The Netherlands

CHROMSYMP. 1561

PURIFICATION OF LABELLED ANTIBODIES BY HYDROPHOBIC INTERACTION CHROMATOGRAPHY

HENRIK ALFTHAN* and ULF-HÅKAN STENMAN
Departments I & II of Obstetrics and Gynecology, Helsinki University Central Hospital, Haartmaninkatu 2, SF-00290 Helsinki (Finland)

SUMMARY

In order to improve the sensitivity of immunometric assays, a chromatographic technique was developed that virtually eliminates components causing non-specific background. Labelled antibodies were applied to a phenyl-Sepharose column in physiological buffer. When labelled antibodies were purified by this technique, the non-specific background of various time-resolved immunofluorometric assays was reduced 3- to 10-fold and was very close to the instrument background. The assay sensitivity was simultaneously increased by a factor of 2 to 16. This purification method might be used to improve the results of immunometric assays in general.

INTRODUCTION

Time-resolved immunofluorometry is a highly sensitive immunochemical technique[1–3], with which it is possible to develop methods 100 times more sensitive than corresponding radioimmunoassays[4]. The method is based on the sandwich principle, in which two antibodies are used[5,6]. One antibody is immobilized on the walls of microtitre strip wells and the other one is labelled with a europium chelate[2]. The high sensitivity of the technique is related to the use of large amounts of antibodies in combination with an highly fluorescent label[7,8]. In order to achieve maximum sensitivity, the background signal, *e.g.*, the fluorescence of the sample containing no analyte, must be low and the specific signal must be as high as possible. Gel chromatography is used mostly to purify the labelled antibody, but after this purification step, some antibodies still show high non-specific binding, causing an high background.

Hydrophobic interaction between the labelled antibody and the solid phase is a potential cause of non-specific binding. To test this hypothesis we have purified antibodies by hydrophobic interaction chromatography (HIC). On the basis of the results we have developed a rapid and simple technique by which the non-specific background can be reduced 2- to 10-fold and the sensitivity improved by a similar factor.

0021-9673/89/$03.50

EXPERIMENTAL

Materials

hCG and free hCGα and hCGβ subunits were obtained from Boehringer Mannheim (Mannheim, F.R.G.).

T-buffer is 0.05 mol/l Tris–HCl (pH 7.7), containing 9 g/l NaCl and 0.5 g/l NaN_3. C-buffer is 0.1 mol/l Na_2CO_3 (pH 9.1). The washing solution contained 9 g/l NaCl, 0.2 g/l Tween 20 and 0.5 g/l NaN_3. The assay buffer used in the immunofluorometric assays (IFMA) was T-buffer containing 5 g/l bovine serum albumin (BSA), 0.5 g/l bovine globulin and 0.1 g/l Tween 40. The enhancement solution contained 6.8 mmol/l potassium hydrogenphthalate, 100 mmol/l acetic acid, 1 g/l Triton X-100, 50 μmol/l tri-*n*-octylphosphine oxide and 15 μmol/l 2-naphthoyltrifluoroacetone (Wallac Biochemical Labs., Turku, Finland).

Six monoclonal antibodies (MAbs) were used. MAbs 1–5 were kindly provided by Drs. Jim Schröder (Department of Genetics, University of Helsinki, Helsinki, Finland) and Robin Fraser (Monoclonal Antibodies, Mountain View, CA, U.S.A.). MAbs 1 and 2 are specific for the free α subunit of the gonadotropins, MAb 3 is specific for the free β subunit of hCG and MAbs 4 and 5 detect both hCG and the free β subunit of hCG. MAb 6 was obtained from Medix Biochemica (Helsinki, Finland). The antibody is specific for hCG and the free β subunit of hCG.

Methods

MAbs 1–5 were purified from ascites by precipitation with Na_2SO_4. Equal amounts of ascites and 36% Na_2SO_4 were mixed and incubated for 10 min at 20°C. After centrifugation at 5000 *g* for 10 min, the precipitate was washed twice with 18% Na_2SO_4 and finally dissolved in C-buffer. After purification with Na_2SO_4, 1 mg of MAb 5 in T-buffer was applied to an 11-ml chromatography column equipped with a frit (Econo-Column®; Bio-Rad Labs., Richmond, CA, U.S.A.), packed with 1.5 ml phenyl-Sepharose (Pharmacia LKB Biotechnology, Uppsala, Sweden) and eluted with T-buffer. Fractions containing non-adsorbed protein were pooled and used to coat microtitre strip wells. The columns were discarded after a single use.

Coating

Antibodies were coated onto the walls of microtitre strip wells (Eflab, Helsinki, Finland). A 200-μl volume of C-buffer, containing 5 mg/l of antibody, was pipetted into the wells and incubated overnight at 20°C. To block non-specific adsorption on the plastic surface, 250 μl of T-buffer, containing 10 g/l BSA, were added to the wells and incubated overnight. The solution was discarded, and the wells were stored in a moist atmosphere at 4°C.

Labelling

MAbs, purified from ascites by precipitation with Na_2SO_4, were labelled with an isothiocyanatophenyl derivative of diethylenetriaminetetraacetate (isothiocyanatophenyl-DTTA), complexed with europium at 100-fold molar excess in C-buffer[2]. After 20 h at 4°C, unreacted chelate was separated from labelled antibody by gel chromatography on a 50 cm × 1 cm Sephacryl S-300 column (Pharmacia LKB Biotechnology) in T-buffer at a flow-rate of 15 ml/h. Fractions of 0.5 ml were collected in tubes, prefilled with 100 μl assay buffer.

HIC

Labelled MAbs were further purified by HIC. The sample was applied to a chromatography column (Econo-Column) packed with 0.8 ml phenyl-Sepharose (Pharmacia LKB Biotechnology) and equilibrated with T-buffer. After application of the sample, the column was eluted at hydrostatic pressure with 10 ml T-buffer. The non-adsorbed fractions were collected and used as a label in IFMA. The columns were discarded after a single use.

Immunofluorometric assay

A 25-μl volume of sample and 200 μl assay buffer were pipetted into the coated wells. After incubation for 2 h, the wells were washed, and 50 ng europium-labelled antibody in 200 μl assay buffer were added. After a further incubation for 1 h, the wells were washed four times and filled with 200 μl enhancement solution. The fluorescence was measured after 5 min in an Arcus 1230 fluorometer. The sensitivity of the assays was calculated from the mean +2 S.D. of twelve replicates of assay buffer (Table I).

RESULTS

Europium-labelled antibodies were purified by gel chromatography. The MAbs were eluted as one smooth peak, and the peak fractions were used as tracers in immunofluorometric assay (Fig. 1). In the immunofluorometric assay with labelled antibody 5 the background was moderately elevated (2200 $\pm$ 363 cps, mean $\pm$ S.D.). When the tracer was further purified by HIC, 80–90% was recovered in the non-adsorbed fractions. When this fraction was used as tracer the background dropped to 275 $\pm$ 29 cps (Fig. 2). This should be compared with the instrument background (53 $\pm$ 8.4 cps), the background of the microtitre strip wells (147 $\pm$ 11 cps) and the enhancement solution (256 $\pm$ 17 cps). The fraction adsorbed to the column was not studied further. The assay sensitivity before and after HIC purification was 2.9 and 0.18 pmol/l, respectively. Similar results were obtained with other HIC-purified antibodies (Fig. 3, Table II). Purification of the europium-labelled MAbs by HIC did not change the maximum signal obtained by immunofluorometric assay.

Normally, the solid phase antibody was purified only by sodium sulphate precipitation. When this antibody was further purified by HIC, 5% was retained on the column. When the non-adsorbed fraction was used for coating, no further reduction of non-specific binding was obtained. However, a two-fold increase in the maximum signal was observed when HIC-purified solid-phase MAb was used in

TABLE I

SPECIFICITY OF THE IMMUNOFLUOROMETRIC ASSAYS

Solid-phase antibody	*Labelled antibody*	*Specificity*
1	2	hCGα
6	3	hCGβ
4	5	hCG, hCGβ

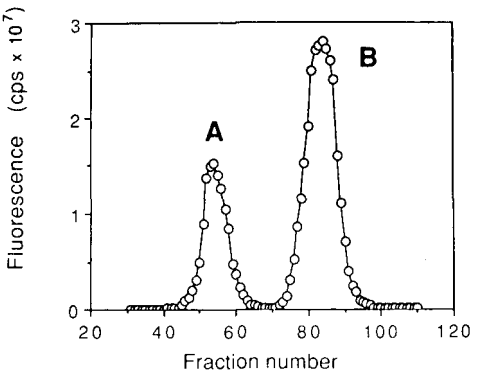

Fig. 1. Gel chromatography of anti-hCG antibody 5, labelled with isothiocyanatophenyl-DTTA-Eu. The labelled antibody corresponds to peak A and the free chelate to peak B.

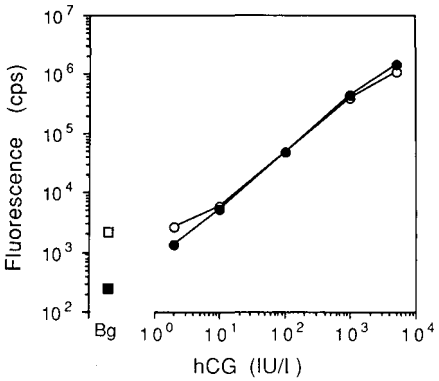

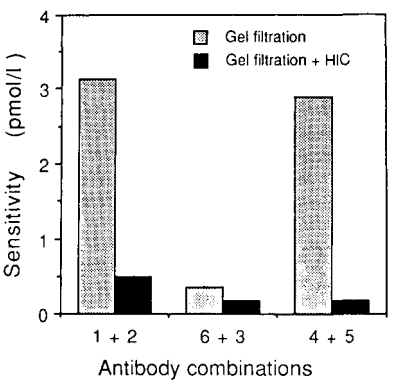

Fig. 2. Standard curve of an hCG immunofluorometric assay. The labelled antibody was purified by gel chromatography (@) and by gel chromatography and HIC (⅛). The background signal (Bg) is denoted by squares.

Fig. 3. Sensitivity of the immunofluorometric assays before and after purification of the labelled antibody by HIC.

TABLE II

SENSITIVITY OF hCG IMMUNOFLUOROMETRIC ASSAYS BEFORE AND AFTER PURIFICATION OF THE LABELLED ANTIBODY BY HIC

Purification method	*Solid-phase antibody*	*Labelled antibody*	*Background fluorescence (mean ± S.D.)*	*Sensitivity (pmol/l)*	*Sensitivity increase (factor)*
Gel chromatography	1	2	2017 ± 250	3.1	
Gel chromatography + HIC	1	2	443 ± 37	0.5	6.2
Gel chromatography	6	3	2156 ± 265	0.36	
Gel chromatography + HIC	6	3	622 ± 91	0.17	2.1
Gel chromatography	4	5	2200 ± 363	2.9	
Gel chromatography + HIC	4	5	275 ± 29	0.18	16.1

combination with a labelled antibody that had been purified by gel filtration and HIC (results not shown).

DISCUSSION

We have developed a novel technique for purification of antibodies used in immunometric assays, based on HIC. This method lowers the background and improves the sensitivity 2- to 16-fold in three different model assays. Earlier, the labelled antibodies were purified by gel chromatography. By this method we have obtained extreme sensitivity for immunofluorometric methods, *i.e.*, an 100-fold improvement over conventional radioimmunoassays. Even these sensitive assays can be further enhanced by a factor of 2 to 3 by using HIC.

The purification technique is simple and rapid. It utilizes small disposable polypropylene chromatography columns, packed with phenyl-Sepharose, and the chromatography is completed within 10 min. After this step, the labelled antibodies show virtually no non-specific binding in the immunofluorometric assay. Our results indicate that the main cause of the background is the presence of hydrophobic europium-labelled proteins. These may be formed as a result of denaturation during the labelling procedure, or hydrophobic proteins may be labelled, contaminating the immunoglobulin G (IgG) preparation. When HIC was used to purify the solid-phase antibody, an increased maximum signal was also obtained. This may have resulted from removal of hydrophobic components from the rather crude IgG preparation which interfered with the binding of the specific MAb to the solid phase.

The sensitivities of the immonofluorometric assays used in this study were all improved remarkably by purifying the labelled antibody by HIC. We use this purification technique routinely for all of our assays.

This technique should also be applicable to other immunometric techniques in which different labels are used and may also improve the specificity of other immunochemical techniques, *e.g.*, immunohistochemistry. Studies are in progress to clarify this possibility.

ACKNOWLEDGEMENTS

This study was supported by grants from the Sigrid Juselius Foundation, the Academy of Finland and the Finnish Cancer Society.

REFERENCES

1 E. Soini and H. Kojola, *Clin. Chem.*, 29 (1983) 65.
2 I. Hemmilä, S. Dakubu, V.-M. Mukkala, H. Siitari and T. Lövgren, *Anal. Biochem.*, 137 (1984) 335.
3 T. Lövgren, I. Hemmilä, K. Pettersson, J. U. Eskola and E. Bertoft, *Talanta*, 31 (1984) 909.
4 U.-H. Stenman, H. Alfthan, T. Ranta, E. Vartiainen, J. Jalkanen and M. Seppälä, *J. Clin. Endocrinol. Metab.*, 64 (1987) 730.
5 L. E. M. Miles and C. N. Hales, *Nature (London)*, 219 (1968) 186.
6 L. Wide, H. Bennich and S. G. O. Johansson, *Lancet*, ii (1967) 1105.
7 T. M. Jackson and R. P. Ekins, *J. Immunol. Methods*, 87 (1986) 13.
8 H. Alfthan, *J. Immunol. Methods*, 88 (1986) 239.

Journal of Chromatography, 470 (1989) 391–399
Elsevier Science Publishers B.V., Amsterdam — Printed in The Netherlands

CHROMSYMP. 1572

RECENT ADVANCES IN THE PREPARATION AND USE OF MOLECULARLY IMPRINTED POLYMERS FOR ENANTIOMERIC RESOLUTION OF AMINO ACID DERIVATIVES

DANIEL J. O'SHANNESSY*, BJÖRN EKBERG, LARS I. ANDERSSON and KLAUS MOSBACH
Pure and Applied Biochemistry, Chemical Center, University of Lund, P.O. Box 124, S-22100 Lund (Sweden)

SUMMARY

Acrylate-based molecular imprints were prepared, using L-phenylalanine anilide as the print molecule and methacrylic acid as the functional monomer, which is believed to interact both ionically and through hydrogen bonding with the print molecule. Several aspects of the polymer preparation were investigated, including the solvent of polymerization, the initiation system and the effect of the molar ratio of functional monomer to print molecule on the ability of the polymers to separate the enantiomers of the print molecule. Polymers were analysed by high-performance liquid chromatography where the effect of particle size and eluent composition were investigated for enantiomeric resolution of the print molecule. The ability of the polymers to separate racemic mixtures of amide derivatives of amino acids other than phenylalanine anilide (print molecule) was also investigated. It was thus shown that efficient enantiomeric resolution of amide derivatives of amino acids including the anilides, *p*-nitroanilides, *β*-naphthylamides and amides of amino acids, ranging from alanine to tryptophan, was possible on a single polymer imprinted with L-phenylalanine anilide. Such separations were highly specific and dependent on the presence of both the print molecule and functional monomer in the polymerization mixture. The mechanism of recognition was shown to involve ionic bonding to the primary amine and hydrogen bonding to the amide function of the substrate by acid groups of the polymer, "immobilized" in a stereospecific manner. Both interactions were necessary for efficient enantiomeric resolution. Molecular imprints, prepared from L-phenylalanine anilide, were also shown to give efficient enantiomeric resolution of phenylalanine-containing dipeptides and may be useful for preparative-scale separations.

INTRODUCTION

Two basically similar approaches have been followed for the preparation of molecular imprints for a variety of molecules (for a review see ref. 1). The first involves the formation of reversible covalent adducts between the print molecule and functional monomers. Examples of this include the formation of Schiff bases[2,3], boronic esters[4,5] and ketals[6]. The second approach involves the use of non-covalent

0021-9673/89/$03.50

interactions, such as ionic and hydrogen bonding, between the print molecule and functional monomers[7]. In both cases, these interactions are allowed to occur in solution prior to initiation of polymerization and are subsequently responsible for recognition of molecules by the polymer.

In our laboratory, we have used the approach of non-covalent interactions for the preparation of molecular imprints for amino acid derivatives[7–12]. These polymers are subsequently used in high-performance liquid chromatography (HPLC) for enantiomeric resolution of racemic mixtures of amino acid derivatives. In the present paper we present some recent advances in the preparation and use of molecular imprints with amino acid derivatives as the print molecules. A new polymerization procedure, which allows the preparation of polymers at 0°C, is presented. The method of preparation of the polymers is simpler to perform, is less time-consuming and results in polymers exhibiting greater separation abilities than those previously presented. In addition, several factors affecting the performance of such polymers in HPLC for enantiomeric resolution were investigated. Finally, the versatility of molecular imprints to separate racemic mixtures of molecules other than the print molecule has been demonstrated and the results allow some conclusions to be drawn on the mechanism of recognition.

EXPERIMENTAL

Methacrylic acid (MAA) and ethylene glycol dimethacrylate (EDMA) were obtained from Aldrich Chemie (Steinheim, F.R.G.), 2,2′-azobis(2-methylpropionitrile) (AIBN) from Janssen Chimica (Beerse, Belgium) and 2,2′-azobis(2,4-dimethylvaleronitrile) (ABDV) from Polysciences (Warrington, PA, U.S.A.). The print molecule, L-phenylalanine anilide, was synthesized as previously described[11]. D-Phenylalanine anilide and D- and L-tyrosine and tryptophan anilides were synthesized in a similar manner. D- and L-phenylalanylglycine ethyl esters were synthesized from glycine ethyl ester and D- and L-Boc-phenylalanine, respectively, using dicyclohexyl carbodiimide and hydroxybenzotriazole as condensing agents[13] in dimethylformamide. The Boc protecting group was then removed by treatment with trifluoroacetic acid in dichloromethane. All other amino acid derivatives were obtained from either Bachem (Bubendorf, Switzerland) or Nova Biochem (Läufelfingen, Switzerland) and were used without further purification. Solvents were of either analytical or HPLC grades. HPLC analyses were performed with a LKB (Bromma, Sweden) system comprising a Model 2152 HPLC controller, two Model 2150 HPLC pumps and a Model 2151 variable-wavelength monitor.

Polymer preparation

Polymers were prepared by either thermal initiation or photolytic initiation with azobisnitriles (AIBN or ABDV)[11]. The composition of the standard polymerization mixture, determined from the experiments described herein, is shown in Table I. The crystalline print molecule (L-phenylalanine anilide), functional monomer (MAA), cross-linking monomer (EDMA), initiator and solvent (most commonly chloroform) were weighed into 50-ml borosilicate glass ampoules (Wheaton Scientific, Melvill, NJ, U.S.A.). Solubilization was achieved by sonication and the mixture was then cooled on ice. The mixture was degassed under vacuum in a sonicating bath

TABLE I

STANDARD POLYMERIZATION MIXTURE

Crystalline print molecule (L-phenylalanine anilide), functional monomer (MAA), cross-linking monomer (EDMA), initiator (AIBN) and solvent (chloroform) were added to 50-ml borosilicate glass ampoules, and complete solubilization was achieved by sonication.

Addition	*mg*	*mmol*	*mol %*[a]
Print molecule	474	1.956	4
MAA	677	7.86	16
EDMA	7790	39.3	80
AIBN	94.5	0.57	–
Solvent		12 ml	

[a] Calculated by neglecting the initiator (AIBN). Molar ratio MAA/print molecule is 4:1.

and sparged with nitrogen for 5 min. Then the ampoules were sealed with Parafilm. For thermal initiation, the ampoules were placed in a water-bath at the temperature of decomposition of the initiator (AIBN, 60°C; ABDV, 40°C). For photoinitiation, the ampoules were irradiated at 366 nm, using a standard laboratory UV source, at 4°C. In all cases, polymerization was allowed to proceed overnight (18 h), after which the ampoules were smashed. The polymer was ground in a mortar and wet-sieved in water to the desired size distribution. Particles which passed through a 25-μm sieve constituted a fraction of <25 μm. In all cases, dust was removed by flotation in acetonitrile, and the particles were finally dried under vacuum.

High-performance liquid chromatography

For particles of 45–63 μm, HPLC columns (100 mm × 5 mm or 200 mm × 5 mm) were dry-packed. Particles <25 μm were slurried by sonication in water–acetonitrile–acetic acid (10:9:1; v/v/v) and packed using the same solvent at 300 bar using an air-driven fluid pump (Haskel Engineering Supply, Burbank, CA, U.S.A.). All columns were then washed on-line with acetonitrile–acetic acid (9:1; v/v) at a flow-rate of 1 ml/min until a stable baseline was obtained. HPLC analyses were performed isocratically with either 19:1 (v/v) or 9:1 (v/v) acetonitrile–acetic acid at a flow-rate of 1 ml/min and detection at 260 nm. Analyses were performed at room temperature. Samples to be analysed were prepared in either acetonitrile or acetic acid, depending on their solubility, and were injected in a total volume of 20 μl. Routinely, a mixture of 25 μg of each of the L- and D-enantiomers of a given compound was injected for analysis. Enantiomeric resolution was confirmed by separate injections of each of the enantiomers. All samples analysed contained 1 μg of a non-interacting, non-excluded void marker, Boc-L-phenylalanine anilide purified as an intermediate in the synthesis of the print molecule, L-phenylalanine anilide[11].

RESULTS

Factors affecting printing efficiency and column performance

Previous descriptions of the preparation of molecular imprints have predominantly involved the use of thermal initiators[1–10]. Most commonly, AIBN has been

used at polymerization temperatures of 60–120°C. We were interested in investigating the effect of the polymerization temperature on the subsequent performance of the polymers for two major reasons. First, it was considered that the interactions between the print molecule and the functional monomers would be stronger at lower temperature, thereby increasing the printing efficiency. Secondly, polymerization at elevated temperatures was considered to be inappropriate for the imprinting of temperature-sensitive molecules.

Initial investigations on the effect of polymerization temperature involved the preparation of polymers at 60°C, using AIBN, and at 40°C using ABDV as the initiators. Analyses of these polymers in HPLC for the separation of the enantiomers of the print molecule (L-phenylalanine anilide) showed that polymerization at 40°C resulted in a small but significant increase in the observed separation. We therefore sought to decrease the temperature of polymerization even further through the use of photosensitizers and photoinitiators. It was subsequently realized that the azobisnitriles undergo photolytic decomposition when irradiated at 366 nm (refs. 14 and 15) and it was demonstrated that molecular imprints could be prepared using this type of initiation at temperatures as low as 0°C[11]. Polymers prepared in this manner resulted in excellent enantiomeric resolution of a racemic mixture of the print molecule (Fig. 1). The results shown in Fig. 1 were obtained with a polymer prepared using photoini-

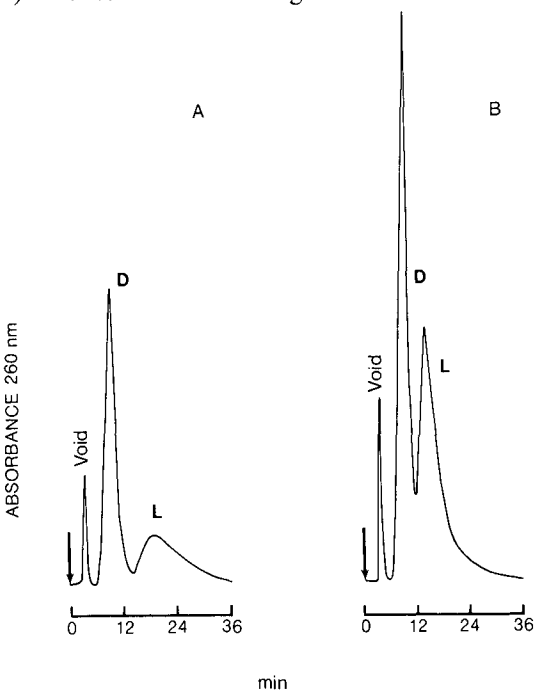

Fig. 1. Resolution of the enantiomers of the print molecule. Particles < 25 μm were packed into a 200 mm × 5 mm stainless-steel column. Analyses were performed at room temperature under isocratic conditions using acetonitrile–acetic acid (9:1, v/v) as the eluent at a flow-rate of 1 ml/min. Detection was at 260 nm. Samples consisted of a mixture of either 5 (A) or 100 μg (B) of each of the enantiomers of phenylalanine anilide. Boc-L-Phenylalanine anilide was included in each sample as a non-interacting, non-excluded void marker. The arrows indicate the point of sample injection. Peaks corresponding to the void and the D- and L-enantiomers of phenylalanine anilide are clearly indicated.

tiation with AIBN at 0°C and chloroform as the polymerization solvent. As is seen, baseline separations were obtained with low sample loads (5 μg of each enantiomer; A). The polymer also exhibited a rather high capacity in that acceptable separations were obtained with sample loads of 100 μg of each enantiomer (B). It should be noted that the results presented in Fig. 1 were obtained under isocratic conditions at room temperature. This contrasts with previous reports where separations needed to be performed at column temperatures of up to 90°C[10].

As has been described for other HPLC matrices, the use of small particles and long, thin columns, increased the separations obtained on molecularly imprinted polymers (data not shown). Routinely therefore, particles of < 25 μm and columns of 200 mm × 5 mm were used in subsequent experiments.

A previous report suggested that the functional monomer, methacrylic acid, interacts with the print molecule, phenylalanine anilide, in a 2:1 complex involving an ionic bond to the free primary amine and an hydrogen bond to the amide[10]. We were interested in defining these interactions from the point of view of polymer preparation and specificity. Therefore, a series of polymers, listed in Table II, were prepared and analysed in HPLC for their ability to separate the enantiomers of phenylalanine anilide. Polymer 1, prepared in the absence of print molecule, and polymer 2, prepared using a non-interacting monomer (methyl methacrylate), did not retain phenylalanine anilide. This result shows that recognition of molecules by molecularly imprinted polymers depends on both the print molecule and the functional monomer and is therefore a "specific" event. Polymer 3 was also unable to recognize phenylalanine anilide. This indicates that a one-point interaction between the print molecule and the polymer is insufficient for enantiomeric resolution, at least in this system and under the conditions used for analysis. The results of analyses of polymers 4–6 indicated that the "optimum" ratio of functional monomer/print molecule was 4:1 (not shown).

Enantiomeric resolution of other amino acid amides

We considered that a polymer prepared using phenylalanine anilide as the print molecule may also be able to separate the enantiomers of other amide derivatives of amino acids, since the positioning of functional groups within the polymer was de-

TABLE II

POLYMER PREPARATIONS

Polymer[a] *(monomer:print)*	*mmol component added*[b]			
	PA	*MAA*	*MM*	*EDMA*
1 (0)	0	7.5	0	36.62
2 (0)	1.956	0	7.86	39.3
3 (1:2)	1.956	0.975	6.885	39.3
4 (2:1)	1.956	3.93	3.93	39.3
5 (4:1)	1.956	7.86	0	39.3
6 (8:1)	1.31	10.48	0	50.26

[a] (monomer:print) refers to the molar ratio of functional monomer (MAA) to print molecule (PA).

[b] PA = L-Phenylalanine anilide; MAA = methacrylic acid; MM = methyl methacrylate; EDMA = ethylene glycol dimethacrylate.

TABLE III

ENANTIOMERIC RESOLUTION OF AMIDE DERIVATIVES OF AMINO ACIDS ON POLYMER 5 (TABLE II)

A mixture of 25 μg of each of the enantiomers of the amide derivative of the amino acid was injected into the column in a total volume of 20 μl and eluted with acetonitrile–acetic acid (9:1, v/v) at room temperature. Detection was at 260 nm. The (+) indicates that enantiomeric resolution was obtained. NT indicates that the compound was not tested, either because both enantiomers were not commercially available or UV detection was not possible, *e.g.*, for the amides of leucine and alanine.

Amino acid	*Derivative*[a]			
	A	*p-NA*	*β-NA*	*Amide*
Phenylalanine	(+)	(+)	NT	(+)
Tyrosine	(+)	NT	NT	NT
Tryptophan	(+)	NT	NT	(+)
Leucine	NT	(+)	(+)	NT
Alanine	NT	(+)	(+)	NT

[a] A = Anilide; *p*-NA = *p*-nitroanilide; *β*-NA = *β*-naphthylamide.

fined. A number of derivatives of amino acids, including amides, esters and dipeptides, were thus analysed on polymer 5 (Table II). In all cases investigated, enantiomeric resolution was obtained for the amide derivatives of amino acids (see Table III) and representative elution profiles are shown in Fig. 2.

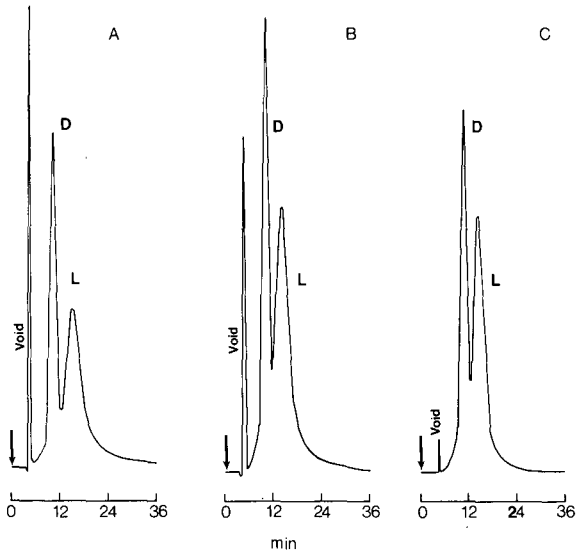

Fig. 2. Enantiomeric resolution of amide derivatives of amino acids on polymer 5 (Table II). Particles < 25 μm, prepared from polymer 5 (Table II), were packed into a 200 mm × 5 mm column. Analyses were performed at room temperature with acetonitrile–acetic acid (9:1, v/v) as the eluent at 1 ml/min. Detection was at 260 nm. In all experiments, a mixture of 25 μg of each of the enantiomers of the compound was analysed. Boc-L-Phenylalanine anilide was included as a void marker. The analyses shown are: (A) D,L-tryptophan anilide; (B) D,L-leucine-*β*-naphthylamide; (C) D,L-alanine-*p*-nitroanilide.

From these data it is clear that a single polymer is able to recognize and separate enantiomers of molecules having structures similar to that of the original print molecule. The most important factor for enantiomeric resolution in this system would appear to be the presence of both an amine and an amide, in the correct spatial orientation, on the molecule being analysed. This is clearly demonstrated by the fact that removal of the amine, as in Boc-L-phenylalanine anilide, results in elution of this compound with the solvent front (see Figs. 1 and 2). In addition, removal of the amide, as in D,L-phenylalanine benzyl ester, results in retention but no enantiomeric resolution (not shown).

Preliminary experiments also indicate that the enantiomers of phenylalanine-containing dipeptides such as D,L-phenylalanylglycine ethyl ester are resolved on this polymer, whereas glycyl-D,L-phenylalanine is retained but no enantiomeric resolution is obtained. Therefore, polymers prepared by the technique of molecular imprinting may find use in the identification and purification of peptides.

Proposed mechanism of enantiomeric resolution

Both a free primary amine and an amide, in the correct spatial orientation, are required to achieve enantiomeric resolution. Initial recognition probably occurs via "ion pairing" between the free primary amine of the molecule and a free carboxylic acid group of the polymer. This relatively strong interaction places the molecule in a position to hydrogen bond through the amide function to another carboxylic acid function of the polymer. Since polymers prepared in the absence of either print molecule or functional monomer (polymers 1 and 2, Table II) do not subsequently recognize the print molecule, it can be concluded that enantiomeric discrimination by polymers, such as polymer 5, is a specific event and dependent on the interaction(s) of print molecules with functional monomers in solution prior to polymerization. These interactions result in a polymer which has carboxylic acid functions exactly positioned to interact with the print molecule in a stereospecific manner. In addition, the mechanism of recognition cannot be of a simple ion-exchange type, since this would also be expected to occur in a polymer with randomly distributed carboxylic acid functions, as in polymer 1 (Table II). Therefore, it can be assumed that the stereospecific interaction of molecules with the polymer occurs within specific sites of the polymer which are a direct result of the interactions of molecules in solution prior to polymerization.

DISCUSSION

The technique of molecular imprinting is gaining acceptance as a means of producing specialty separation media, particularly for enantiomeric resolution of chiral molecules[1]. In the present paper, we have presented some of our recent work on the preparation of molecular imprints for the enantiomeric resolution of amino acid derivatives. The method involves the formation of non-covalent interactions between the print molecule and functional monomers, in solution, prior to the initiation of polymerization. These interactions are subsequently responsible for the recognition of molecules by the polymer.

The method of polymerization presented herein shows distinct advantages over those previously presented from the point of view of simplicity and speed of prep-

aration of polymers. From an operational standpoint, polymers prepared by this technique exhibit excellent enantiomeric resolution under standard HPLC conditions. HPLC analyses were performed at room temperature and at flow-rates of 1 ml/min, resulting in pressures of 60—70 bar for a 200 mm × 5 mm column, packed with particles < 25 μm. Previous descriptions of the use of molecular imprints in the HPLC mode required column temperatures of up to 90°C, and flow-rates of only 0.3 ml/min were used to achieve separations comparable to those presented here[1,4,10]. In addition, the demonstration that efficient molecular imprints can be prepared simply at temperatures down to 0°C adds a degree of flexibility to the method of preparation of polymers and should be particularly valuable for the imprinting of temperature-sensitive molecules. However, it is important to note that, even in the system studied here, better printing was obtained with polymerization at 0°C than at 60°C. Therefore, the preparation of molecular imprints at low temperature should be considered as a general method. It should also be stressed that the initiator used in the present system, AIBN, is the same initiator used by previous workers for the preparation of molecular imprints at temperatures ranging from 60 to 120°C[1,10].

The interactions between the print molecule and functional monomer prior to polymerization are, of course, central to the successful preparation of molecular imprints. Two factors affecting these interactions are the temperature (discussed above) and solvent of polymerization. Similar to work of other investigators[1] we have shown that it is possible to "tailor" the strength of the interactions by manipulation of the solvent of polymerization[11]. This may prove useful in certain situations. Of course, the same effect(s) of solvent should apply to the elution of compounds from molecularly imprinted polymers. However, little work has been done in this area. It is possible that a thorough investigation of elution conditions may further improve the separations, particularly the peak shape. It should be noted that extremely irregular particles of relatively poorly defined size have been used for the analysis of molecular imprints. The preparation of molecular imprints in a beaded form, with small particle size, as is common for other HPLC packings, may also prove advantageous.

The ability of a single polymer to separate the enantiomers of molecules other than the print molecule, as presented here, is an important concept. This may allow the design and preparation of molecular imprints by using a "soluble" derivative of a molecule which is itself insoluble in the polymerization mixture. An example of this is D,L-phenylalanine amide, which is insoluble in the polymerization mixture but may be applied and separated on a polymer prepared using L-phenylalanine anilide as the "soluble" print molecule. We are following this approach for the imprinting of molecules other than amino acid derivatives. Another potential application of molecular imprinting is in preparative-scale chiral separations of biological or pharmaceutical preparations. This would be of particular value in situations where other chiral separation methods do not achieve the required enantiomeric enrichment.

REFERENCES

1 G. Wulff, *ACS Symp. Ser.*, 308 (1986) 186.
2 Y. Fujii, K. Matsutani and K. Kikuchi, *J. Chem. Soc., Chem. Commun.*, (1985) 415.
3 G. Wulff, B. Heide and G. Helfmeier, *J. Am. Chem. Soc.*, 108 (1986) 1089.
4 G. Wulff, H-G. Poll and M. Minárik, *J. Liq. Chromatogr.*, 9 (1986) 385.
5 O. Norrlöw, M.-O. Månsson and K. Mosbach, *J. Chromatogr.*, 396 (1987) 374.

6 K. J. Shea and T. K. Dougherty, *J. Am. Chem. Soc.*, 108 (1986) 1091.
7 L. Andersson, B. Sellergren and K. Mosbach, *Tetrahedron Lett.*, 25 (1984) 5211.
8 B. Sellergren, B. Ekberg and K. Mosbach, *J. Chromatogr.*, 347 (1985) 1.
9 L. Andersson, B. Ekberg and K. Mosbach, *Tetrahedron Lett.*, 26 (1985) 3623.
10 B. Sellergren, M. Lepistö and K. Mosbach, *J. Am. Chem. Soc.*, 110 (1988) 5853.
11 D. J. O'Shannessy, B. Ekberg and K. Mosbach, *Anal. Biochem.*, in press.
12 D. J. O'Shannessy, L. I. Andersson and K. Mosbach, *J. Mol. Recog.*, in press.
13 W. König and R. Geiger, *Chem. Ber.*, 103 (1970) 788.
14 F. M. Lewis and M. S. Matheson, *J. Am. Chem. Soc.*, 71 (1949) 747.
15 R. D. Burkhart and J. C. Merrill, *J. Phys. Chem.*, 73 (1969) 2699.

Journal of Chromatography, 470 (1989) 401–406
Elsevier Science Publishers B.V., Amsterdam — Printed in The Netherlands

CHROMSYMP. 1564

DETECTION OF TRYPSIN- AND CHYMOTRYPSIN-LIKE PROTEASES USING *p*-NITROANILIDE SUBSTRATES AFTER SODIUM DODECYL SULPHATE POLYACRYLAMIDE GEL ELECTROPHORESIS

ERKKI KOIVUNEN
Clinical Laboratory, Departments I & II of Obstetrics and Gynecology, Helsinki University Central Hospital, Haartmaninkatu 2, SF-00290, Helsinki (Finland)

SUMMARY

Specific chromogenic *p*-nitroanilide substrates have proved useful for localizing proteolytic enzymes, such as trypsin, chymotrypsin and elastase after separation by agarose gel electrophoresis and when immobilized on nitrocellulose. This procedure was further developed for use with sodium dodecyl sulphate-polyacrylamide gel electrophoresis (SDS-PAGE). After SDS-PAGE, proteins were transferred electrophoretically to a nitrocellulose membrane. The membrane was incubated for 10–60 min with Bz-Ile-Glu-Gly-Arg-*p*-nitroanilide as a substrate for detection of trypsin-like proteases and with MeO-Suc-Arg-Pro-Tyr-*p*-nitroanilide for detection of chymotrypsin. The yellow *p*-nitroanilide released at the site of proteolytic activity was converted into a visible and stable red azo dye. By this method was identified and determined the molecular weight of a trypsin-like protease that occurs at high concentrations in mucinous ovarian tumour cyst fluid together with its specific inhibitor peptide, tumour-associated trypsin inhibitor (TATI). The method was also used to visualize trypsin and chymotrypsin in human pancreatic juice. Using the trypsin substrate, three proteolytic bands, corresponding to M_r of 22 000, 24 000 and 26 000 daltons, were visualized in pancreatic juice, while the proteolytic zones in cyst fluid had M_r of 25 000 and 28 000 daltons. With the chymotrypsin substrate, a band of 29 000 daltons was visualized in pancreatic juice, whereas no activity was detected in cyst fluid. By incubation of the blotted cyst fluid proteins with ^{125}I-labelled TATI, a pattern of bands at 25 000 and 28 000 daltons was detected identical to that obtained with the chromogenic substrate.

INTRODUCTION

Several methods have been developed for the qualitative detection of proteases after electrophoresis. Protein substrates have been impregnated in polyacrylamide gel prior to electrophoresis[1,2], or included in an agarose or agar film, placed in contact with an electrophorogram[3–6]. Alternatively, proteases have been localized by staining with specific chromogenic peptide substrates. In these methods, the liberated chromophore, usually *p*-nitroanilide or β-naphthylamide, must be visualized in the

0021-9673/89/$03.50

gel by coupling to an azo reagent[7,8]. However, with *p*-nitroanilide substrates a practical problem has been the poor resolution and preservation of the dye that does not precipitate in the gel. These disadvantages were recently overcome by enzymoblotting[9]. The substrate reaction was carried out on a nitrocellulose membrane, onto which proteases were transferred by capillary diffusion after agarose gel electrophoresis. This immobilizing matrix restricts diffusion of the enzymatic products and preserves a red azo dye generated from *p*-nitroanilide.

Here it is reported that the chromogenic substrate reaction can be utilized for the detection of proteinases after their separation by sodium dodecyl sulphate-polyacrylamide gel electrophoresis (SDS-PAGE) and after electroblotting. This method was used to visualize a trypsin-like protease in cyst fluid of mucinous ovarian tumours. Previous studies have suggested that this protease is similar to or closely homologous with pancreatic trypsin[10]. It is strongly and specifically inhibited by the Kazal-type inhibitor peptide, tumour-associated trypsin inhibitor (TATI). For comparison, the procedure was also used to study the molecular weight of trypsin and chymotrypsin in human pancreatic juice. In addition, it was shown that [^{125}I]TATI provides an alternative method for localizing trypsin-like proteases immobilized on nitrocellulose.

EXPERIMENTAL

Materials

Bovine trypsin (Type 1, twice crystallized) was obtained from Sigma (St. Louis, MO, U.S.A.). TATI was purified from urine of cancer patients, as described[11]. It was iodinated by the lactoperoxidase method[12].

Cyst fluid of mucinous ovarian tumours was obtained from patients undergoing surgery for removal of the tumour. Pancreatic juice was collected by catheterization of the pancreatic duct in patients with biliary or pancreatic diseases. All samples were stored at –20°C until used.

The chromogenic substrates were dissolved in 50 m*M* Tris–HCl + 20 m*M* $CaCl_2$ + 0.1% Triton X-100 (pH 8.0) at a concentration of 1 mg/ml. The solution was stored at –20°C. N-Benzoyl-L-isoleucyl-L-glutamylglycyl-L-arginine *p*-nitroanilide (S-2222) was used as a substrate for the measurement of trypsin-like activity and 3-methoxycarbonyl propionyl-L-arginyl-L-propyl-L-tyrosine *p*-nitroanilide (S-2586) (Kabi, Stockholm, Sweden) for chymotrypsin-like enzymes.

SDS-PAGE

Sample preparations and electrophoresis were performed according to Laemmli[13] under non-reducing conditions. Prior to electrophoresis, trypsin standards, cyst fluid and pancreatic juice were mixed with an equal volume of Laemmli sample buffer (double concentration), and heated for 2 min in boiling water or incubated for 2 h at 25°C. A sample of 50 μl was applied per lane in the vertical slab gels (16 cm × 18 cm). The acrylamide concentration in the resolving gel was 10 (Fig. 3) or 12.5% (Figs. 1 and 2).

Blotting onto nitrocellulose

Porteins were transferred electrophoretically from SDS gels onto nitrocellulose

(Transblot, Bio-Rad), as described by Towbin *et al.*[14]. Transfer was performed at room temperature for 90 min using a constant current of 250 mA or overnight at 50 mA. Proteins blotted onto the nitrocellulose membrane were first stained reversibly with 0.2% Ponceau S (Chroma, Stuttgart, F.R.G.) in 3% trichloroacetic acid for 2 min in order to facilitate cutting of the lanes into strips. The strips were destained and simultaneously saturated with 2% bovine serum albumin (BSA) in 50 m*M* Tris buffer (pH 7.4), containing 0.9% Triton X-100. Protein standards (Pharmacia, Uppsala, Sweden) were stained with Amido black (Merck, Darmstadt, F.R.G.) Apparent molecular weights of proteases were estimated by comparison with the protein standards.

Detection of proteolytic activity

Incubation with [^{125}I]TATI was performed for 16 h at 25°C, using 500 000 cpm/ml in 50 m*M* Tris buffer (pH 9.0), containing 20 m*M* $CaCl_2$ and 0.1% Triton X-100. After extensive washing of the nitrocellulose sheets with 2% BSA in 50 m*M* Tris buffer (pH 7.4), containing 0.9% Triton X-100 and 0.1 *M* NaCl (BSA buffer), an autoradiogram was generated by placing the dried nitrocellulose paper against X-ray film for 3 d at –70°C. To inhibit immobilized proteases after blotting, nitrocellulose strips were preincubated with TATI at a concentration of 1 μg/ml in BSA buffer for 60 min at 37°C, and then with the chromogenic substrate. The substrate was allowed to react for 10–60 min, and to prevent background staining the incubation was stopped when faintly yellow *p*-nitroanilide bands appeared. The released *p*-nitroanilide was then diazotized by immersing the nitrocellulose membrane for 5 min in a solution of 0.1% sodium nitrite in 1.0 *M* HCl and then for another 5 min in 0.5% ammonium sulphamate in 1.0 *M* HCl. Dark red bands were developed with a fresh solution of 0.05% N-(1-naphthyl)ethylenediamine (Sigma) in 47.5% ethanol[9,15]. After the bands had reached their maximum intensity (1–5 min), the nitrocellulose membrane was washed with water and stored at –20°C. The red bands were best visualized by wetting the nitrocellulose with water.

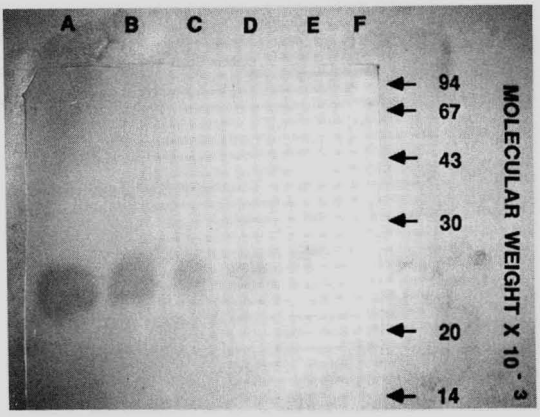

Fig. 1. Estimation of the detection limit for bovine trypsin with substrate S-2222. Lanes A–F contained 500, 300, 100, 50, 20 and 1 ng of trypsin, respectively, separated by SDS-PAGE and electroblotted onto nitrocellulose. The molecular weight marker proteins, treated in parallel, are shown to the right: phosphorylase b (94 000), albumin (67 000), ovalbumin (43 000), carbonic anhydrase (30 000), soy bean trypsin inhibitor (20 000) and lactalbumin (14 000 daltons).

RESULTS

Sensitivity of the method

The sensitivity of this method was tested by analysing decreasing amounts of commercial bovine trypsin. The trypsin activity on the nitrocellulose membrane was developed by incubating for 40 min with S-2222 as a substrate. Fig. 1 shows that bovine trypsin migrates with an apparent M_r of 23 000 daltons, the minimum detectable amount of trypsin is 20 ng. When samples were reduced with 2-mercaptoethanol before electrophoresis, no proteolytic activity was detected.

Detection of pancreatic trypsin and chymotrypsin

Fig. 2A shows a typical staining pattern with 25 μl of pancreatic juice using S-2222 as a substrate. Three amidolytic zones at 22 000, 24 000 and 26 000 daltons are observed, demonstrating molecular weight heterogeneity. With the chymotrypsin substrate S-2586, only one active band, migrating at 29 000 daltons, was discovered in pancreatic juice (Fig. 2C).

Visualization of the trypsin-like protease in mucinous ovarian cyst fluid

Of twelve cyst fluid samples studied, three contained detectable amidolytic activity migrating at 25 000 daltons, and in one sample a minor active band of 28 000 daltons was also detected, by using S-2222 as a substrate (Fig. 2B). In addition, a faint amidolytic band emerged at M_r 75 000 daltons when the substrate reaction was performed at pH 9.0 (not shown). With the chymotrypsin substrate S-2586, no activity was detected.

Binding of TATI to proteases immobilized onto nitrocellulose

When the nitrocellulose membranes were preincubated with TATI no amido-

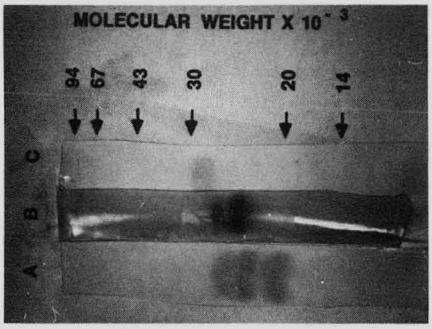

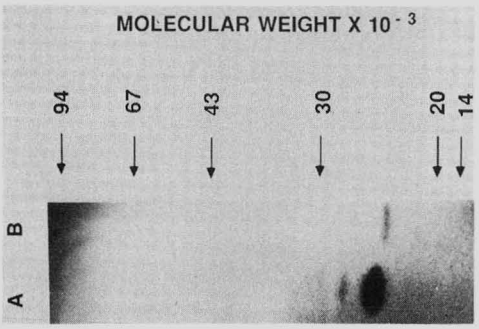

Fig. 2. Visualization of human pancreatic trypsin, ovarian tumour-associated trypsin-like protease and pancreatic chymotrypsin with chromogenic substrates. After SDS-PAGE, proteins were transferred onto nitrocellulose. (A) Pancreatic juice (25 μl), stained for trypsin activity with S-2222 as a substrate (30-min incubation); (B) mucinous ovarian tumour cyst fluid (25 μl), stained for activity against S-2222 (60-min incubation); (C) pancreatic juice (25 μl), stained for chymotrypsin activity with substrate S-2586 (30-min incubation). The positions of the molecular mass standards are indicated on the right (*cf.*, Fig. 1).

Fig. 3. Binding of [^{125}I]TATI to immobilized proteases. Lanes A and B contained 25 μl of mucinous ovarian cyst fluid and of pancreatic juice, respectively, separated by SDS-PAGE and electroblotted onto nitrocellulose. After extensive washing, the complexes labelled with TATI were visualized by autoradiography. The positions of the molecular weight standards are shown to the right.

lytic activity was detected in cyst fluid samples with S-2222 as a substrate (not shown). Incubation of nitrocellulose membranes containing cyst fluid and pancreatic juice proteins with ^{125}I-labelled TATI showed that TATI is bound to the cyst fluid proteins of 25 000 and 28 000 daltons and to pancreatic trypsin of 24 000 daltons (Fig. 3). Weak binding of TATI to the cyst fluid protein of 75 000 daltons was also observed (not shown).

DISCUSSION

This paper describes a simple, sensitive method for visualization of proteases, blotted onto a nitrocellulose membrane after separation by SDS-PAGE. Proteases are detected by incubation with specific *p*-nitroanilide substrates and coupling the hydrolysed *p*-nitroanilide to an azo dye. The dark red bands that form against a white background are stable for years when the nitrocellulose is stored at –20°C.

The chromogenic substrate reaction on the nitrocellulose was originally reported by Ohlsson *et al.*[9] for localizing trypsin, chymotrypsin and elastase, separated by agarose gel electrophoresis. This study shows that proteases, such as trypsin, chymotrypsin and the trypsin-like protease associated with ovarian tumour, are recovered in active form on nitrocellulose, even after the denaturating conditions in SDS-PAGE and electroblotting. An apparent advantage of the use of SDS and heating of samples before electrophoresis is the dissociation of complexes between a protease and its inhibitor, which enables detection of proteolytic activity in crude biologic samples containing an excess of inhibitors.

By the present method the apparent molecular weights of proteases can be determined. Using the substrate S-2222, three trypsin bands (M_r 22 000, 24 000 and 26 000 daltons) were found in human pancreatic juice. Two trypsin isozymes differing slightly in mobility in SDS-PAGE have been characterized in detail earlier[16,17]. Using the chymotrypsin substrate S-2586, I observed one band in pancreatic juice migrating at 29 000 daltons, which corresponds to the molecular weight of human chymotrypsin, reported earlier[17]. The analysis of mucinous ovarian tumour cyst fluid with the S-2222 substrate revealed two proteolytic bands, a major one at 25 000 and a minor one at 28 000 daltons.

The sensitivity of the method depends on the hydrolysis rate of the chromogenic substrate used for a given protease. Using a temperature of 37°C and pH 8.0, a detection limit of 20 ng was obtained for commercial bovine trypsin after incubating for 40 min with S-2222 as a substrate. Lowering the temperature to 25°C decreased the substrate reaction but did not improve the sharpness of protease bands. Interestingly, by elevating the pH of the incubation media to 9.0, a faint amidolytic band was observed in cyst fluid migrating at 75 000 daltons that also bound labelled TATI. The identity of this proteolytic activity is unknown.

Immobilization of proteases on a nitrocellulose matrix offers several advantages. Once immobilized, proteases are stable for long periods of time, and they are accessible to different detection procedures and chemical reactions, *e.g.*, it is possible to activate the zymogen forms of proteases[9]. The binding of ^{125}I-labelled TATI to blotted proteases was also studied. Autoradiography of the bound TATI yielded a pattern of two bands identical with that obtained by the chromogenic substrate reaction in mucinous ovarian cyst fluid. Furthermore, inhibition of the proteolytic activ-

ity by TATI was used to demonstrate the inhibitor specificity of the bound protease.

Several *p*-nitroanilide substrates that allow sensitive and selective detection are now available for various proteases, for example plasminogen activators, plasmin, elastase and thrombin. If used as described here, they might provide useful alternatives to protein substrates for detection of proteolytic activity after SDS-PAGE.

ACKNOWLEDGEMENTS

I thank U.-H. Stenman for critical reading of this manuscript and H. Alfthan for advice in photography. This study was supported by grants from the Academy of Finland, the Finnish Cancer Society and the Sigrid Juselius Foundation.

REFERENCES

1 C. Heussen and E. B. Dowdle, *Anal. Biochem.*, 102 (1980) 196.
2 E. F. Plow, *Biochim. Biophys. Acta*, 630 (1980) 47.
3 O. Vesterberg and R. Eriksson, *Biochim. Biophys. Acta*, 285 (1972) 393.
4 J. Dijkhof and C. Poort, *Anal. Biochem.*, 83 (1977) 315.
5 J. L. Westergaard, C. Hackbarth, M. W. Treuhaft and R. C. Roberts, *J. Immunol. Methods*, 34 (1980) 167.
6 D. Every, *Anal. Biochem.*, 116 (1981) 519.
7 P. Fric, J. Slaby, E. Kasafirek and F. Malis, *Clin. Chim. Acta*, 63 (1975) 309.
8 J. S. Mort and M. Leduc, *Anal. Biochem.*, 119 (1982) 148.
9 B. G. Ohlsson, B. R. Weström and B. W. Karlsson, *Anal. Biochem.*, 152 (1986) 239.
10 U.-H. Stenman, E. Koivunen and M. Vuento, *Biol. Chem. Hoppe-Seyler*, 369 (1988) 9.
11 M.-L. Huhtala, K. Pesonen, N. Kalkkinen and U.-H. Stenman, *J. Biol. Chem.*, 257 (1982) 13713.
12 S.-L. Karonen, P. Mörsky, M. Siren and U. Seuderling, *Anal. Biochem.*, 67 (1975) 1.
13 U. K. Laemmli, *Nature (London)*, 227 (1970) 680.
14 H. Towbin, T. Staehelin and J. Gordon, *Proc. Natl. Acad. Sci. U.S.A.*, 76 (1979) 4350.
15 F. Willig and W. Körber, *Z. Gastroenterol.*, 5 (1967) 33.
16 O. Guy, D. Lombardo, D. C. Bartelt, J. Amic and C. Figarella, *Biochemistry*, 17 (1978) 1669.
17 G. Scheele, D. Bartelt and W. Bieger, *Gastroenterology*, 80 (1981) 461.

Journal of Chromatography, 470 (1989) 407–414
Elsevier Science Publishers B.V., Amsterdam — Printed in The Netherlands

CHROMSYMP. 1597

ISOTACHOPHORESIS OF PROTEINS

FERNANDO ACEVEDO
Department of Dermatology, Karolinska Hospital, Karolinska Institute, 104 01 Stockholm (Sweden)

SUMMARY

The analytical separation of proteins by isotachophoresis (ITP) was achieved in a short electrophoretic path and with a resolution comparable to that of isoelectric focusing by the appropriate selection of (1) a mixture of ampholytes as spacers to generate linear gradients of electrophoretic mobility and (2) the counter ions chosen to buffer the complete pH gradient generated. This ITP technique is exemplified by the analysis of plasma proteins in agarose gels. Up to 46 samples in the same gel plate were analysed. The resolution was such that at least 30 clear and discrete bands per sample could be observed after staining with Coomassie Brilliant Blue. The resolving power of ITP could be further increased for the study of a particular protein or zone by the selection of suitable spacers and counter ions.

INTRODUCTION

Isotachophoresis (ITP) has the resolving capacity inherent in isoelectric focusing (IEF) and the advantage of flexibility of pH and ionic strength, which confers great potential for analytical and preparative separations of proteins. However, the use of ITP for the separation of proteins has been scant. Two major problems that limit this application have been pointed out by Nguyen and Chrambach[1]: first, the lack of spacers to generate a continuous gradient of electrophoretic mobility, and second, the length of the electrophoretic path required to obtain a steady state. In this paper, we present an ITP technique for the analytical separation of proteins in which mixtures of commercially available ampholytes are used as spacers. The analytical separation of plasma proteins in agarose gels is used as a model system to illustrate the technique.

THEORETICAL

Theoretically, in ITP the components of the mixture should migrate at the same velocity and stack according to their electrophoretic mobilities (U). The Kohlrausch function, defined as

$$\omega_i = \sum_j C_{ij}/U_{ij},$$

where C_{ij} is the concentration of the jth component in the ith phase, should have the

0021-9673/89/$03.50

same value in all phases. The concentration of each component in the stack is given by the concentration and electrophoretic mobility of the components in the leading zone, and the system is self-regulated against diffusion[2]. The leading ion should have (1) an electrophoretic mobility slightly higher than that of any component in the mixture, in order to avoid conductivity jumps, and (2) a concentration such that all the components in the mixture stack in an adequate length.

Two aspects require attention in the design of an isotachophoretic system for the separation of proteins: the counter ions and the spacers.

Counter ions

Electroneutrality requires that the concentration of ions of different sign should be equal in any phase. Therefore, the charge provided by the counter ions is an important factor in the stablishment of an ITP system. To illustrate this, let us consider IEF as a special case of ITP where the final velocities of the components are close to zero (Fig. 1A).

The addition of a strong ion, for instance Na^+, to ampholytes which are focused in an electric field causes the migration of the stack of ampholytes and the pH gradient towards the anode. As the counter ion is strong, it will cause the protonation of weakly ionized groups of the ampholytes. Consequently, the charges of all stacked ampholytes

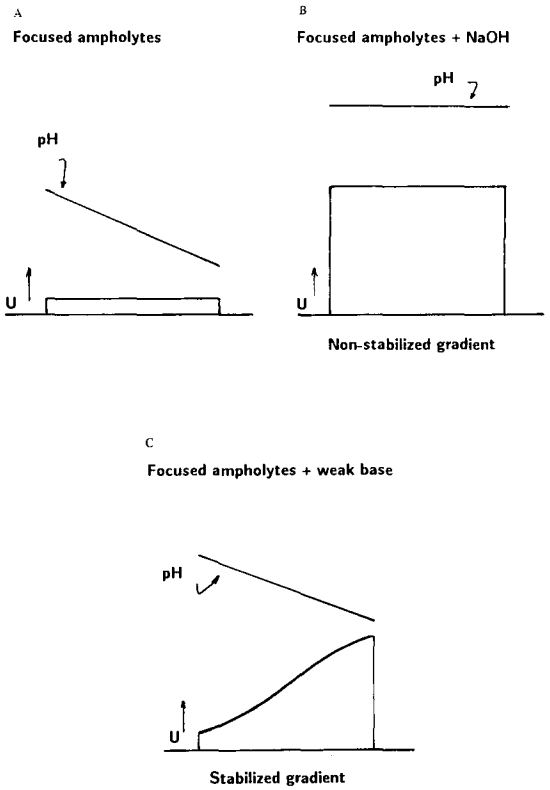

Fig. 1. Electrophoretic mobility *vs.* distance. (A) Focused ampholytes; (B) focused ampholytes after addition of a strong base; (C) focused ampholytes after the addition of a weak base.

will be similar and they will mix, with the consequence that the pH gradient will vanish during the migration (Fig. 1B). On the other hand, the addition of a weak ion, *i.e.*, with a pK_b value in the p*I* zone of the focused ampholytes, will stabilize the pH gradient; the ampholytes on the acidic side of the pK_b will migrate faster than those on the basic side towards the anode, owing to the higher charge conferred upon the former by the weak base used as the counter ion (Fig. 1C).

Spacers

The separation of proteins by ITP is based on their differences in electrophoretic mobility. Therefore, suitable spacers for analytical ITP should generate a continuous linear gradient of electrophoretic mobility. According to the Kohlrausch function for a moving boundary, the concentration of the ions in the different zones obtained by ITP is determined by their electrophoretic mobility. Consequently, in order to develop a linear gradient of electrophoretic mobility, the amount of any particular spacer should be proportional to its electrophoretic mobility. Commercially available ampholyte mixtures are designed for IEF where an equal concentration of all the different p*I* ampholytes is desired. Therefore, a non-linear gradient of electrophoretic mobility will be generated when these ampholyte mixtures are used in ITP. However, IEF ampholytes can be used as spacers for ITP if the concentration of each component is adjusted to its electrophoretic mobility. This can be achieved by fractionating commercially available ampholytes according to their p*I* and then preparing a mixture with concentrations inversely proportional to their p*I* values. Commercially available ampholytes of narrow pH range can be mixed to generate nearly linear gradients of electrophoretic mobility and produce good results, as illustrated in this paper. The addition of a terminating ion with a lower mobility will, together with the leading ion, set the limits of the migration velocities and complete the isotachophoretic system.

EXPERIMENTAL

Human plasma samples were supplied by the blood centre at the Karolinska Hospital. Ampholytes and paper electrode strips were obtained from LKB (Bromma, Sweden), agarose, electrode strips and paper sample applicators from Pharmacia (Uppsala, Sweden), rabbit immunoglobulins (Igs) against human antigens and horseradish peroxidase-conjugated swine antibodies against rabbit Igs from Dakopatts (Copenhagen, Denmark), Gelbond from FMC Bioproducts (Rockland, ME, U.S.A.), swine serum from Flow Laboratories (Uxbridge, Middlesex, U.K.) and dry defatted milk from Semper (Stockholm, Sweden). All chemicals were of analytical-reagent grade.

Isotachophoresis in agarose gels

The procedure was basically as described by Acevedo[3]. The plasma proteins were electrophoresed towards the anode in 0.1 × 12 × 24 cm 1% agarose IEF, 12% sorbitol gels, at 10°C, on a flat-bed electrophoresis apparatus (Pharmacia FBE3000).

The gels were cast in buffers formed by the leading ion and the counter ion or counter ions. The spacers were either included in the gel, in the electrode solution, or in a small portion of the gel behind the samples. The electrode solutions, 10 or 20 ml, which contained the leading and counter ions (anode) or the terminating ion (cathode),

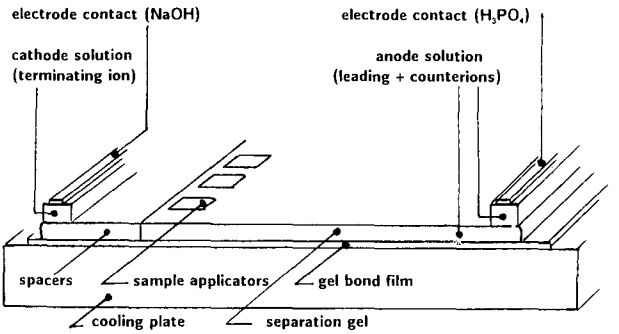

Fig. 2. Assembly for agarose gel ITP. The use of electrode vessels for the electrode solutions connected to the gel by means of paper wicks produces the same results.

were absorbed in electrode strips, placed on the edge of the gel. The use of 500-ml electrode vessels for the electrode solutions, connected to the gel by means of paper wicks, produced the same results. In the former instance, the contact between the electrode wires and the strips containing the electrode solutions was mediated by either 1 *M* phosphoric acid or sodium hydroxide, respectively (see Fig. 2).

The gels were pre-run for about 1 h at 5–10 W until the isotachophoretic front reached 1.5–2 cm from the cathode. Then the samples (8 μl of 20% plasma in 5% Ampholytes 5–7) were applied on paper sample applicators, cut to half the width (1 × 0.25 cm) and placed behind the front and perpendicular to it. Electrophoresis was carried at 5–20 W (300–1200 V) until the steady state was reached. This was observed by the formation of sharp lines at the front and rear ends, which migrated at the same velocity, or until the leading front reached the anode, after *ca.* 3–5 h at 10°C. In some instances, the gel shrank at the cathodic side. This was observed as a decrease in the current and a flattening of the gel surface immediately at the electrode contact. In such an event, to avoid burning of the gel, the electrode contact was advanced a few millimetres (2–10) and electrophoresis was continued at a lower power setting. The protein bands were revealed with Coomassie Brilliant Blue (CBB) or by immuno techniques and scanned in a LKB laser gel scanner.

Conductivity and pH measurements

Pieces of gel of 1 × 0.5 cm were cut and left overnight at room temperature in 1.5 ml of distilled water for conductivity measurements or in 1 ml of 10 m*M* potassium chloride solution for pH measurements.

Immunodetection

The proteins were transferred to a nitrocellulose (NC) filter by overlaying the gel with a stack, consisting of a wet NC filter, a layer of wet blotting paper, eight layers of dry blotting paper (Munktell, Stora, Sweden), a glass plate and, on the top, a 5-kg weight for 20 min at room temperature. The immunological detection of proteins on NC filters was performed essentially as described by Andrews[4], except that 5% dry defatted milk in 0.9% NaCl–10 m*M* Tris–HCl buffer (pH 7.4) (TBS) was used instead of bovine serum albumin. The Igs were diluted 1:1000 in 5% dry defatted milk–10% swine serum in TBS. Peroxidase-labelled antibodies were detected with 4-chloro-1-naphthol.

RESULTS

The result of an isotachophoretic separation of plasma proteins is illustrated in Fig. 3A. The protein bands, stained after ITP, are as sharp as expected for IEF, in spite of the 1-cm-long application zone, and more than 30 clear and discrete bands, stained with Coomassie Brilliant Blue, as illustrated by the scanning result shown in Fig. 4. The result of conductivity and pH measurements on a gel similar to that shown in Fig. 3A is illustrated in Fig. 5 and shows a linear pH gradient, from 5 at the front to 9 at the terminating zone, and a non-linear conductivity gradient, which are conditions expected for an ITP stack. Other characteristics of the ITP system described here were that the migration velocities of the leading and the terminating fronts were the same, and consequently the length of the ITP train was constant (this length was dependent on the type and amount of ampholytes used and the type and concentration of the leading ion), and the pH value for any protein zone in the stack was higher than the protein's isoelectric point.

The resolution can be increased for a particular protein or pH zone by the selection of ampholyte mixtures with a narrow p*I* interval as spacers and counter ions with pK_b in this interval, as illustrated in Fig. 3. Two different transferrin forms,

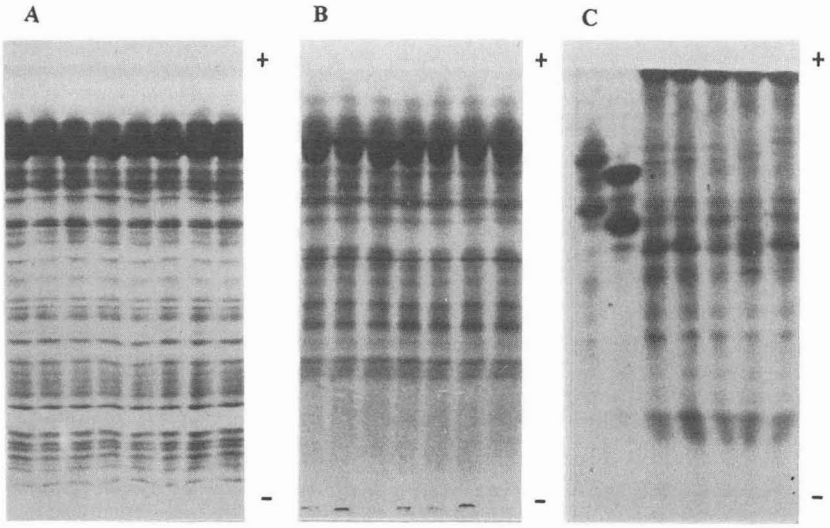

Fig. 3. Agarose gel ITP of plasma proteins. CBB staining. (A) The spacers (pH 3.5–10) were placed behind the separation gel. Separation gel (24 × 10 × 0.1 cm): 120 m*M* glutamic acid–40 m*M* Tris-base–20 m*M* imidazole–20 m*M* Bis-Tris–40 m*M* pyridine. Spacer-containing gel (24 × 2 × 0.1 cm): 565 μl of Ampholytes 3.5–10, 175 μl of 7–9, 175 μl of 6–8, 350 μl of 5–7, 350 μl of 4–6, 400 μl of 3.5–5 and 120 m*M* lysine. Terminating ion: lysine. Anode: 20 ml of 400 m*M* Tris–200 m*M* imidazole–200 m*M* Bis-Tris–400 m*M* pyridine–400 m*M* glutamic acid. Cathode: 10 ml of 120 m*M* lysine. Power setting: 10 W. (B) The spacers (pH 3.5–7) were included in the separation gel (24 × 12 × 0.07 cm): 120 m*M* glutamic acid–30 m*M* imidazole–90 m*M* histidine. 600 μl of Ampholytes 3.5–5, 400 μl of 4–6 and 400 μl of 5–7. Terminating ion: β-alanine. Anode: 20 ml of 150 m*M* imidazole–450 m*M* histidine–300 m*M* glutamic acid. Cathode: 10 ml of 1 *M* β-alanine–250 m*M* histidine. Power setting: 10 W. (C) The spacers (pH 5–7) were included in the separation gel. Separation gel (24 × 12 × 0.07 cm): 20 m*M* glutamic acid–60 m*M* histidine. 500 μl of Ampholytes 5–7 and 500 μl of Pharmalytes 5–6. Terminating ion: histidine. Anode: 20 ml of 250 m*M* histidine–20 m*M* glutamic acid. Cathode: 10 ml of 250 m*M* histidine. Power setting: 5 W. Two different transferrin forms are included as markers.

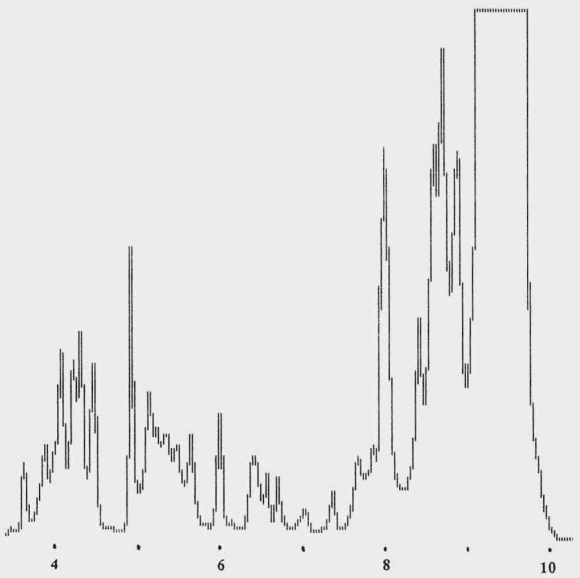

Fig. 4. Scanning of one track of the gel illustrated in Fig. 3A (LKB laser scanner). Abscissa, distance in cm; ordinate, absorbance.

prepared in our laboratory, are included as markers in Fig. 3C. The application of immuno techniques after ITP is illustrated in Fig. 6.

Results obtained with T_5C_3 polyacrylamide gel slabs were similar to those on agarose gels (not shown), but the latter are easier to handle and more suitable for immunological and preparative purposes.

DISCUSSION

Two aspects demand special attention in the design of an isotachophoretic system for the analytical separation of proteins: first, commercially available mixtures of ampholytes, designed for IEF, generate non-linear gradients of electrophoretic

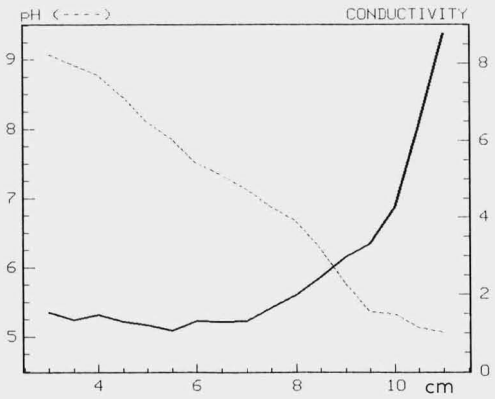

Fig. 5. Conductivity and pH measurements after agarose gel ITP, as illustrated in Fig. 3A.

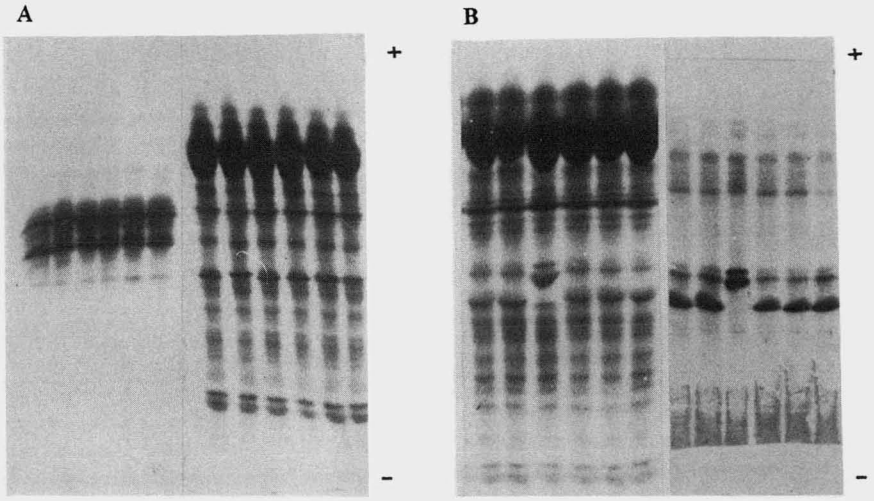

Fig. 6. Agarose gel ITP of plasma proteins, followed by immunoblot. (A) Transferrin and CBB stain. The spacers (pH 4–7) were included in the separation gel (24 × 12 × 0.1 cm): 80 m*M* glutamic acid–20 m*M* imidazole–60 m*M* histidine. 1.4 ml of Ampholytes 4–6, 700 μl of 5–7. Terminating ion: histidine. Anode: 20 ml of 400 m*M* glutamic acid–100 m*M* imidazole–300 m*M* histidine. Cathode: 10 ml of 250 m*M* histidine–80 m*M* imidazole. Power setting: 20 W. (B) CBB stain and C_3 complement. The spacers (pH 3.5–7) were included in the separation gel. Separation gel (24 × 12 × 0.07 cm): 40 m*M* glutamic acid–40 m*M* histidine. 600 μl of Ampholytes 3.5–5, 400 μl of 4–6, 400 μl of 5–7. Terminating ion: β-alanine. Anode: 20 ml of 250 m*M* histidine–20 m*M* glutamic acid. Cathode: 10 ml 1 *M* β-alanine–250 m*M* histidine. Power setting: 10 W.

mobility on ITP and therefore for this application they should be remixed inversely proportional to their p*I* value, as outlined above, and second, the buffer capacity of the counter ion(s) should cover the complete pH zone used for the separation.

For the design of the ITP systems illustrated in this paper, the electrophoretic mobilities of the leading, spacer and terminating ions were considered to be proportional to their charge. When the ITP condition is established, the total charge of the spacer in a particular pH zone in the system is defined by the charge of the counter ions in the zone, as the condition of electroneutrality must be satisfied. Therefore, the relative proportions between the leading ion and the counter ion(s) at the start, which gives the pH in the separation gel, regulate the charge of the spacers in the zones. Then, according to the Kohlrausch function, the starting pH regulates the concentration of spacers in the zones and thereby the length of the stack. The distance required to reach the steady state will be shorter for starting pH values closer to the p*I* of the fastest spacer ampholyte used, where its mobility is low. The starting pH is determined by all ions present in the separation gel: the leading ion, the counter ion(s) and the spacers, if they are included in the separation gel. In the latter instance, the spacers can also initially act as counter ions.

CONCLUSIONS

The separation of proteins by ITP offers, first, a high resolving capacity, which is adjustable for the study of any particular protein and, second, flexibility in pH and

ionic strength for the separation. The use of mixtures of ampholytes that generate linear gradients of electrophoretic mobility as spacers and the selection of counter ions to buffer the complete pH gradient generated are critical factors for the analytical separation of proteins by ITP. The analytical application of ITP illustrated in this paper is simple and rapid, comparable to gel electrophoresis or IEF, and it does not require special equipment or training.

ACKNOWLEDGEMENTS

This work was supported by grants from the Swedish Medical Research Council (12-5665), the Karolinska Institute, the Swedish Medical Association, the Swedish Psoriasis Association and the Foundations of Magnus Bergvall, Finsen and Edvard Wellander.

REFERENCES

1 N. Y. Nguyen and A. Chrambach, in B. D. Hames and D. Rickwood (Editors), *Gel Electrophoresis of Proteins: a practical approach*, IRL Press, London, 1981, Ch. 3, p. 145.
2 P. Boček, M. Deml, P. Gebauer and V. Dolník, in B. J. Radola (Editor), *Analytical Isotachophoresis*, VCH, Weinheim, 1988, pp. 25, 43.
3 F. Acevedo, in C. Schafer-Nielsen (Editor), *Electrophoresis '88*, VCH, Weinheim, 1988, p. 112.
4 A. T. Andrews, *Electrophoresis—Theory, Techniques, and Biochemical and Clinical Applications*, Oxford Science Publications, Oxford, 1986, p. 67.

International Symposium on Current Separation Techniques for Macromolecules
Uppsala (Sweden), August 22–24, 1988

END OF SYMPOSIUM PAPERS

Author Index to Volume 470

PUBLICATION SCHEDULE FOR 1989

Journal of Chromatography and Journal of Chromatography, Biomedical Applications

MONTH	J	F	M	A	M	J	J	A	S
Journal of Chromatography	461 462 463/1	463/2 464/1	464/2 465/1 465/2	466 467/1 467/2	468 469 470/1 470/2	471 472/1 472/2 473/1		The publication schedule for further issues will be published later	
Bibliography Section		486/1		486/2		486/3		486/4	
Biomedical Applications	487/1	487/2	488/1 488/2	489/1 489/2	490/1 490/2	491/1	491/2	492 493/1	493/2

INFORMATION FOR AUTHORS

(Detailed *Instructions to Authors* were published in Vol. 445, pp. 453–456. A free reprint can be obtained by application to the publisher, Elsevier Science Publishers B.V., P.O. Box 330, 1000 AH Amsterdam, The Netherlands.)

Types of Contributions. The following types of papers are published in the *Journal of Chromatography* and the section on *Biomedical Applications:* Regular research papers (Full-length papers), Notes, Review articles and Letters to the Editor. Notes are usually descriptions of short investigations and reflect the same quality of research as Full-length papers, but should preferably not exceed six printed pages. Letters to the Editor can comment on (parts of) previously published articles, or they can report minor technical improvements of previously published procedures; they should preferably not exceed two printed pages. For review articles, see inside front cover under Submission of Papers.

Submission. Every paper must be accompanied by a letter from the senior author, stating that he is submitting the paper for publication in the *Journal of Chromatography*. Please do not send a letter signed by the director of the institute or the professor unless he is one of the authors.

Manuscripts. Manuscripts should be typed in double spacing on consecutively numbered pages of uniform size. The manuscript should be preceded by a sheet of manuscript paper carrying the title of the paper and the name and full postal address of the person to whom the proofs are to be sent. Authors of papers in French or German are requested to supply an English translation of the title of the paper. As a rule, papers should be divided into sections, headed by a caption (*e.g.*, Summary, Introduction, Experimental, Results, Discussion, etc.). All illustrations, photographs, tables, etc., should be on separate sheets.

Introduction. Every paper must have a concise introduction mentioning what has been done before on the topic described, and stating clearly what is new in the paper now submitted.

Summary. Full-length papers and Review articles should have a summary of 50–100 words which clearly and briefly indicates what is new, different and significant. In the case of French or German articles an additional summary in English, headed by an English translation of the title, should also be provided. (Notes and Letters to the Editor are published without a summary.)

Illustrations. The figures should be submitted in a form suitable for reproduction, drawn in Indian ink on drawing or tracing paper. Each illustration should have a legend, all the *legends* being typed (with double spacing) together on a *separate sheet*. If structures are given in the text, the original drawings should be supplied. Coloured illustrations are reproduced at the author's expense, the cost being determined by the number of pages and by the number of colours needed. The written permission of the author and publisher must be obtained for the use of any figure already published. Its source must be indicated in the legend.

References. References should be numbered in the order in which they are cited in the text, and listed in numerical sequence on a separate sheet at the end of the article. Please check a recent issue for the layout of the reference list. Abbreviations for the titles of journals should follow the system used by *Chemical Abstracts*. Articles not yet published should be given as "in press" (journal should be specified), "submitted for publication" (journal should be specified), "in preparation" or "personal communication".

Dispatch. Before sending the manuscript to the Editor please check that the envelope contains three copies of the paper complete with references, legends and figures. One of the sets of figures must be the originals suitable for direct reproduction. Please also ensure that permission to publish has been obtained from your institute.

Proofs. One set of proofs will be sent to the author to be carefully checked for printer's errors. Corrections must be restricted to instances in which the proof is at variance with the manuscript. "Extra corrections" will be inserted at the author's expense.

Reprints. Fifty reprints of Full-length papers, Notes and Letters to the Editor will be supplied free of charge. Additional reprints can be ordered by the authors. An order form containing price quotations will be sent to the authors together with the proofs of their article.

Advertisements. Advertisement rates are available from the publisher on request. The Editors of the journal accept no responsibility for the contents of the advertisements.